

**Enhancing brain/neural-machine interfaces for upper
limb motor restoration in chronic stroke
and cervical spinal cord injury**

**Thesis submitted as requirement to fulfill the degree
“Doctor of Philosophy” (Ph.D)**

at the
Faculty of Medicine
Eberhard Karls Universität
Tübingen

by

Nann, Marius

2021

Dean: Professor Dr. B. Pichler

First reviewer: Professor Dr. S. Soekadar
Second reviewer: Professor Dr. C. Braun

Date of oral examination: 20.10.2021

*In every winter's heart there is a quivering spring,
and behind the veil of each night there is a shining dawn.*

Khalil Gibran (1883-1931)

Table of contents

1. Introduction.....	1
1.1 Individual and social implications of brain and spinal cord lesions	1
1.2 Conventional methods for upper limb motor restoration and their limitations	2
1.2.1 Stroke	2
1.2.2 Spinal cord injury	3
1.3 Brain-computer/machine interfaces	3
1.4 Current hybrid brain/neural-machine interface control paradigms and their limitations.....	6
1.4.1 Whole-arm exoskeleton control strategies after stroke.....	8
1.4.2 Bilateral exoskeleton control strategies after spinal cord injury	9
1.4.3 Predictive biomarker for declining sensorimotor rhythm control.....	11
2. Results.....	13
2.1 Feasibility and safety of shared EEG/EOG and vision-guided autonomous whole-arm exoskeleton control to perform activities of daily living	14
2.2 Restoring activities of daily living using an EEG/EOG-controlled semiautonomous and mobile whole-arm exoskeleton in chronic stroke	24
2.3 Feasibility and safety of bilateral hybrid EEG/EOG brain/neural-machine interaction	33
2.4 Heart rate variability predicts decline in sensorimotor rhythm control.....	47
3. Discussion.....	59
4. Summary	65
5. Bibliography.....	67
6. German summary	75
7. Declaration of contribution others.....	78
Acknowledgments	81

1. Introduction

1.1 Individual and social implications of brain and spinal cord lesions

Individuals suffering a brain or spinal cord lesion are often substantially affected in their daily life routines due to the loss of motor function and cognitive impairments. Especially brain lesions caused by stroke are the second leading cause of long-term disabilities above the age of 50 worldwide (Vos et al., 2020) with 13.7 million new stroke cases in 2016 across the globe (GDB Stroke Collaborators, 2019). Most stroke survivors are hemiparetic with related motor inabilities. In particular, the loss of hand function has considerable implications for the ability to engage in daily life activities, especially for activities in which bimanual manipulations are required, e.g., eating with cutlery or dressing on a pant (Rosamond et al., 2008). Besides these limitations in motor function, stroke survivors often experience cognitive impairments, e.g., post-stroke fatigue (Acciarresi et al., 2014) or reduced attentive capabilities (Lincoln et al., 2000). As consequence of such disabilities, they are often incapable to meet their basic needs limiting autonomy and quality of life. It was found that motor impairments can lead to general life dissatisfaction and depression in many cases (Laurent et al., 2011). Restoration of lost hand function after stroke is therefore an important medical goal of great social relevance for the affected persons and society as a whole. Also, the socioeconomic costs for treatment and post-stroke care are considerable (GDB Stroke Collaborators, 2019).

Even though the absolute cases of spinal cord injuries (SCIs) are distinctly lower than in stroke, the prevalence of traumatic SCI was approx. 27 million across the globe (James et al., 2019), while 41.1 % of them results in loss of motor function in all four extremities called tetraplegia (National Spinal Cord Injury Statistical Center, 2019). Contrary to stroke, SCIs have commonly no negative impact on cognitive capabilities, but cause substantial impairments in daily life activities due to paralysis. Dependent on the lesion location, inabilities in motor function vary considerably. Tetraplegics with injuries at the spinal motion sections C5 to C7, i.e., approximately 50 % of all tetraplegics (National Spinal Cord Injury Statistical Center, 2019), have some residual shoulder and arm function, but no

movement in wrist and fingers (Ahuja et al., 2017). Therefore, restoration of hand function is a crucial goal for tetraplegics to improve their autonomy and quality of life (Campbell et al., 1999).

1.2 Conventional methods for upper limb motor restoration and their limitations

1.2.1 Stroke

Several methods of task-oriented and task-specific physical therapy were shown to be effective under certain circumstances in all phases post-stroke, e.g., mental practice with motor imagery, neuromuscular stimulation of wrist/finger extensors or robotic-assisted training with the paretic arm (for review: Veerbeek et al., 2014). A very effective rehabilitation method based on physical therapy focuses on the existing motor function of the paretic limb while restricting the use of the non-paretic limb to avoid compensatory strategies. Several studies proved significance of the so-called constrained-induced movement therapy (CIMT) promoting substantial and long-lasting improvements in motor function (Wolf et al., 2006).

However, all methods in task-oriented physical therapy have in common that they require sufficient residual motor function to be applicable, and are therefore not suitable for stroke survivors with severe paralysis. For these severe cases, approximately one third of all stroke survivors (Ullberg et al., 2015; Wolfe et al., 2011), there is currently no accepted and standardized treatment strategy (Hatem et al., 2016; Veerbeek et al., 2014). Moreover, the absent of any motor function has the effect that these individuals perform the majority of their everyday life activities with the non-paretic extremity. This leads to the so-called “learned non-use”, which further aggravates existing deficits (Molle Da Costa et al., 2019). Extensive therapeutic effort can counteract such “learned non-use” to a certain extent in the post-acute phase, but is limited in time and reach to be effective against compensatory routines and habits in daily life. As a consequence, stroke survivors with severe hand and arm paralysis develop a chronic motor deficit, which is quite often rigidified over decades.

1.2.2 Spinal cord injury

Therapeutic options after a spinal cord injury (SCI) are still very limited and their rehabilitation outcome in terms of improved motor function strongly depends on the lesion type, i.e., whether the spinal cord lesion is complete and incomplete. Approximately half of all SCIs face complete injury with no motor and sensory function being preserved in spinal segments below the lesion location (Wyndaele & Wyndaele, 2006). Although descending axons can stay intact after clinically complete SCI (Sherwood et al., 1992), the prospect of recovery is very restricted. In case of incomplete lesions, there are rehabilitation methods to improve remaining motor and sensory function below the neurological level of injury, e.g., exercise therapy, electrical stimulation or robotic training. However, such interventions showed low effects and low power in clinical studies (for review: Lu et al., 2015). Further, similar to stroke rehabilitation, these methods require intensive therapy over several months. While there were recently some promising results in neural-controlled robotic-assisted rehabilitation (Donati et al., 2016), these studies predominately focused on lower extremities to augment walking function with motorized exoskeletons (for review: Mekki et al., 2018).

Regardless of the specific type of lesion and its chances for rehabilitation, up to date, the most applied method for upper limb motor restoration are surgical interventions (Bunketorp-Käll et al., 2017), such as tendon transfer or tenodesis (Bednar & Woodside, 2018). While these interventions can restore arm and hand function after SCI to a certain degree, their success strongly depends on individual factors as, e.g., quality and availability of tendons and residual muscles. Further, risks associated with surgery compromise their general application in restoration of upper extremity following SCI.

1.3 Brain-computer/machine interfaces

By considering that there are no standardized and accepted (non-surgical) therapeutic options for upper limb motor restoration in approximately one third of all stroke survivors and in all tetraplegics constitute a burden for all affected individuals and underline the need for alternative treatment approaches. The development of novel neurotechnology-aided methods over the past decades

rose hope in providing alternative strategies for movement restoration in such patient population (for review: Coscia et al., 2019). In particular, brain-computer/machine interface (BCI/BMI) systems promise aid in severe paralysis by bypassing non-functional corticospinal motor pathways for control of external devices without any motor output (Wolpaw et al., 2002). BCI/BMI systems translate electric, magnetic or metabolic brain activity into control commands, e.g., of computers, robotic devices, exoskeletons or devices applying functional electrical stimulation (FES) to paralyzed muscles. The remarkable potential of BMIs was shown with implantable as well as non-invasive systems in tetraplegics, e.g., controlling a robotic arm (Collinger et al., 2013; Hochberg et al., 2012) or an exoskeleton (Soekadar et al., 2016). Besides providing assistance, recent studies indicate that repeated use of such systems can trigger neural recovery (Biasiucci et al., 2018; Donati et al., 2016; Ramos-Murguialday et al., 2013). However, optimal training parameters, e.g., frequency, dose and intensity of training, remain unclear (Lang et al., 2016; Soekadar et al., 2015a; Young et al., 2015).

Even though BCI research has its beginning already in the late 1960s / beginning 1970s (Vidal, 1973), the first clinically relevant BCI was just demonstrated decades later in 1999 by Niels Birbaumer allowing locked-in patients, i.e., individuals, who are cognitively awake but unable to move or speak, to communicate by volitional modulation of their brain activity (Birbaumer et al., 1999). Since then, clinical applications of BCI/BMI systems including first approaches of brain-controlled movement restoration after brain or spinal cord lesions (Pfurtscheller et al., 2003) further emerged, also thanks to substantial improvements in sensor technology as well as in hardware for signal transmission and digital processing.

Brain activity can be recorded either invasively or non-invasively. Even though implantable BCIs/BMIs¹ show superior decoding performance, the majority of applied systems are based on non-invasive imaging techniques being applicable without any risk of infections or bleedings. While the most frequently used non-invasive recording methods for BCI/BMI paradigms are

¹ e.g., braingate2 neural interface system (www.braingate.org)

electroencephalography (EEG) (Pfurtscheller et al., 2008) and functional near-infrared spectroscopy (fNIRS) (Naseer & Hong, 2015; Soekadar et al., 2021) due to their relatively low cost and portability, also magnetoencephalography (MEG) (Buch et al., 2008) and functional magnetic resonance imaging (fMRI) (Liew et al., 2016) was shown to be feasible. However, especially in the field of brain-controlled motor restoration, EEG has been predominantly favored in most clinical studies (Van Dokkum et al., 2015). Therefore, the following paragraphs will focus on this imaging technique only.

For BCI/BMI control, a pattern change in commonly one EEG feature is translated into control commands. Several EEG features from four main subgroups have been tested so far: event-related potentials (ERPs) (Farwell & Donchin, 1988), slow cortical potentials (Birbaumer et al., 1999), steady-state visually or auditory evoked potentials (SSVEP/SSAEP) (Sakurada et al., 2013) and oscillatory brain activity (McFarland et al., 1993; Pfurtscheller et al., 2006; for review: Soekadar et al., 2015a). For instance, ERP-based BCI/BMI systems, as for example the P300 speller (Farwell & Donchin, 1988), are very reliable, but require by nature external stimuli, which is a shortcoming in practicability and usability in everyday life environments. The most common approach for brain-controlled movement restoration utilizes sensorimotor rhythms (SMR, 8-12 Hz) recorded from sensorimotor cortical areas (supplementary motor area, SMA, and M1) (Babiloni et al., 1999). Pfurtscheller and Neuper (1994) found out that SMR modulation appears during motor planning, motor imagination or motor execution and can be volitionally manipulated, e.g., by imagining grasping movements. Moreover, the somatotopic arrangement facilitates focal recording at the respective EEG recording site, e.g., at C3 for SMR modulations related to the right-hand knob representation. Thus, SMRs are very well suited as specific BCI/BMI feature for motor restoration allowing intuitive and self-paced control, e.g., of a hand exoskeleton.

Besides the advantages of SMR-based BCI/BMI systems, there are two main shortcomings. First, contrary to ERPs and evoked potentials, SMR control requires usually learning over several training sessions and is cognitively demanding as control tasks, e.g., imagination of grasping movements, request

for focus and concentration. This is especially challenging for users who suffer from cognitive impairments, e.g., due to a stroke (Soekadar et al., 2015c). In general, learning of volitional SMR control is based on operant conditioning of neuro-electric responses. Such operant conditioning can be trained by receiving contingent visual, auditory or haptic online neurofeedback of SMR modulation induced, e.g., by imagined movements (Soekadar et al., 2015a).

The second major problem is the relatively low average performance as well as the high variability from a day to another or even from trial to trial within a single session. Especially in self-paced (asynchronous) control paradigms, i.e., onsets of trials are randomly initiated by the user, control performance of SMR-based systems ranges at around 70-80 % accuracy (Grosse-Wentrup & Schölkopf, 2013). This would mean, that users, who manipulate daily life objects with a SMR-controlled hand exoskeleton would drop such objects in one of five cases limiting reliable and safe applicability in daily life environments as well as user acceptability. Thus, before broad use in clinical settings or everyday life environments is feasible, it is necessary to optimize BCI control paradigms to improve BCI learning and performance.

1.4 Current hybrid brain/neural-machine interface control paradigms and their limitations

To improve reliability of brain/neural controlled systems outside the laboratory, in particular when brain activity is recorded non-invasively with scalp EEG, further biosignals, e.g., electromyography (EMG) or electrooculography (EOG), have been merged with EEG to enhance control accuracy (for reviews: Amiri et al., 2013; Pfurtscheller et al., 2010). During the last decade, many studies investigated the advances of so-called hybrid brain/neural-machine interfaces (B/NMIs). For instance, Chowdhury et al. (2017) demonstrated improved exoskeleton control with a hybrid EEG/EMG paradigm and Wang et al. (2014) could show reliable wheelchair control based on fused EEG/EOG commands. The first remarkable clinical study demonstrated restoration of simple activities of daily living, e.g. eating with a fork, in tetraplegics with a hybrid EEG/EOG-based B/NMI hand exoskeleton outside the laboratory (Soekadar et al., 2016). This

study was a first important step transferring assistive neurotechnology towards uncontrolled daily life environments.

However, even though the development of hybrid B/NMI control has considerably improved applicability, brain-controlled neurotechnology has not yet entered more complex clinical or in-home environments. Apart from the need for more user-friendly recording and robotic systems, e.g., self-applicable EEG headsets instead of cap-based systems, two major reasons have been identified and are described below.

The first major reason is that current control paradigms still do not properly account for the characteristic motor inabilities of chronic stroke and SCI survivors. The majority of stroke survivors suffer from paralysis in the entire upper limb, i.e., there is a spastic flexion in finger, wrist as well as elbow joints (Colebatch & Gandevia, 1989; Pain et al., 2015). Current B/NMI systems could restore hand function, but do not allow simultaneous control of more proximal joints for whole-arm motor coordination. As a consequence, stroke survivors can hardly reach out for and grasp an object, e.g., in front of them on a table, as all joints need to be extended for such a task. In contrast to stroke survivors, tetraplegics after a cervical SCI lack motor function in both hands. Given that most activities of daily living (ADL) involve bimanual manipulation, e.g., to open the lid of a bottle, unilateral restoration of hand function is not sufficient in most cases. Instead, bilateral exoskeleton control is required but was not yet demonstrated in clinical studies.

The second major reason is that control paradigms are rarely personalized (Remsik et al., 2016). This means that there is no adaptive component to account for individual differences, e.g., how fast a user learns reliable SMR control or how fast a user gets fatigued as SMR control tasks are cognitively demanding. Especially, stroke survivors reach faster a state of exhaustion, because attentive capabilities are limited (Acciarresi et al., 2014; Christensen et al., 2008). As a consequence, B/NMI control performance can considerably deteriorate over time in this patient population.

To further enhance B/NMI systems towards broader clinical use, we have addressed the previously outlined points in several studies. First, we investigated

whether B/NMI whole-arm exoskeleton control in hemiplegia after chronic stroke is feasible and safe. Thereafter, feasibility and safety of bilateral B/NMI control after cervical SCI was evaluated. Lastly, as reliable B/NMI control is cognitively demanding, e.g., by imagining or attempting the desired movements, we investigated whether physiological biomarkers can predict a potential decline in control performance, a circumstance that should be avoided, but often occurs in stroke survivors. Details of the conducted studies are outlined in the following three paragraphs.

1.4.1 Whole-arm exoskeleton control strategies after stroke

During the last decade, various robotic systems for upper limb movement restoration have been developed. Most of these systems have been predominantly designed for stationary rehabilitation therapies in clinics, e.g., after stroke, but less for assistive purposes. However, recent developments in research and industry targeted the need of portable and light-weight hand (Cempini et al., 2015) or whole-arm exoskeletons² (Pedrocchi et al., 2013; Mohammad Habibur Rahman et al., 2015; Ren et al., 2012) for assistive support in daily life environments. While there are passive versions, e.g., with gravity compensation (Housman et al., 2007; Hull et al., 2020), also active ones were developed for more complex assistive support (Sanchez et al., 2005).

However, control of such complex assistive exoskeletons with non-invasive recording technique remains challenging. Several studies proposed exoskeleton control approaches based on EMG (Pernel et al., 2016; Mohammad H Rahman et al., 2015) or merged EMG/EEG control commands (Kawase et al., 2017). However, they all rely on residual and purposeful muscle activity often not present in severely affected stroke survivors. Other researchers suggested fusion of gaze and brain control, but often just showed partial mobilization of upper limb without wrist and hand (Frisoli et al., 2012). Moreover, while another study suggested a novel camera-based control, where different grasping types are optically selected via changing tracking patterns on the exoskeleton (Hazubski et al., 2020), such neural-free methods might be a feasible alternative, but lack intuitiveness and

² commercially available whole-arm exoskeleton MyoPro, Myomo Inc., Cambridge, USA

potential rehabilitative advances shown with brain-controlled strategies. To sum up, there is currently no established whole-arm exoskeleton B/NMI control that is intuitive, safe and effective.

In contrast to simple grasping (Soekadar et al., 2016), B/NMI control of more complex tasks involving the entire upper limb was not shown yet because high-dimensionality of such multiple joint systems require a large amount of control commands, which is not feasible with non-invasive recording methods to date. Thus, we blended B/NMI control with camera-based vision-guidance to receive a semiautonomous whole-arm exoskeleton control. Such setup allowed to divide ADL tasks into a sequence of EEG/EOG-triggered sub-tasks reducing complexity for the user. While, for instance, a drinking task was resolved into EOG-induced reaching, lifting and placing back the cup, grasping and releasing movements were based on intuitive SMR control. Feasibility of such shared vision-guided B/NMI control was assumed when executions were initialized within 3 s (fluent control) and a minimum of 75 % of subtasks were executed within that time (reliable control). The definition of fluent control as an average initialization of 3 s was reasoned based on the fact that human SMR control is temporally integrated within a 3-second window (Mates et al., 1994; Poppel, 2004). We showed feasibility in healthy participants as well as stroke survivors without report of any side effects documenting safe use. While results with healthy participants were published in “*Feasibility and safety of shared EEG/EOG and vision-guided autonomous whole-arm exoskeleton control to perform activities of daily living*”, results with severely affected stroke survivors were presented in “*Restoring activities of daily living using an EEG/EOG-controlled semiautonomous and mobile whole-arm exoskeleton in chronic stroke*”.

1.4.2 Bilateral exoskeleton control strategies after spinal cord injury

Soekadar et al. (2016) demonstrated full restoration of hand motor function in tetraplegia by using a hybrid EEG/EOG-controlled hand exoskeleton. Besides the use of motorized hand exoskeletons to passively move the fingers, also other restorative techniques like functional electrical stimulation (FES) were shown to be feasible in SCI survivors with flaccid spasticity (for review: Marquez-Chin &

Popovic, 2020). Regardless of the applied end effector, up to date, clinical studies restored only *unilateral* hand function. However, to conduct most ADLs, e.g., opening a bag of potato chips or a water bottle, *bimanual* manipulation is required, but was not yet implemented in tetraplegics.

During the last 10 to 15 years, extensive research in the BCI/BMI field have been carried out to classify movement intentions (Lotte et al., 2018). Numerous classification algorithms have been developed to solve not only the standard two-classes problem, i.e., movement vs. non-movement, but also multiclass problems with more than two states. Simultaneous control of two exoskeletons is such a multiclass problem: The algorithm needs to interpret whether either the left or right exoskeleton, both exoskeletons, or none of them should be activated. The simplest approach is a classifier, which distinguishes between lateralized activation patterns (León, 2017; Meng et al., 2016). This would mean that the attempt to move the right paralyzed hand induce a strong activation pattern over the contralateral hemisphere, here over C3, when recorded with EEG. However, even though Meng et al. (2016) showed proof-of-principle in healthy subjects, such classification method requires a strong lateralization of SMR for reliable functioning, which is often absent in chronic tetraplegics (Dahlberg et al., 2018; Osuagwu et al., 2016). Therefore, a method based on lateralized brain activation might not be suitable for a clinical study with SCI survivors.

A possible solution was to implement a reliable switch to select either the left or right exoskeleton. To enable bilateral B/NMI control, established EEG-based grasping and EOG-based releasing or stop commands were complemented with a novel EOG command allowing to switch laterality by performing prolonged horizontal eye movements (>1 s) to the left or to the right.

Similar to the previous study with stroke survivors, feasibility and safety of bilateral B/NMI control after cervical SCI was evaluated. Study results with healthy subjects and tetraplegics document fluent initialization of grasping motions below 3 s as well as safe use as unintended grasping could be stopped before a full motion was conducted. Superiority of novel bilateral control was documented by a higher accuracy of up to 22 % in tetraplegics compared to a bilateral control without prolonged EOG command. Results are documented in

the publication “*Feasibility and safety of bilateral hybrid EEG/EOG brain/neural-machine interaction*”.

1.4.3 Predictive biomarker for declining sensorimotor rhythm control

Current BCI/BMI control paradigms are rarely personalized meaning that they do not account for individual differences, e.g., how well and lasting focus and concentration can be maintained (Remsik et al., 2016). It is known that SMR control performance can vary from session to session depending on day-specific capabilities including factors like subjective fatigue or motivation (Curran & Stokes, 2003; Myrden & Chau, 2015). Especially stroke survivors suffering from side effects caused by their brain lesion have difficulties to sustain attention and concentration over longer period of time, e.g., potentially caused due to post-stroke fatigue (Acciarresi et al., 2014). As SMR control is cognitively demanding, it was shown that increasing fatigue correlates with diminished BCI/BMI performance (Foong et al., 2019). This study indicated that diminished BCI/BMI performance would not only limit applicability in assistive BCI, but also reduces efficacy of BCI training.

It would be thus important to identify a biomarker that predicts deterioration of BCI/BMI performance over time within an ongoing session. Even though extensive research was conducted to find predictive SMR performance markers in psychological (Hammer et al., 2012) or neurophysiological measures like resting alpha EEG power (Blankertz et al., 2010), such markers provide an estimate how well subjects potentially perform in average, but do not allow for predicting individual SMR performance within an ongoing session. However, this would be necessary to avoid potential contradictory effects, e.g., increasing frustration with progressing decline in BCI performance.

During the last decade, neuroadaptive human-computer interaction systems have been developed to passively monitor cognitive states without interfering with an active task (Zander & Kothe, 2011). Such monitoring methods were mainly applied in cognitive workload estimation. Besides features based on EEG brain activity, it was shown that also peripheral physiological measures as heart rate provide suitable classification information (Hogervorst et al., 2014).

We thus investigated whether heart rate variability (HRV) can be used as biomarker to predict declining control performance. More precisely, the parasympathetic activity quantified as high frequency (HF-) HRV (0.15 to 0.4 Hz) (Berntson et al., 1997) was shown to be sensitive for cognitive processes and decrease during demanding cognitive tasks (Muth et al., 2012; Stuiver et al., 2014). We showed with healthy subjects that a decline in HF-HRV is specific as well as predictive to a decline in SMR control performance within a single training session. Predictive link was revealed by a Granger-causality analysis. Results are documented in the publication *“Heart rate variability predicts decline in sensorimotor rhythm control”*.

2. Results

The following section contains four original publications, which were published as first or co-first author in international peer-reviewed journals. These publications summarize the research being conducted to answer the research questions introduced in the first section.

2.1 Feasibility and safety of shared EEG/EOG and vision-guided autonomous whole-arm exoskeleton control to perform activities of daily living

Crea, S.*, Nann, M.*[,], Trigili, E.*[,], Cordella, F., Baldoni, A., Badesa, F. J., Catalan, J. M., Zollo, L., Vitiello, N., Aracil, N. G., Soekadar, S. R. (2018). Feasibility and safety of shared EEG/EOG and vision-guided autonomous whole-arm exoskeleton control to perform activities of daily living. *Scientific Reports*, 8(1), 10823.

* authors contributed equally to this work

SCIENTIFIC REPORTS



OPEN

Feasibility and safety of shared EEG/EOG and vision-guided autonomous whole-arm exoskeleton control to perform activities of daily living

Received: 4 January 2018

Accepted: 3 July 2018

Published online: 17 July 2018

Simona Crea^{1,2}, Marius Nann³, Emilio Trigili¹, Francesca Cordella⁴, Andrea Baldoni¹, Francisco Javier Badesa⁵, José María Catalán⁶, Loredana Zollo⁶, Nicola Vitiello^{1,2}, Nicolas García Aracil¹ & Surjo R. Soekadar^{3,7}

Arm and finger paralysis, e.g. due to brain stem stroke, often results in the inability to perform activities of daily living (ADLs) such as eating and drinking. Recently, it was shown that a hybrid electroencephalography/electrooculography (EEG/EOG) brain/neural hand exoskeleton can restore hand function to quadriplegics, but it was unknown whether such control paradigm can be also used for fluent, reliable and safe operation of a semi-autonomous whole-arm exoskeleton restoring ADLs. To test this, seven able-bodied participants (seven right-handed males, mean age 30 ± 8 years) were instructed to use an EEG/EOG-controlled whole-arm exoskeleton attached to their right arm to perform a drinking task comprising multiple sub-tasks (reaching, grasping, drinking, moving back and releasing a cup). Fluent and reliable control was defined as average 'time to initialize' (TTI) execution of each sub-task below 3 s with successful initializations of at least 75% of sub-tasks within 5 s. During use of the system, no undesired side effects were reported. All participants were able to fluently and reliably control the vision-guided autonomous whole-arm exoskeleton (average TTI 2.12 ± 0.78 s across modalities with 75% successful initializations reached at 1.9 s for EOG and 4.1 s for EEG control) paving the way for restoring ADLs in severe arm and hand paralyses.

Arm and hand paralysis due to lesions of the central or peripheral nervous system is the most common reason for long-term disability in the adulthood¹. Particularly high-cervical spinal cord injuries, stroke or plexus brachialis avulsions resulting in a complete loss of arm and finger function have a substantial impact on the ability to perform various activities of daily living (ADLs), e.g. eating and drinking independently^{2,3}.

Over the last years, various upper-limb robotic systems were developed to mobilize the upper limb and fingers, e.g. in the context of rehabilitation therapies^{4–7}. Other promising robotic approaches to restore ADLs include gaze-based teleprosthetics⁸. While these systems were often immobile and designed to be used in rehabilitation facilities, recent advances in systems integration yielded the development of portable robotic arms with grippers^{9,10} or lightweight whole-arm¹¹ or hand exoskeletons^{12,13} that can be used in everyday life environments to assist in ADLs. While assistive robotic arms were mainly designed for individuals with complete tetraplegia and

¹The BioRobotics Institute, Scuola Superiore Sant'Anna, Pisa, Italy. ²Fondazione Don Carlo Gnocchi, Milan, Italy.

³Applied Neurotechnology Laboratory, Department of Psychiatry and Psychotherapy, University Hospital of Tübingen, Tübingen, Germany. ⁴Unit of Biomedical Robotics and Biomicrosystems, University Campus Bio-Medico of Rome, Rome, Italy. ⁵Applied Robotics, Departamento de Ingeniería en Automática, Electrónica, Arquitectura y Redes de Computadores, Universidad de Cádiz, Cádiz, Spain. ⁶Biomedical Neuroengineering, Departamento de Ingeniería de Sistemas y Automática, Universidad Miguel Hernández de Elche, Elche, Spain. ⁷Clinical Neurotechnology Laboratory, Neuroscience Research Center (NWFZ) & Department of Psychiatry and Psychotherapy, Charité – University Medicine Berlin, Berlin, Germany. Simona Crea, Marius Nann and Emilio Trigili contributed equally to this work. Correspondence and requests for materials should be addressed to S.C. (email: simona.crea@santannapisa.it) or S.R.S. (email: surjo.soekadar@uni-tuebingen.de)

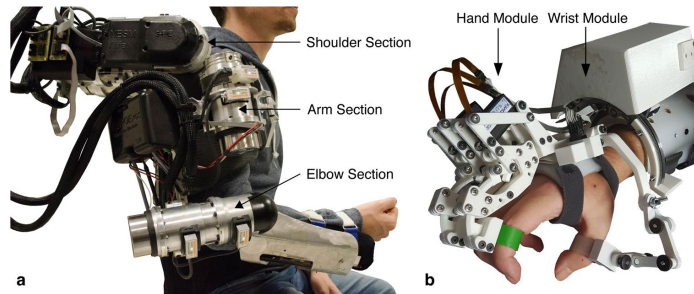


Figure 1. Illustration of the different components of the whole-arm exoskeleton. (a) NeuroExos Shoulder-elbow Module (NESM) exoskeleton consisting of three sections: shoulder, arm and elbow. (b) Hand-wrist exoskeleton comprising two modules: the hand module allows hand opening or closing motions, while the wrist module allows for pronation or supination movements.

inability to move their arms due to severe osteoporosis, atrophy of muscles and contractions of connective tissue, whole-arm exoskeletons that actuate the paralyzed upper-limb are particularly appealing for individuals with some remaining, but severely compromised arm and shoulder function. In this context, upper-limb exoskeletons can be either passive, for arm gravity compensation¹⁴, or active, for more complex assistive strategies¹⁵.

The main challenge to integrate such systems into everyday life environments relates to the individualization and user-friendliness of the hardware on one side, and the versatility, reliability and safety of robotic arm or exoskeleton control on the other side. Currently, there is no established paradigm for whole-arm exoskeleton control that is intuitive, safe and effective.

A very promising approach to provide intuitive control is based on direct translation of movement-related brain activity into robotic arm or exoskeleton control commands. The most impressive demonstrations of such approach required, however, the implantation of electrode-grids¹⁶ or microelectrode arrays¹⁷ with the risk of bleedings or infections.

Recently it was demonstrated that also non-invasive brain/neural recordings, such as electroencephalography (EEG) and electrooculography (EOG), allowed for intuitive and reliable hand exoskeleton control enabling quadriplegic patients with complete finger paralysis e.g. to eat and drink independently outside the laboratory¹⁸. In this study, EEG signal modulations related to the intention to grasp were translated online into actual grasping motions driven by a motorized hand exoskeleton system integrated into the users' wheelchair. Hand exoskeleton opening motions as well as interruption of unintended hand closing motions were controlled by EOG signals related to voluntary horizontal oculoversions (HOV). While the majority of established control paradigms translating non-stationary and non-linear brain activity into control signals use a dual state approach (i.e. synchronous mode of operation)¹⁹, the applied system allowed for *asynchronous* mode of operation, i.e. end-users could initiate hand grasping motions at any time¹⁸.

In contrast to a simple grasping task, operating a whole-arm exoskeleton, for example to drink, involves a series of sub-tasks such as reaching, grasping and lifting. A seven degrees-of-freedom (DOF) system like the human arm in which each joint can assume e.g. three discrete joint positions would result in an actions space with a dimensionality of 2187 (3⁷). The necessity to increase the number of possible joint positions for fine finger control, as required to e.g. drink from a cup, would exponentially increase the dimensionality. Currently, information transfer rates (ITR) required for such high-dimensional control of a robotic whole-arm exoskeleton exceeds ITRs of any established (implantable or non-invasive) brain-machine interface (BMI) system. Thus, blending of BMI and e.g. vision-guided autonomous robotics was suggested to improve control performance²⁰.

However, feasibility and safety of such novel control paradigm to restore ADLs, e.g. drinking, was not demonstrated yet. Here we tested whether an EEG/EOG control paradigm used to operate a vision-guided autonomous whole-arm exoskeleton across a series of sub-tasks (reaching, grasping, lifting and drinking, as well as placing back and releasing a cup) is feasible and safe.

While hand opening and closing motions to grasp and release a cup were controlled by motor imagery-related EEG desynchronization of sensorimotor rhythms (SMR, 9–15 Hz), reaching, lifting and placing back of the cup were controlled by EOG signals related to horizontal oculoversions (HOV) to the right (HOV_r). At any time, the participants could re-set the system to the initial state by using HOV to the left (HOV_l) (Figs 1 and 2). The movement trajectories of the whole-arm exoskeleton were continuously calculated and adapted using optical object tracking. Fluency, defined as average 'time to initialize' (TTI) execution of each of the sub-tasks, and reliability, defined as time to successfully initialize 75% of sub-tasks, as well as safety of operation were assessed. We reasoned that an average TTI of more than 3 seconds across control modalities would not be conceived as fluent operation, given that temporal integration in human sensorimotor control occurs in a 3-second time window^{21,22}. Reliable control was assumed if 75% of sub-tasks were successfully initialized within a time window of 5 seconds, a value comparable to other state-of-the-art BMI systems using an asynchronous mode of operation for

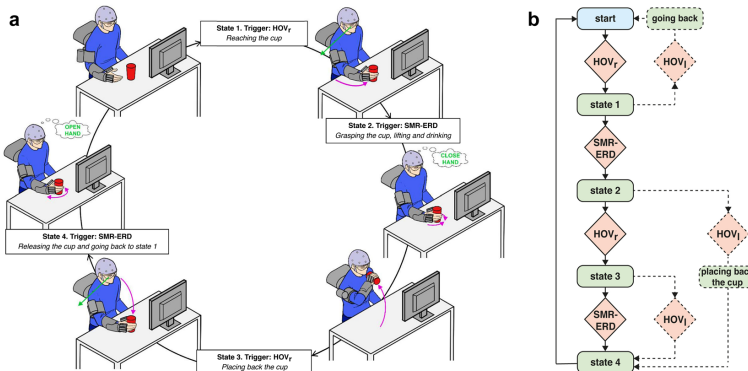


Figure 2. Shared-human robot control strategy based on a finite-state machine (FSM) triggered by electroencephalography/electrooculography (EEG/EOG). (a) Visualization of whole-arm exoskeleton actions controlled by EEG/EOG. Green arrows indicate horizontal oculoversions to the right (HOV_r) recorded with EOG, while “close hand” and “open hand” indicate EEG desynchronization of sensorimotor rhythms (SMR-ERD, 9–15 Hz) related to motor imagery of grasping and releasing motions. Purple arrows represent actions of the whole-arm exoskeleton. (Drawings: D. Marconi, The BioRobotics Institute, Scuola Superiore Sant’Anna, Pisa, Italy). (b) Flowchart of the whole-arm exoskeleton control loop.

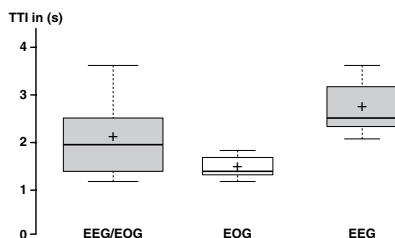


Figure 3. Fluency. ‘Time to initialize’ (TTI) across control modalities (EEG/EOG) as well as for individual EOG and EEG control mode across all participants. Average TTIs ranged below 3 s documenting fluent control. Crosses show the means, while centralines show the medians. Box limits indicate the 25th and 75th percentiles.

exoskeleton^{18,23}. Additionally, EEG/EOG control performance was assessed by calculating the sensitivity index (SI²³) that reflects the average rate of false positive classifications. At the end of the sessions, all participants were asked to report any discomforts or undesired side-effects.

Results

Feasibility. The average TTI (\pm s.d.) across control modalities ranged at 2.12 ± 0.78 s (median = 1.96 s [interquartile range = 1.46–2.48 s]) documenting fluent whole-arm exoskeleton control. The average EOG TTI was 1.49 ± 0.25 s (median = 1.40 s [1.32–1.69 s]), while average EEG TTI ranged at 2.75 ± 0.57 s (median = 2.52 s [2.34–3.18 s]) (Fig. 3).

Time to initialize 75% of the EOG-controlled sub-tasks was 1.9 s, while time to initialize 75% of the EEG-controlled sub-tasks was 4.1 s. Thus, time for 75% of successful initializations ranged below 5 s documenting reliable control (Fig. 4).

Safety. At the end of the session, none of the participants reported any discomforts or side-effects during whole-arm exoskeleton control.

Control performance. All participants were able to control the whole-arm exoskeleton using EEG/EOG control. SI (\pm s.d.) reached an average value of 1.43 ± 0.62 for EEG and 3.63 ± 1.21 for EOG across participants

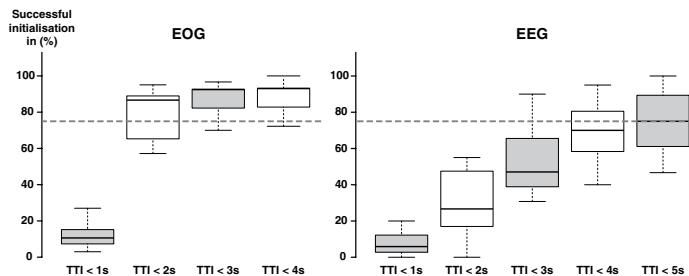


Figure 4. Reliability. Successful initializations during EEG and EOG control for discrete time intervals. Box plots show the relative number of successful initializations with TTIs smaller or equal to discrete time intervals ranging from 1 to 5 s for EEG and 1 to 4 s for EOG. Dashed line indicates 75% threshold of successful initializations representing reliable control, which was assumed when the time for successful initializations ranged below 5 s. The exact time to initialize 75% of the EOG-controlled sub-tasks was 1.9 s, while time to initialize 75% of the EEG-controlled sub-tasks was 4.1 s. Centrelines show the medians. Box limits indicate the 25th and 75th percentiles.

	EEG	EOG
Hit rate in % (\pm s.d.)	64.7 ± 5.0	94.3 ± 7.3
False alarm rate in % (\pm s.d.)	17.0 ± 21.4	5.7 ± 7.3

Table 1. Hit and false alarm classification rates across control modalities.

indicating good separation of EEG and EOG mean power values during rest and task and low false positive rate during use of the system (see classification rates, Table 1).

Discussion

Various neurological disorders related to brain lesions, neurodegeneration or neuroinflammation can lead to complete loss of hand and arm function. To restore this function, we developed a whole-arm exoskeleton²⁴ and tested whether a novel shared human–robot control strategy based on EEG/EOG signals can be used for its fluent and reliable operation, e.g. to reach out, lift and drink from a cup. While average TTIs during EOG control required less than 2 seconds (1.49 ± 0.25 s), brain control was associated with longer TTIs (2.75 ± 0.57 s), but still ranged below 3 seconds. This longer duration before initialization may relate to the time required for task-switching. Moreover, the delay in maximum ERD usually ranging between 800 milliseconds and up to 2 seconds^{18,25}. Performance of EEG/EOG control during use of this novel shared human–robot control strategy was comparable to other EEG/EOG control paradigms, e.g. asynchronous operation of a brain/neural hand exoskeleton²³ or a robotic arm²⁶. None of the participants complained about any discomfort or undesirable effects. Clinical studies are needed that investigate whether these findings can be generalized to individuals suffering from severe arm and hand paralysis.

While using EEG alone to control a complex multi-joint exoskeleton would be impractical due to the limited bandwidth and reliability, combined EEG and electromyography (EMG) control would provide higher bandwidth and reliability. However, because most people who require an exoskeleton suffer from a neurological condition that affects muscle control (often resulting in early fatigue), reliable EMG control often requires precise placing of the electrodes, extensive training and repeated individual calibration. Besides EOG, another viable tool for shared brain/neural- and vision-guided autonomous robot control might be eye tracking, an approach worth further exploring. Particularly, in more complex tasks with many branches, predominant use of EOG or eye tracking might be appealing. Besides using the system to perform a drinking task, it is conceivable that also other ADLs can be restored. In such case, the different tasks could be selected using sensor glasses to initiate different movement trajectories depending on the user's gaze direction.

Before whole-arm exoskeletons can enter everyday life environments, some technical challenges need to be addressed. These challenges relate to their weight, mobility and adaptability to the specific anatomical characteristics of possible end-users. Especially the presence of a stationary camera limits the portability of the current system. Portability could be improved by integrating the camera (possibly a set of cameras) into the wheelchair. Another challenge relates to the safety of such systems: while our study was performed in a controlled lab environment, further studies are needed to investigate possible safety constraints in everyday life scenarios. In this respect, implementation of a reliable veto function²⁷, i.e. the ability to interrupt unintended motions or behaviours of the system, will be critical. In our setup, the user could re-set the system to the initial state by eliciting HOV to the left (HOV_L). Such veto function will be required for any brain-controlled device, as none of the existing BMI approaches provide sufficient reliability in decoding brain activity to exclude false positive classifications.

(ranging at $17.0 \pm 21.4\%$ in our control paradigm with an asynchronous mode of operation, Table 1). Future studies should investigate the practicality and reliability of different veto-mechanisms across various everyday life scenarios, an issue not investigated in our study.

While voluntary muscle contractions have a “point of no return” approximately 200 milliseconds before their execution^{28,29}, voluntary acts can still be modified or vetoed after this “point of no return”. However, such “last minute” modification cannot be provided by any means of a BMI system, as the time window for detection of a false positive classification and corresponding brain response (usually a P300, i.e. a positive EEG deflection approximately 300 ms after error detection) would exceed this period. It is conceivable, however, that once the neural substrate of vetoing was identified, a veto function based on brain activity classification is feasible.

Previous studies indicated that the majority of individuals with damaged brain areas, e.g. following a stroke, can successfully use a brain-machine interface (BMI) to open and close a hand-orthosis^{30–32}. Whereas in healthy volunteers, EEG signals from electrode positions C3 or C4 (located over the motor cortex) are usually used, electrode positioning for BMI control may need to be adapted after a brain lesion due to cortical reorganization³³. Given the growing evidence that repeated use of a brain-controlled exoskeleton can trigger neurological recovery^{34,35}, larger studies that also investigate this aspect are needed³⁶. Currently, there is no study that investigated whether shared EEG/EOG and vision-guided autonomous whole-arm exoskeleton control would result in similar neurorehabilitation effects as EEG exoskeleton control alone. In this context, characterizing the optimal training schedules for specific patient populations will be important. Implementation of other bio-signals into shared human-robot interaction, such as physiological measures reflecting the user's workload or mental state, e.g. heart-rate variability³⁷, might improve their applicability and provide important information to optimize training schedules in the context of neurorehabilitation. By demonstrating feasibility and safety of shared EEG/EOG and vision-guided autonomous whole-arm exoskeleton control as accomplished in our study, such further clinical testing is now rendered possible.

Materials and Methods

Participants. Seven healthy volunteers (seven males, mean age (\pm s.d.): 30 ± 8 years) were invited to a single-session experiment at the Università Campus Biomedico di Roma (Rome, Italy). Before entering the study, all participants provided written informed consent. To enter the study, the following inclusion criteria had to be met: (i) absence of neurological or physical disorders, (ii) no regular medication intake, (iii) no history of neurological or psychiatric disorders and (iv) ability to speak and understand Italian or English. The study protocol complied with the Declaration of Helsinki and was approved by the local ethics committee (Comitato Etico Università Campus Biomedico di Roma, reference number: 01/17 PAR ComEt CBM) and by the Italian Ministry of Health (Registro - classif. DGDMF/I.5.i.m.2/2016/1096).

Whole-arm exoskeleton. The whole-arm exoskeleton comprises two components: A shoulder-elbow exoskeleton and a hand-wrist exoskeleton.

Shoulder-elbow exoskeleton. The shoulder-elbow exoskeleton (NeuroExos Shoulder-elbow Module, NESM) is a robotic upper-limb exoskeleton for shoulder/elbow mobilization^{24,38} (Fig. 1a). The exoskeleton was hanging from a standing structure and provides four active DOFs that are all rotational joints mounted in a serial kinematic chain. The exoskeleton mechanical structure is composed of three main blocks: the shoulder section, the arm section and the elbow section. The shoulder section includes the actuation units and motor drivers for the shoulder adduction/abduction (sA/A) and flexion/extension (sF/E). Both the sA/A and sF/E actuation units can exert a maximum continuous torque of 60 N·m. The arm section includes a shoulder intra/extra (sI/E) rotation joint. The actuation unit can exert a maximum continuous torque of 30 N·m. Moreover, the arm support consists of carbon-fiber shell structures with aluminium inserts and an ergonomic cuff. Finally, the elbow section includes an elbow flexion/extension (eF/E) joint. This joint can exert a maximum torque of 30 N·m.

Each actuation unit has a series elastic actuation (SEA) architecture comparable to Vitiello, *et al.*³⁹ that includes the following components: A brushless direct current (DC) motor, a reduction stage, two absolute encoders, a custom spring and an Elmo® Gold Solo Whistle servo driver. In each joint, the two encoders are placed at the two sides of the spring with respect to the mechanical frame: the encoder more proximal to the human joint (i.e. the joint position encoder) provides the joint angular value, while the difference between the two encoder readings provides the spring deformation, thus the transmitted torque. The support structure of the exoskeleton consists of a wheeled platform endowed with a vertical stand, which carries an articulated parallelogram functioning as a weight-relief system and supports the exoskeleton through a passive rotational joint. The wheeled platform also hosts the box containing the control and interface electronics. The total weight of the device (with the support structure, counterweight and electronics) was around 136 kg whereas the only wearable exoskeleton module weights approximately 13 kg. Passive DOFs allowing the rotation axis to follow the axis of the corresponding biological joint, and size regulations allowing to adjust the lengths of the frames to the user's anatomical characteristics, have been designed to ensure user comfort.

The control system was implemented on a real-time controller, a sbRIO-9636 (National Instruments, Austin, Texas, US) endowed with a 400-MHz processor running a NI real-time operating system and a field programmable gate array (FPGA) processor Xilinx Spartan-3. While the high-level layer was running at 100 Hz, the low-level closed-loop controllers were running at 1 kHz.

On the low-level control layer, a joint position control mode was implemented. Each actuation unit drives the joint position along a reference value or trajectory. The closed-loop joint position control of each actuation unit employed a proportional-integrative-derivative (PID) regulator using the error between the desired joint angle and measured joint position to allow for passive guidance in the absence of residual movement capabilities.

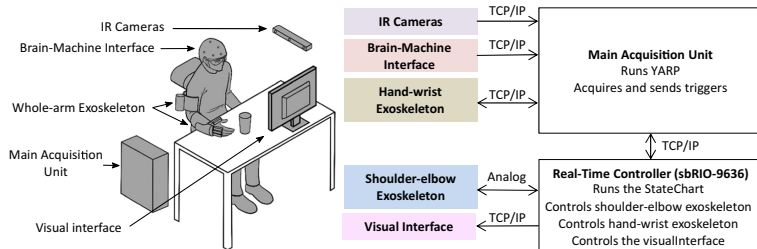


Figure 5. Overview of components and communication architecture based on TCP/IP protocol and analogue communication. (Drawings: D. Marconi, The BioRobotics Institute, Scuola Superiore Sant'Anna, Pisa, Italy).

Hand-wrist exoskeleton. The hand-wrist exoskeleton consists of two modules: The hand and wrist module that can be used separately or in combination⁴⁰ (Fig. 1b).

The hand exoskeleton was an electrical-driven device with 4-active DOFs. The mechanical structure of the exoskeleton can be divided into three main parts: (1) First and second fingers: For each of these fingers, a linkage attached to proximal and middle phalanges is driven by a linear actuator, performing a movement of both proximal interphalangeal (PIP) and metacarpophalangeal (MCP) joints. (2) Third and fourth fingers: A similar linkage is used for the third finger, while the linkage for the fourth finger is only attached to the proximal phalanx. Both linkages are driven by the same linear actuator, performing a movement of the third finger's PIP and MCP and fourth finger's MCP. (3) Thumb: For the thumb only, the flexion/extension movement is actuated, while adduction/abduction movement is fixed in an abduction position in order to achieve thumb opposition. In the same way as the fourth finger, a linear actuator drove a linkage to perform the movement of the thumb.

The wrist exoskeleton was a 1-active DOF device for the mobilization of the pronation/supination movement of the wrist. It consisted of a direct current (DC) motor with a reduction stage that drove a geared ring guide. The circular guide was attached to an orthosis that aligned the forearm with the axis of the guide. In addition, two load cells were used to estimate the interaction forces between the device and the user and ensured a safe human-robot interaction.

The wrist exoskeleton was designed to be easily connected to the NESM exoskeleton: by simply removing the forearm cuff from the NESM, the cuff integrated to the wrist exoskeleton could be attached to the elbow actuation unit's output frame.

EEG/EOG control interface. A 5-channel, wireless EEG (Enobio®, Neuroelectrics Barcelona S.L., Spain) was recorded from the following conventional 10/20 system recording sites: F3, T3, C3, Cz and P3 using polyamide-based solid-gel electrodes⁴¹. Ground and reference electrodes were placed at AFz and FCz, respectively. One additional channel was used to detect HOV using EOG signals recorded from the left outer canthus referenced to left mastoid. EEG and EOG were sampled at 500 Hz and band pass-filtered at 0.1–30 Hz. To increase signal-to-noise ratio, EEG was pre-processed using a surface Laplacian filter⁴². A customized version of the open-source BCI2000 software^{43,44} was used to translate the EEG and EOG signals into whole-arm exoskeleton control commands. To compute SMR event-related desynchronization (SMR-ERD), the power method by Pfurtscheller and Lopes da Silva⁴⁵ was used.

Motion capturing system. To capture the position and motion of the whole-arm exoskeleton and the graspable object (e.g. a cup) allowing vision-guided control, an IR-camera was used (OptiTrack®, Corvallis, USA). The system was placed on a vertical stand and tracked objects in 6 DOFs using reflective markers that were attached to the graspable object.

System component communication. The communication among all the integrated components, i.e. the whole-arm exoskeleton, EEG/EOG control interface and motion capturing system, was managed by the messaging system YARP (Yet Another Robotic Platform)^{45,46}. YARP external nodes were created in C++, MATLAB, LabVIEW and Linux environment for sending and receiving data to and from other nodes via a TCP/IP connection. Each node receiving and sending data was identified by a label and had a unique communication port on the YARP server. For the study, all data were received and transmitted at a frequency of 20 Hz. After starting the YARP server, all other nodes could connect independently and, if a node suddenly disconnected, the others could continue sending and receiving data without jeopardizing communication. The scheme of the communication architecture is given in Fig. 5.

Experimental setup and protocol. All participants were comfortably seated at a desk and equipped with a whole-arm exoskeleton as well as wearable devices including EEG and EOG. Before any calibration procedures, participants were familiarized with each of the components and received detailed instructions about the sequence of the drinking task. The drinking task comprised the following sub-tasks: 1. reaching a cup, 2. grasping and drinking from the cup, 3. placing back the cup and 4. releasing the cup. To evaluate fluency and reliability of EEG/

EOG control, participants received visual instructions when to execute each of the sub-tasks. While sub-tasks 1 and 3 were initialized by EOG signals, sub-tasks 2 and 4 were controlled by EEG signals. Over all, each participant performed the whole drinking task 20 times (i.e. 80 sub-tasks in total).

After detailed instruction, all devices for EEG/EOG assessment including amplifier and electrode cap were mounted. The EEG/EOG control interface was calibrated at the beginning of the session and remained unchanged for the entire session. During calibration, detection thresholds for SMR-ERD and HOV were determined as in Soekadar, *et al.*¹⁸. For calibration of the EEG/EOG control interface, a reference value (RV) of SMR-ERD related to externally-paced imagined hand opening or closing movements of the right hand was calculated by using a power spectrum estimation based on an autoregressive model of order 16 (Burg algorithm). Calculation of the RV comprised a total of 42 trials, each lasting 5 s, followed by an inter-trial interval (ITI) of 4 s, during which participants were inactive (rest condition). The optimal frequency for SMR-ERD detection [frequency of interest (FOI)] was set to the frequency showing the highest SMR-ERD modulation during imagined movements. For online classification of SMR-ERD, a frequency filter with an FOI of ± 1.5 Hz was used. A detection threshold for movement initiation and execution was calculated on the basis of the additional 42 trials, during which participants received online visual feedback of SMR-ERD provided on the display in front of them. The detection threshold was set at two standard deviations (s.d.) above average SMR-ERD and used for online EEG control. SMR-ERD was translated into a control command if detection threshold was exceeded. As a next step, participants were instructed to perform 10 externally paced HOV to the left or right following a visual cue while EOG was recorded. In analogy to EEG calibration, a HOV detection threshold was set at two s.d. below the average EOG signal recorded during maximum HOV. While HOV to the right (HOV_r) was defined as confirmatory signal in states 1 and 3, the user could re-set the system to the initial state at any time by HOV to the left (HOV_l) (Fig. 2). Mounting and calibration of the EEG/EOG control interface required approximately 15–20 minutes per participant. Since there was just one session per participant, the whole donning and calibration procedure was performed only once at the beginning of the session.

Before performing 20 trials with the whole-arm exoskeleton to drink from a glass, participants were familiarized with wearing and moving the whole-arm exoskeleton by performing one complete drinking sequence.

Shared human-robot control. To operate the multi-DOF whole-arm exoskeleton, a shared-human robot control strategy was used based on a finite-state machine (FSM) blending vision guidance and BMI control. FSM was implemented within the 100 Hz main loop of the NESM high-level control layer. The following states were implemented in the FSM (Fig. 2):

State 1. *Reaching the cup:* Detection of HOV results in a whole-arm exoskeleton reaching movement guided by the motion capturing system.

State 2. *Grasping the cup, lifting and drinking:* Detection of SMR-ERD exceeding the SMR-ERD detection threshold results in exoskeleton-driven hand closing motions. Once the grasping motion is complete, the whole-arm exoskeleton automatically lifts the cup and moves it to the user's mouth without any additional trigger elicited by the participant.

State 3. *Placing back the cup:* After drinking from the cup, detection of HOV results in moving the whole-arm exoskeleton back to the position from where the cup was lifted.

State 4. *Releasing the cup and going back to state 1:* Detection of SMR-ERD results in exoskeleton-driven hand opening motions. Once the grasping motion is complete, the whole-arm exoskeleton automatically moves back to state 1, without any additional trigger.

An inverse kinematics algorithm calculated the joint angles to achieve the desired end-effector position as described in Lauretti, *et al.*⁴⁷. The end-effector moves along a linear 3D trajectory, as each joint moves along a pre-defined trajectory with a stereotyped sigmoid time-position profile, executed within 5 s. Moreover, the exoskeleton end-effector position was finely adjusted via a *visual-servoing* algorithm: the error between the end-effector and object position was calculated online. End-effector positions were corrected until the error dropped below a certain threshold (i.e. 2 cm).

A graphical user interface (GUI) allowed to visualize the inputs and outputs of the FSM as well as communication flow between the different system components. Moreover, a user display was used to provide the following visual cues that were synchronized with the system's FSM state:

1. EOG control 1: "Please look to the right to initialize reaching movement." (State 1)
2. EEG control 1: "Cup reached! Please imagine hand closing to grasp the cup." (State 2)
3. EOG control 2: "Please look to the right for placing back the cup?" (State 3)
4. EEG control 2: "Initial cup position reached! Please imagine hand opening to release the cup." (State 4)

A green square indicated when the sub-task was successfully initialized.

Data collection and analyses. During use of the system, all system parameters as well as physiological data were stored for offline analysis. EEG/EOG TTIs were evaluated as time between visual indication and detection of EEG/EOG signals exceeding the EEG/EOG detection thresholds. Reliability of control was assessed by calculating the time for successful initializations of at least 75% of sub-tasks. Reliable control was assumed when the time for successful initializations ranged below 5 s. To evaluate the average rate of false positive EEG/EOG classifications as measure of control performance, the sensitivity index (SI, Eq. 1) was calculated and averaged across all participants. SI of EEG and EOG, respectively, was assessed based on 20 trials, which were recorded at the end of the calibration phase.

$$d' = Z(\text{hit_rate}) - Z(\text{false_alarm_rate}) \quad (1)$$

For EEG, 'hit_rate' was defined as the relative number of sample blocks during the task in which EEG activity exceeded the EEG-detection threshold, whereas 'false_alarm_rate' was defined as the relative number of sample blocks during rest in which the EEG-detection threshold was exceeded. For EOG, a 'hit' (true positive) was assumed if EOG signals exceeded the EOG-detection threshold upon visual instruction, whereas 'false_alarm' (false positive) was assumed if EOG signals exceeded the EOG-detection threshold although no visual instruction was provided.

Data availability. The datasets generated during and/or analysed during the current study are available from the corresponding author on reasonable request.

References

1. Salomon, J. A. *et al.* Common values in assessing health outcomes from disease and injury: disability weights measurement study for the Global Burden of Disease Study 2010. *Lancet* **380**, 2129–2143, [https://doi.org/10.1016/S0140-6736\(12\)61680-8](https://doi.org/10.1016/S0140-6736(12)61680-8) (2012).
2. Filiault, J., Arsenault, A. B., Dutil, E. & Bourbonnais, D. Motor function and activities of daily living assessments: a study of three persons for persons with hemiplegia. *Am. J. Occup. Ther.* **45**, 806–810 (1991).
3. Mercier, L., Audet, T., Hebert, R., Rochette, A. & Dubois, M. Impact of motor, cognitive, and perceptual disorders on ability to perform activities of daily living after stroke. *Stroke* **32**, 2602–2608 (2001).
4. Veerbeek, J. M., Langbroek-Amersfoort, A. C., van Wegen, E. E., Meskers, C. G. & Kwakkel, G. Effects of Robot-Assisted Therapy for the Upper Limb After Stroke. *Neurorehabil Neural Repair* **31**, 107–121, <https://doi.org/10.1177/154968316666957> (2017).
5. Maciejasz, P., Eschweiler, J., Gerlach-Hahn, K., Jansen-Troy, A. & Leonhardt, S. A survey on robotic devices for upper limb rehabilitation. *J. Neuroeng. Rehabil.* **11**, 3, <https://doi.org/10.1186/1743-0003-11-3> (2014).
6. Masiero, S., Celia, A., Rosati, G. & Armani, M. Robotic-assisted rehabilitation of the upper limb after acute stroke. *Arch. Phys. Med. Rehabil.* **88**, 142–149, <https://doi.org/10.1016/j.apmr.2006.10.032> (2007).
7. Colombo, R. *et al.* Robotic techniques for upper limb evaluation and rehabilitation of stroke patients. *IEEE Trans. Neural Syst. Rehabil. Eng.* **13**, 311–324, <https://doi.org/10.1109/TNSRE.2005.848352> (2005).
8. Dzienian, S., Abbott, W. W. & Faisal, A. A. In *Biomedical Robotics and Biomechatronics (BioRob), 6th IEEE International Conference on*, 1277–1282 (IEEE) 2016.
9. Maheu, V., Archambault, P. S., Frappier, J. & Routhier, F. In *Rehabilitation Robotics (ICORR), IEEE International Conference on*, 1–5 (IEEE) 2011.
10. Brose, S. W. *et al.* The role of assistive robotics in the lives of persons with disability. *Am. J. Phys. Med. Rehabil.* **89**, 509–521, <https://doi.org/10.1097/PHM.0b013e3181cf569f> (2010).
11. Pedrocchi, A. *et al.* MUNDUS project: Multimodal neuroprosthesis for daily upper limb support. *J. Neuroeng. Rehabil.* **10**, 66, <https://doi.org/10.1186/1743-0003-10-66> (2013).
12. Campini, M., Cortese, M. & Vittolo, N. A Powered Finger-Thumb Wearable Hand Exoskeleton With Self-Aligning Joint Axes. *IEEE/ASME Transactions on Mechatronics* **20**, 705–716, <https://doi.org/10.1109/Tmech.2014.2315528> (2015).
13. Gandolla, M. *et al.* Artificial neural network EMG classifier for functional hand grasp movements prediction. *J. Int. Med. Res.* **45**, 1831–1847, <https://doi.org/10.1177/0300060516656689> (2017).
14. Housman, S. J., Le, V., Rahman, T., Sanchez, R. J. & Reinkensmeyer, D. J. In *Rehabilitation Robotics, 2007. ICORR. IEEE International Conference on*, 562–568 (IEEE) 2007.
15. Sanchez, R. *et al.* In *Rehabilitation Robotics, 2005. ICORR. 9th International Conference on*, 500–504 (IEEE) 2005.
16. Ajiboye, A. B. *et al.* Restoration of reaching and grasping movements through brain-controlled muscle stimulation in a person with tetraplegia: a proof-of-concept demonstration. *Lancet* **389**, 1821–1830, [https://doi.org/10.1016/S0140-6736\(17\)30601-3](https://doi.org/10.1016/S0140-6736(17)30601-3) (2017).
17. Hochberg, L. R. *et al.* Reach and grasp by people with tetraplegia using a neurally controlled robotic arm. *Nature* **485**, 372–375, <https://doi.org/10.1038/nature1076> (2012).
18. Soekadar, S. R. *et al.* Hybrid EEG/EOG-based brain/neural hand exoskeleton restores fully independent daily living activities after quadriplegia. *Science Robotics* **1** (2016).
19. Soekadar, S. R. *et al.* ERD-based online brain-machine interfaces (BMI) in the context of neurorehabilitation: optimizing BMI learning and performance. *IEEE Trans. Neural Syst. Rehabil. Eng.* **19**, 542–549, <https://doi.org/10.1109/TNSRE.2011.2166809> (2011).
20. Downey, J. E. *et al.* Blending of brain-machine interface and vision-guided autonomous robotics improves neuroprosthetic arm performance during grasping. *J. Neuroeng. Rehabil.* **13**, 28, <https://doi.org/10.1186/s12984-016-0134-9> (2016).
21. Poppel, E. Lost in time: a historical frame, elementary processing units and the 3-second window. *Acta Neurobiol Exp (Wars)* **64**, 295–301 (2004).
22. Mates, J., Muller, U., Radil, T. & Poppel, E. Temporal integration in sensorimotor synchronization. *J. Cogn. Neurosci.* **6**, 332–340, <https://doi.org/10.1162/jocn.1994.6.4.332> (1994).
23. Witkowski, M. *et al.* Enhancing brain-machine interface (BMI) control of a hand exoskeleton using electrooculography (EOG). *J. Neuroeng. Rehabil.* **11**, 165, <https://doi.org/10.1186/1743-0003-11-165> (2014).
24. Crea, S. *et al.* In *Biomedical Robotics and Biomechatronics (BioRob), 6th IEEE International Conference on*, 1248–1253 (IEEE) 2016.
25. Neuper, C., Schlogl, A. & Pfurtscheller, G. Enhancement of left-right sensorimotor EEG differences during feedback-regulated motor imagery. *J. Clin. Neurophysiol.* **16**, 373–382 (1999).
26. Minati, L., Yoshimura, N. & Koike, Y. Hybrid Control of a Vision-Guided Robot Arm by EOG, EMG, EEG Biosignals and Head Movement Acquired via a Consumer-Grade Wearable Device. *IEEE Access* **4**, 9528–9541, <https://doi.org/10.1109/Access.2017.2647851> (2016).
27. Clausen, J. *et al.* Help, hope, and hype: Ethical dimensions of neuroprosthetics. *Science* **356**, 1338–1339, <https://doi.org/10.1126/science.aam7731> (2017).
28. Deeecke, L. & Soekadar, S. R. Beyond the point of no return: Last-minute changes in human motor performance. *Proc Natl Acad Sci USA* **113**, E2876, <https://doi.org/10.1073/pnas.1604257113> (2016).
29. Schultz-Kraft, M. *et al.* The point of no return in vetoing self-initiated movements. *Proc. Natl. Acad. Sci. USA* **113**, 1080–1085, <https://doi.org/10.1073/pnas.1513569112> (2016).
30. Soekadar, S. R., Birbaumer, N., Slutsky, M. W. & Cohen, L. G. Brain-machine interfaces in neurorehabilitation of stroke. *Neurobiol. Dis.* **83**, 172–179, <https://doi.org/10.1016/j.neuro.2014.11.025> (2015).
31. Buch, E. *et al.* Think to move: a neuromagnetic brain-computer interface (BCI) system for chronic stroke. *Stroke* **39**, 910–917, <https://doi.org/10.1161/STROKEAHA.107.505313> (2008).
32. Birbaumer, N. & Cohen, L. G. Brain-computer interfaces: communication and restoration of movement in paralysis. *J. Physiol.* **579**, 621–636, <https://doi.org/10.1113/jphysiol.2006.125633> (2007).
33. Luft, A. R. *et al.* Lesion location alters brain activation in chronically impaired stroke survivors. *Neuroimage* **21**, 924–935 (2004).

34. Donati, A. R. *et al.* Long-Term Training with a Brain-Machine Interface-Based Gait Protocol Induces Partial Neurological Recovery in Paraplegic Patients. *Sci Rep* **6**, 30383. <https://doi.org/10.1038/srep30383> (2016).
35. Ramos-Murguialday, A. *et al.* Brain-machine interface in chronic stroke rehabilitation: a controlled study. *Ann Neurol* **74**, 100–108. <https://doi.org/10.1002/ana.23879> (2013).
36. Ushiba, J. & Soekadar, S. R. Brain-machine interfaces for rehabilitation of poststroke hemiplegia. *Prog Brain Res* **228**, 163–183. <https://doi.org/10.1016/bs.pbr.2016.04.020> (2016).
37. Madden, K. & Savard, G. K. Effects of mental state on heart rate and blood pressure variability in men and women. *Clin. Physiol.* **15**, 557–569 (1995).
38. Crea, S. *et al.* In *Converging Clinical and Engineering Research on Neurorehabilitation II* 495–499 (Springer, 2017).
39. Vitello, N. *et al.* Functional Design of a Powered Elbow Orthosis Toward its Clinical Employment. *IEEE/ASME Transactions on Mechatronics* **21**, 1880–1891. <https://doi.org/10.1109/Tmech.2016.2558646> (2016).
40. Díez, J. A. *et al.* In *Converging Clinical and Engineering Research on Neurorehabilitation II* 531–535 (Springer, 2017).
41. Toyama, S., Takano, K. & Kansaku, K. A non-adhesive solid-gel electrode for a non-invasive brain-machine interface. *Front. Neurol.* **3**, 114. <https://doi.org/10.3389/fneur.2012.00114> (2012).
42. McFarland, D. J. The advantage of the surface Laplacian brain-computer interface research. *Int. J. Psychophysiol.* **97**, 271–276. <https://doi.org/10.1016/j.ijpsycho.2014.07.009> (2015).
43. Schalk, G. In *Engineering in Medicine and Biology Society, 2009. EMBC. Annual International Conference of the IEEE*. 5498–5501 (IEEE) 2009.
44. Pfurtscheller, G. & da Silva, L. F. H. Event-related EEG/MEG synchronization and desynchronization: basic principles. *Clin. Neurophysiol.* **110**, 1842–1857. [https://doi.org/10.1016/S1388-2457\(99\)00141-8](https://doi.org/10.1016/S1388-2457(99)00141-8) (1999).
45. Fitzpatrick, P. *et al.* A middle way for robotics middleware. *Journal of Software Engineering for Robotics* **5**, 42–49 (2014).
46. Metta, G., Fitzpatrick, P. & Natale, L. YARP: yet another robot platform. *International Journal of Advanced Robotic Systems* **3**, 8 (2006).
47. Lauretti, C. *et al.* Learning by Demonstration for Motion Planning of Upper-Limb Exoskeletons. *Front. Neurorobot.* **12**, 5. <https://doi.org/10.3389/fnbot.2018.00005> (2018).

Acknowledgements

This study was funded by the European Commission under the project AIDE (G.A. no: 645322), the European Research Council (ERC) under the project NGBMI (759370), the Baden-Württemberg Stiftung (NEU007/1), and supported by the Open Access Publishing Fund of the University of Tübingen. SRS received special support by the Brain & Behavior Research Foundation as 2017 NARSAD Young Investigator Grant recipient and P&S Fund Investigator. We thank D. Marconi for providing the drawings in Figures 2a and 5.

Author Contributions

S.C., M.N., E.T., F.C. and S.R.S. designed the study. S.C., M.N., E.T., F.C., F.J.B. and J.M.C. collected the data. S.C., M.N., E.T. and F.C. analysed the data. F.C. and L.Z. organised the experimental session. A.B. developed the shoulder-elbow exoskeleton. S.C., M.N., E.T., F.C., L.Z., N.V. and S.R.S. interpreted the data and performed the literature search. S.C., M.N., E.T. and S.R.S. wrote the manuscript. S.C., M.N., E.T. and J.M.C. created the figures. S.C., M.N., E.T., F.C., F.J.B., J.M.C., L.Z., N.V., N.G.A. and S.R.S. edited the manuscript.

Additional Information

Competing Interests: S.C. and N.V. have interests in a spin-off company (IUVO S.r.l.) developing and commercializing exoskeleton technology that may benefit in the future from research presented in this article. The IP protecting the NESM technology has currently been licensed to IUVO S.r.l.

Publisher's note: Springer Nature remains neutral with regard to jurisdictional claims in published maps and institutional affiliations.



Open Access This article is licensed under a Creative Commons Attribution 4.0 International License, which permits use, sharing, adaptation, distribution and reproduction in any medium or format, as long as you give appropriate credit to the original author(s) and the source, provide a link to the Creative Commons license, and indicate if changes were made. The images or other third party material in this article are included in the article's Creative Commons license, unless indicated otherwise in a credit line to the material. If material is not included in the article's Creative Commons license and your intended use is not permitted by statutory regulation or exceeds the permitted use, you will need to obtain permission directly from the copyright holder. To view a copy of this license, visit <http://creativecommons.org/licenses/by/4.0/>.

© The Author(s) 2018

2.2 Restoring activities of daily living using an EEG/EOG-controlled semiautonomous and mobile whole-arm exoskeleton in chronic stroke

Nann, M.*, Cordella, F.*., Trigili, E., Lauretti, C., Bravi, M., Miccinilli, S., Catalan, J. M., Badesa, F. J., Crea, S., Bressi, F., Garcia-Aracil, N., Vitiello, N., Zollo, L.*., Soekadar, S. R.* (2021). Restoring Activities of Daily Living Using an EEG/EOG-Controlled Semiautonomous and Mobile Whole-Arm Exoskeleton in Chronic Stroke. *IEEE Systems Journal*, 15(2), 2314-2321.

* authors contributed equally to this work

Restoring Activities of Daily Living Using an EEG/EOG-Controlled Semiautonomous and Mobile Whole-Arm Exoskeleton in Chronic Stroke

Marius Nann¹, Francesca Cordella¹, Emilio Trigili¹, Clemente Lauretti¹, Marco Bravi¹, Sandra Miccinilli¹, Jose M. Catalan, Francisco J. Badesa, Simona Crea², Federica Bressi², Nicolas Garcia-Aracil, Nicola Vitiello, Loredana Zollo, and Surjo R. Soekadar¹

Abstract—Stroke survivors with chronic paralysis often have difficulties to perform various activities of daily living (ADLs), such as preparing a meal or eating and drinking independently. Recently, it was shown that a brain/neural hand exoskeleton can restore hand and finger function, but many stroke survivors suffer from motor deficits affecting their whole upper limb. Therefore, novel hybrid electroencephalography/electrooculography (EEG/EOG)-based brain/neural control paradigms were developed for guiding a whole-arm exoskeleton. It was unclear, however, whether hemiplegic stroke survivors are able to reliably use such brain/neural-controlled device. Here, we tested feasibility, safety, and user-friendliness of EEG/EOG-based brain/neural robotic control across five hemiplegic stroke survivors engaging in a drinking task that consisted of several subtasks (e.g., reaching, grasping, manipulating, and drinking). Reliability was assumed when at least

75% of subtasks were initialized within 3 s. Fluent control was assumed if average “time to initialize” each subtask ranged below 3 s. System’s safety and user-friendliness were rated using Likert-scales. All chronic stroke patients were able to operate the system reliably and fluently. No undesired side effects were reported. Four participants rated the system as very user-friendly. These results show that chronic stroke survivors are capable of using an EEG/EOG-controlled semiautonomous whole-arm exoskeleton restoring ADLs.

Index Terms—Activities of daily living (ADL), brain-computer interface (BCI), brain-machine interface (BMI), chronic stroke, electroencephalography (EEG), electrooculography (EOG), exoskeletons, hemiparesis, rehabilitation robotics, sensorimotor rhythms, shared control.

I. INTRODUCTION

STROKE is one of the leading causes for long-term disability in the adulthood worldwide [1]. Besides cognitive and sensory impairments, particularly loss of hand and arm function impedes the ability of stroke survivors to engage in various activities of daily living (ADLs) such as preparing a meal or eating and drinking independently. As a consequence, stroke survivors frequently reported reduced quality of life and limited autonomy [2]. Therefore, effective restoration of hand and arm motor function after stroke is of great importance. However, there is no accepted gold standard in the treatment of stroke survivors with little or no capacity to move the arm or fingers [3], [4]. Most established rehabilitation methods such as constraint-induced movement therapy [5] require some remaining grasp function and are therefore not applicable for stroke survivors with complete hand and finger paralysis. Moreover, many stroke survivors also suffer from limited or nonexistent arm and shoulder function.

Recently, it was shown that brain/neural hand exoskeletons (B/NHEs) are capable of fully restoring hand and finger function despite complete paralysis, e.g., due to cervical spinal cord injury [6]. Such devices translate modulations of electric, magnetic, or metabolic brain activity, e.g., related to imagined or attempted movements of the paralyzed fingers, into actual finger movements driven by electromechanical actuators [7]–[10]. The best established approach for such application uses modulations of sensorimotor rhythms (SMR, 8–12 Hz) recorded by EEG

Manuscript received December 31, 2019; revised June 28, 2020 and August 28, 2020; accepted August 30, 2020. This work was supported in part by the European Commission under the Project AIDE under Grant 645322, in part by the European Research Council under the Project NGBMI under Grant 759370, in part by the Baden-Württemberg Stiftung under Grant NEU007/1 and the Einstein Stiftung Berlin, and in part by the Italian Institute for Labour Accidents with the RehabRobo@Work under Grant CUP:C82F17000040001. The work of Surjo R. Soekadar was supported by Brain and Behavior Research Foundation as 2017 NARSAD Young Investigator Grant recipient and P&S Fund Investigator. (*Marius Nann, Francesca Cordella, Loredana Zollo, and Surjo R. Soekadar contributed equally to this work.*) *Corresponding author:* Surjo R. Soekadar.)

Marius Nann and Surjo R. Soekadar are with the Charité – Universitätsmedizin, 10117 Berlin, Germany, and also with the University Hospital of Tübingen, 72076 Tübingen, Germany (e-mail: marius.nann@uni-tuebingen.de; surjo.soekadar@charite.de).

Francesca Cordella, Clemente Lauretti, Marco Bravi, Sandra Miccinilli, Federica Bressi, and Loredana Zollo are with the Università Campus Bio-Medico di Roma, 00128 Rome, Italy (e-mail: f.cordella@unicampus.it; c.lauretti@unicampus.it; m.bravi@unicampus.it; s.miccinilli@unicampus.it; f.bressi@unicampus.it; l.zollo@unicampus.it).

Emilio Trigili is with the BioRobotics Institute, Scuola Superiore Sant’Anna, 56025 Pontedera, Italy (e-mail: emilio.trigili@santannapisa.it).

José M. Catalan and Nicolas Garcia-Aracil are with Bioengineering Institute at Miguel Hernández University of Elche, 03202 Alicante, Spain, and also with the New Technologies for Neurorehabilitation Laboratory, 28054 Madrid, Spain (e-mail: jcatalan@umh.es; nicolas.garcia@umh.es).

Francisco J. Badesa is with the Miguel Hernández University of Elche, 03202 Alicante, Spain, with the New Technologies for Neurorehabilitation Laboratory, Madrid, Spain, and also with the Universidad de Cádiz, 11003 Cádiz, Spain (e-mail: javier.badesa@uca.es).

Simona Crea and Nicola Vitiello are with the BioRobotics Institute, Scuola Superiore Sant’Anna, 56025 Pontedera, Italy, with the Department of Excellence in Robotics & AI, Scuola Superiore Sant’Anna, 56127 Pisa, Italy, and also with the IRCCS Fondazione Don Carlo Gnocchi, 50143 Florence, Italy (e-mail: simona.crea@santannapisa.it; nicola.vitiello@santannapisa.it).

Digital Object Identifier 10.1109/JSYST.2020.3021485

and quantified as SMR event-related desynchronization (SMR-ERD).

It was demonstrated that also stroke patients with cortical lesions and severe or complete finger paralysis are able to operate such brain/neural-controlled system, i.e., to drive an orthotic device opening and closing their paralyzed hands [7], [11].

While studies on upper limb motor function after stroke found that distal weakness, particular of finger movements, is more profound than shoulder and elbow weakness [12], motor compensation associated with learned nonuse, joint contractures, and pain [5], [13] may further affect whole-arm motor function.

Using an active hand exoskeleton, stroke survivors may be capable of securely grasping and holding different objects of daily living, but may remain unable to lift up and move these objects. Grasping a glass and drinking, for example, requires hand function and whole arm motor coordination for reaching and grasping a cup before guiding it to the mouth for drinking.

Therefore, we developed a novel brain/neural-controlled whole-arm exoskeleton actuating the shoulder, elbow and hand to assist in ADLs [14]. It was unclear, however, whether chronic stroke patients with upper-limb paraparesis could use such brain/neural-controlled system to perform a complex task, e.g., grasping and drinking from a glass of water. The ability to perform such task would be very important, however, to broaden the scope of assistive brain/neural exoskeletons toward restoration of ADLs in everyday life environments [15].

Here, we investigated feasibility, safety, and user-friendliness of EEG/electrooculography (EOG)-based brain/neural robot control after chronic stroke to operate a vision-guided semi-autonomous whole-arm exoskeleton for restoration of ADLs.

II. METHODS

The EEG/EOG-controlled semiautonomous whole-arm exoskeleton comprised the following components and control modules.

A. Whole-Arm Exoskeleton

The whole-arm exoskeleton consisted of two submodules: the newly developed shoulder-elbow exoskeleton NeuroExos Shoulder-elbow Module β (NESM β , which evolved from NESM α [16]) combined with a wrist-hand exoskeleton described in [17].

The novel second generation shoulder-elbow exoskeleton (NESM β , Fig. 1) [18] features several enhancements toward use for ADLs compared with previous versions, e.g., used in [14]. Foremost, the NESM β allows for mobile use because all elements were fully integrated into a wheelchair. Despite its compact design, essential requirements in terms of compliance, powerful actuation, and safe human-robot interaction are fulfilled. The self-aligning mechanism for improved comfort and wearability allows to follow the same passive movements of the shoulder complex as in NESM α , but integrated into a much more compact structure. The frame to fixate the shoulder-elbow exoskeleton into a wheelchair was customized and offers the possibility to have a battery-operated portable exoskeleton. Moreover, thanks to a flipping mechanism integrated in each



Fig. 1. Image of the NESM β that was fully integrated into a wheelchair for mobile use. The shoulder-elbow exoskeleton can be flipped so that either the left or right upper extremity becomes mobilized.

joint allowing to manually change the arm configuration, the NESM β can mobilize the left or right upper extremity while the previous version could only mobilize the right arm and hand. The mechanical structure of the arm exoskeleton comprised four series-elastic actuation (SEA) units to realize shoulder abduction/adduction (SAA), shoulder flexion/extension (SFE), shoulder intra/extra rotation (SIE) and elbow flexion/extension (EFE). Relative to its zero-configuration with the arm laying parallel to the trunk, the four active joints allow for the following range of motions (ROMs): $[0^\circ, 85^\circ]$ sA/A and sF/E, $[-90^\circ, 30^\circ]$ sI/E and $[10^\circ, 100^\circ]$ eF/E. Additionally, the SEA units can deliver up to 35 Nm for SAA and SFE, and up to 15 Nm for SIE and EFE.

The wrist-hand exoskeleton was composed of a 1-DOF (degree-of-freedom) wrist module that performed the activation of the pronation/supination movement, and of a 4-DOFs hand exoskeleton that allowed for flexion/extension of the thumb, index, middle and ring finger as well as pinky, simultaneously [17]. The abduction/adduction of the thumb was fixed in a predefined position.

B. EEG/EOG Control Interface

EEG was recorded from five conventional recording sites over motor cortical areas of the patient's ipsilesional hemisphere (dependent on the lesion location either F3, T3, C3, Cz, and P3, or F4, T4, C4, Cz, and P4 according to the international 10/20 system). Two additional electrodes were placed at the left and right outer canthus for EOG recordings. Reference and ground electrode were placed at FCZ and FpZ, respectively. All biosignals were sampled at 1 kHz and amplified by a wireless passive-electrode EEG system (LiveAmp, Brain Products

GmbH, Gilching, Germany). Passive polyamide-based solid-gel electrodes [19] were used to provide high wearing comfort and to make hair washing after the experimental session obsolete, a critical point to increase user-friendliness of EEG recordings in patient populations with severe paralysis.

For online processing and classification, the BCI2000 software platform was used [20]. EEG signals were first bandpass-filtered at 1–30 Hz to remove drifts and high frequency noise. Afterwards, surface Laplacian filters were applied to increase signal-to-noise ratio of the targeted electrodes at C3 or C4. Surface Laplacian filtering was shown to be very effective in allowing for specific SMR-ERD detection while suppressing signal modulations due to distant sources (e.g., eye blinks) [21]. Ipsilesional SMR-ERD during the attempt to open or close the right or left hand was calculated based on the power method by Pfurtscheller and Lopez da Silva [22]. In order to remove low-frequency drifts as well as high frequency noise, EOG signals were bandpass-filtered at 0.1–5 Hz.

C. High-Level Control Strategies

For user intention detection and control of the whole-arm exoskeleton, a shared-human robot control strategy based on a finite-state machine (FSM) was adopted. In this article, the FSM allowed the user to effectively perform the drinking task by taking the inputs from the recording devices and by controlling the whole-arm exoskeleton accordingly. In particular, the FSM controlled the transition between the subtasks as triggered by the user's biosignals [14]. In contrast to Crea *et al.* [14], there were no time constraints during activation of the interface.

A central server (based on the Yet Another Robotic Platform messaging system, YARP) managed the communication between all modules.

D. Low-Level Control Strategies

The shoulder-elbow exoskeleton motion was planned by means of a learning by demonstration (LbD) approach based on dynamic movement primitives (DMPs), with a well-defined landscape attractor [23]–[25]. This attractor allowed replicating the recorded trajectory through a weighted sum of optimally spaced Gaussian Kernels. As for a typical LbD method, trajectories performed by a demonstrator were first recorded in the joint space during the execution of ADLs by healthy subject wearing the exoskeleton (i.e., a hands-on approach was applied). Subsequently, distinctive features (called DMP parameters) were extracted using the locally weighted regression algorithm and used to train a neural network (NN) that learned the motion features and the robot's inverse kinematics. In particular, the NN was trained through the Levenberg–Marquardt supervised learning algorithm in order to associate DMP parameters and robot joint target positions to context factors taken as input (i.e., object position and task to be performed).

Thereafter, provided successful detection of the appropriate biosignal, the trained NN provided the proper set of DMP parameters and robot joint target positions for computing the set of DMPs that best fitted the desired task.

TABLE I
DEMOGRAPHIC AND CLINICAL DATA OF STROKE SURVIVORS

	P1	P2	P3	P4	P5
Age	52	49	60	39	69
Gender	M	M	M	M	F
Time from injury (yrs.)	1	6	3	5	16
Impaired limb	Right	Left	Left	Left	Left
FMA S-E-F	28	32	26	29	19
FMA W-H	17	15	9	7	16

For both the shoulder-elbow and wrist-hand exoskeletons, a position control in the joint space was adopted to drive the joint positions along a reference value or trajectory.

E. Participants

Five poststroke patients with severe hemiparesis (time since injury: 6.2 ± 5.8 years) were invited to a 2 h experimental session at the Campus Bio-Medico University of Rome, Italy. Detailed information for each stroke survivor is provided in Table I. Besides demographic data, the side of the hemiparesis as well as the upper-extremity Fugl-Meyer Assessment (FMA) score for the shoulder, elbow and forearm subsection (FMA S-E-F) and for the wrist and hand subsection (FMA W-H) are listed. While the stroke lesion in one participant affected left fronto-parieto-temporal areas, stroke lesions of the other four participants affected the right fronto-parieto-temporal areas. The lesion location was determined based on clinical magnetic resonance imaging.

All participants provided written informed consent before entering the study. The study protocol was in line with the Declaration of Helsinki and was approved by the local ethics committee (Comitato Etico Università Campus Biomedico di Roma, reference number: 01/17 PAR ComEt CBM) and by the Italian Ministry of Health (Registro - classif. DGDMF/I.5.i.m.2/2016/1096).

F. Experimental Setup, Control Paradigm, and Protocol

The study participants were comfortably seated into a wheelchair placed in front of a table where the cup was positioned (Fig. 2). Once the participants were equipped with the biosignal recording devices, EEG/EOG control signals were individually calibrated in [14]. For EOG calibration, the participants were instructed to perform five short horizontal oculoversions (HOVs) to each side. Based on the recorded EOG signals, an individual HOV detection threshold was computed. Afterwards, a SMR-ERD detection threshold was determined based on randomly presented externally paced instructions indicating either the attempt to move the paralyzed hand or to rest. For robust threshold estimation, a total of 42 trials were performed. Each calibration trial lasted 5 s with an inter trial interval of 4 s. To find an optimal SMR-ERD threshold, a

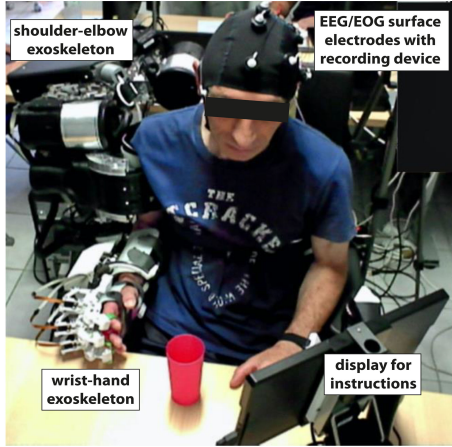


Fig. 2. Experimental setup. The hemiparetic stroke survivors were sitting in a wheelchair equipped with a whole-arm exoskeleton mounted to the patient's paretic arm and hand. EEG and EOG were recorded using surface electrodes attached to the participant's head. In order to calculate reliability and fluent control, participants received visual instructions shown on a display in front of them.

band-pass filter (± 3 Hz) was applied to the frequency showing highest SMR-ERD modulation within the SMR frequency range (8–12 Hz). The SMR-ERD threshold was then set at the two above-mentioned standard deviations the average SMR power during activation. All calibration parameters were determined at the beginning of the session and remained unaltered.

After calibration, all participants received detailed instructions about the experimental paradigm and design once more, and were familiarized with the EEG/EOG control paradigm. After familiarization, all participants were instructed to perform a total of 15 drinking tasks. Each task consisted of the following subtasks (defined by states of the FSM): i) performing HOV to trigger the shoulder-elbow unit to reach the cup. The position of the cup was *a priori* determined by an RGB-D camera; ii) continuously closing the hand exoskeleton by generating SMR-ERD exceeding the SMR-ERD detection threshold to grasp and lift the cup. Once lifted, the cup was autonomously guided to the user's mouth; iii) performing HOV to placing back the cup on the table iv) opening the hand by generating a SMR-ERD exceeding the SMR-ERD detection threshold to release the glass and go back to neutral state (Table II).

During online control within the FSM-states ii) and iv), SMR-ERD modulations were continuously translated into hand opening or closing movements as long as the SMR-ERD threshold was exceeded. Relationship between the time the SMR-ERD detection threshold was exceeded and exoskeleton movements was linear to increase the degree and intuitiveness of control (Fig. 3). This constitutes an important advancement compared to previous studies in which SMR-ERD was used as a trigger for movement initiation in [14]. A full hand exoskeleton opening

TABLE II
BMI CONTROL COMMANDS TO INITIALIZE AND EXECUTE DRINKING TASK

FSM-states	Sub-tasks of drinking	EEG/EOG control command
i.	Reaching the cup	HOV
ii.	Grasping, lifting, moving the cup to the mouth and drinking	SMR-ERD
iii.	Placing back the cup	HOV
iv.	Releasing the cup and moving back to the initial position	SMR-ERD

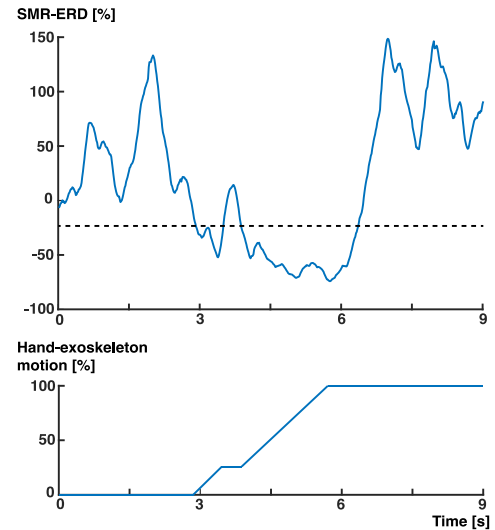


Fig. 3. Upper panel:SMR, 8–13 Hz event-related desynchronization SMR-ERD over time (blue solid line). The black dashed line represents the SMR-ERD detection threshold for hand exoskeleton opening or closing movements determined during calibration. Lower panel: Course of full hand exoskeleton closing motion related to the time the SMR-ERD detection threshold was exceeded (linear relationship).

or closing motion was achieved when the SMR-ERD detection threshold was exceeded for a time of 3 s in total.

At any given moment, participants were able to stop (veto) the ongoing action/subtask by performing HOV and reset the whole-arm exoskeleton to neutral state.

G. Offline Data Analysis

“Time to initialize” (TTI) each subtask was evaluated as time between visual indication to initialize the subtask and detection of the appropriate biosignal, i.e., SMR-ERD or HOV, respectively. Fluent control was assumed when average TTI ranged below 3 s [14]. Reliable control was assumed when at least 75% successful initializations were performed within 3 s. Feasibility

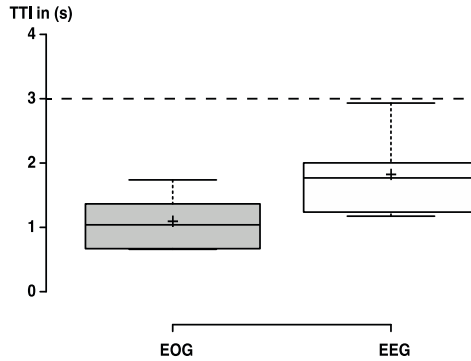


Fig. 4. TTI EOG/EOG control commands. Average TTI ranged below 3s (dashed line) documenting fluent control across both control modalities. Center-lines of boxplot show median, while crosses show the mean. Box limits indicate the 25th and 75th percentiles.

of successful EEG/EOG brain/neural robot control after chronic stroke was assumed if the criteria for reliable and fluent control were met. After the session, user-friendliness and safety aspects were assessed by a five-level Likert scale questionnaire.

III. RESULTS

A. Feasibility

While average TTIs (\pm s.d.) of all EEG-controlled closing and opening hand-exoskeleton motions ranged at 1.82 ± 0.71 s (median = 1.77 s [interquartile range = 1.22–2.24 s]), EOG-controlled commands were initialized in average after 1.09 ± 0.46 s (median = 1.04 s [0.67–1.46 s]) (Fig. 4). 75% successful EEG/EOG-controlled task executions were performed within 1.88 s in average (median = 1.80 s) documenting reliable brain/neural robot control (Fig. 5 shows TTIs for each control modality). Complete hand exoskeleton closing and opening motions required in average 5.79 ± 1.18 s (median = 5.51 s [4.87–6.43 s]).

B. User-Friendliness and Safety

User-friendliness of the system was rated at $87 \pm 21\%$ of the maximum achievable score documenting a very good user experience. With $91 \pm 20\%$ of the maximum achievable score, also system safety was rated as very high by the hemiparetic participants.

Most importantly, none of the stroke survivors reported any side effects or adverse events during the use of the system (such as discomfort or pain). The preparation and mounting procedure were evaluated as comfortable and the participants reported that the calibration instructions were easy to follow. After familiarization, all participants felt safe during the drinking paradigm (Table III).

IV. DISCUSSION

Up to one-third of all stroke survivors suffer from chronic motor deficits that impede their ability to perform ADLs [26], [27]. Driven by recent advancements in the field of wearable robotics and noninvasive neurotechnologies, brain/neural-controlled exoskeletons represent a promising tool to restore intuitive control of movements after stroke. While it was shown that EEG/EOG-based brain/neural control paradigms can be used to restore the ability to eat and drink independently after high cervical spinal cord injury [6], it remained unclear whether chronic stroke patients with severe upper-limb paralysis and different levels of chronicity (1–16 years poststroke) are capable of using such paradigm to reliably operate a semiautonomous whole-arm exoskeleton assisting in ADLs, such as grasping a cup and drinking. Thus, the primary aim of this article was to demonstrate feasibility, safety, and user-friendliness of a noninvasive brain/neural whole-arm exoskeleton for upper limb movement restoration across five chronic stroke patients engaging in a drinking task. Due to the limited bandwidth of EEG-based robotic control (typically allowing for real-time classification of up to three features only, e.g., open versus close, hand versus foot movements, or rest), the drinking task was divided into several subtasks using a FSM and coupled with a context-aware (vision-guided) actuator system. This considerably reduced the amount of necessary control signals that have to be extracted from the stroke survivor's biosignals to execute the task, essentially reducing such information for detection of the target intention and a *veto* signal.

We found that all study participants were able to operate the semiautonomous brain/neural-controlled whole-arm exoskeleton and achieved reliable and fluent control as tested during the drinking task. In average, more than 75% of successful task initializations were reached within 3 s (1.04 s for EOG and at 2.64 s for EEG) documenting reliable control, whereas the average TTI of all EEG/EOG-controlled operations ranged far below 3 reflecting fluent operation (EOG: 1.09 ± 0.46 s, EEG: 1.82 ± 0.71 s). There were no adverse effects reported and all participants felt safe to operate the system.

These results confirm that noninvasive EEG/EOG-based brain/neural robot control is a suitable strategy to restore ADLs in chronic stroke survivors with severe upper-limb motor deficits. While, in principle, EEG or EOG could be used for control of all tasks (e.g., EEG for reaching/retracting or EOG for opening/closing the hand), we reasoned that the chosen combination of EEG/EOG signals would provide a good balance between intuitiveness, reliability, and ease of use. One important rationale for the chosen combination is based on the source location and specificity of motor-related modulation of electric brain activity. Previous studies have shown that the cortical representation of finger and wrist muscles are larger and more lateralized than representations of shoulder and upper arm muscles [28]–[30]. Moreover, besides being more intuitive, EEG exoskeleton control could also trigger neural recovery [31], which makes EEG-control a potentially useful strategy in stroke neurorehabilitation [32]. However, EEG control is also more effortful and less reliable compared to EOG control. We thus

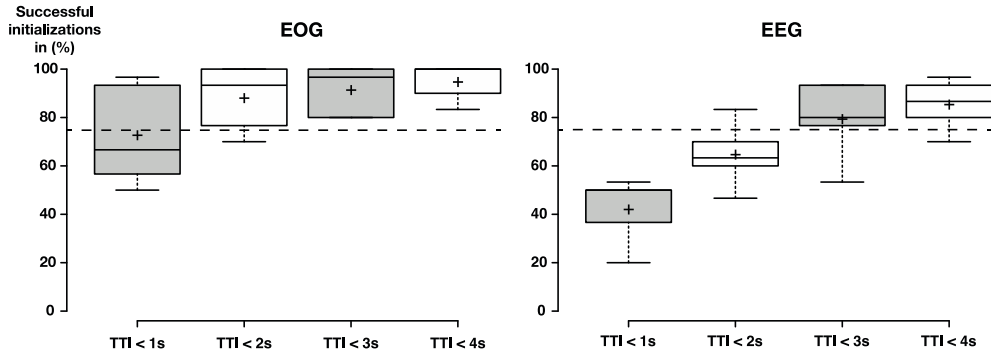


Fig. 5. Fluency of brain/neural robot control using EOG (left panel) and EEG (right panel) signals. Each boxplot summarizes the relative number of successful initializations with TTIs below discrete time intervals. Reliability was assumed when 75% of successful initializations were performed within 3 s (i.e., $TTI < 3s$, dashed line shows 75% threshold). For EOG control, the reliability criterium was met after 1.04 s in average (median = 1.16 s), while EEG control required 2.64 s in average (median = 2.56 s) to meet this criterium. Centerlines of boxplot show median, while crosses show the mean. Box limits indicate the 25th and 75th percentiles.

TABLE III
SUMMARY TABLE OF THE FIVE-LEVEL LIKERT SCALE QUESTIONNAIRE IN %.
(LIKERT SCALE FROM 1 = "STRONGLY AGREE"
TO 5 = "STRONGLY DISAGREE")

Likert Scale	1	2	3	4	5
I experienced side-effects or discomfort during the session	0	0	20	0	80
I felt comfortable with the whole-arm exoskeleton	20	60	20	0	0
Control of the exoskeleton was reliable and practical	60	20	0	20	0
After completing the training, I felt safe using the exoskeleton	80	20	0	0	0
The preparation/attaching process was comfortable	40	40	20	0	0
The calibration instructions were easy to follow	80	20	0	0	0
I felt discomfort/pain while electrodes/ exoskeleton were attached	0	0	0	0	100

reasoned that using EEG for hand opening/closing motions and EOG for reaching/retracting would offer the optimal balance between intuitiveness, reliability, and ease of use. Studies that further investigate the optimal control strategies depending on the purpose of brain/neural control (e.g., assistance in ADLs, neurorehabilitation, or a combination of both, [15]) will be necessary.

While all participants were able to modulate ipsilesional SMR-ERD it cannot be excluded that stroke survivors with extensive cortical lesions show limited or nonexistent ipsilesional SMR-ERD. In such case, calibration with a 64-channel high-density EEG might be necessary to identify remaining

SMR modulations specifically related to movement attempts with the paralyzed hand and finger.

In our study, all participants were brain-machine interface (BMI)-naïve, i.e., they have never engaged in any brain/neural robot control before. Nonetheless, they were all able to reliably perform the drinking task shortly after calibration and familiarization. All participants stated that the calibration instructions were easy to follow. This underlines the applicability and practicality of the presented brain/neural control paradigm to operate assistive robotic devices.

While realtime classification of EEG signals does not allow to reliably differentiate different grasp-types (i.e., palmar grasp, lateral pinch, etc.) or different movement trajectories, such information can be inferred or extrapolated—to some degree—by context-aware robotics. It is important, however, that in such shared-control paradigm a reliable *veto* function is implemented that allows the user to stop unwanted behavior of the robotic device [33]. Future neurotechnologies, e.g., using quantum sensors [34], [35], may overcome the current constraint of limited spatial resolution when recording brain oscillatory activity noninvasively.

While this article paves the way for larger clinical trials, it remains to be shown how our results can be generalized to multiple sessions and to other patient populations, e.g., with traumatic brain injury, multiple sclerosis, or progressive neurodegenerative disorders, such as amyotrophic lateral sclerosis.

Given that a number of randomized clinical trials suggest that repeated use of brain-controlled exoskeletons can trigger neural recovery [36], it is conceivable that the introduced paradigm will also improve adoption of brain-controlled robotics in the context of stroke neurorehabilitation [31]. Ideally, such device should be mounted [37] and operated by the hemiplegic stroke survivor without any assistance [15]. However, to achieve this, a number of technical challenges need to be solved. For instance, the whole-arm exoskeleton is currently integrated into a wheelchair because the gears and motors do not allow for portability. While this may be acceptable for patients who are unable to walk,

e.g., individuals with quadriplegia after brain stem stroke, the majority of stroke survivors are still capable of walking. Here, development of a fully portable and lightweight and modular soft-exoskeleton system [38] for the upper extremity might be a promising venue.

Another technical challenge relates to the EEG-cap. Most EEG electrodes are integrated into a textile cap that cannot be mounted without another person's assistance. Headsets using soft electrodes, e.g., based on felt or conductive polymers, that hemiplegic stroke survivors can put on unassisted are important prerequisites to broaden the applicability of brain/neural assistive systems. Here, minimizing the required recordings sites for brain/neural robot control, particularly from the face region as required for EOG recordings, would be particularly desirable [37].

Due to the heterogeneity of remaining motor functions, any strategy aiming at restoration of movement after stroke should be highly individualized and oriented toward specific individual needs [39], [40]. In this context, implementation of tools that allow for longitudinal quality-of-life assessment and tracking of the actual use of assistive systems in everyday life environments will be critical.

REFERENCES

- [1] G. B. D. S. Collaborators, "Global, regional, and national burden of stroke, 1990–2016: A systematic analysis for the global burden of disease study 2016," *Lancet Neurol.*, vol. 18, no. 5, pp. 439–458, May 2019, doi: [10.1016/S1474-4422\(19\)30034-1](https://doi.org/10.1016/S1474-4422(19)30034-1).
- [2] W. Rosamond *et al.*, "American heart association statistics committee and stroke statistics subcommittee. Disease and stroke statistics—2008 update: A report from the american heart association statistics committee and stroke statistics subcommittee," *Circulation*, vol. 117, no. 4, pp. e25–e146, 2008.
- [3] J. M. Veerbeek *et al.*, "What is the evidence for physical therapy poststroke? A systematic review and meta-analysis," (in English), *PLoS One*, vol. 9, no. 2, pp. e87987–e87987, 2014, doi: [10.1371/JOURNAL.PONE.0087987](https://doi.org/10.1371/JOURNAL.PONE.0087987).
- [4] S. M. Hatem *et al.*, "Rehabilitation of motor function after stroke: A multiple systematic review focused on techniques to stimulate upper extremity recovery," (in English), *Frontiers Human Neurosci.*, vol. 10, pp. 442–442, 2016, doi: [10.3389/FNHUM.2016.00442](https://doi.org/10.3389/FNHUM.2016.00442).
- [5] E. Taub, G. Uswatte, and R. Pidikiti, "Constraint-induced movement therapy: A new family of techniques with broad application to physical rehabilitation—a clinical review," *J. Rehabil. Res. Develop.*, vol. 36, no. 3, pp. 237–251, Jul. 1999. [Online]. Available: <https://www.ncbi.nlm.nih.gov/pubmed/10659807>.
- [6] S. R. Soekadar *et al.*, "Hybrid EEG/EOG-based brain/neural hand exoskeleton restores fully independent daily living activities after quadriplegia," *Sci. Robot.*, vol. 1, no. 1, 2016, Art. no. eaag3296. [Online]. Available: <http://robotics.sciencemag.org/content/1/1/eaag3296.abstract>.
- [7] E. Buch *et al.*, "Think to move: A neuromagnetic brain-computer interface (BCI) system for chronic stroke," *Stroke*, vol. 39, no. 3, pp. 910–917, Mar. 2008, doi: [10.1161/STROKEAHA.107.505313](https://doi.org/10.1161/STROKEAHA.107.505313).
- [8] S. Soekadar, N. Birbaumer, and L.G. Cohen, "Brain–computer interfaces in the rehabilitation of stroke and neurotrauma," *Systems Neuroscience and Rehabilitation*, K. Kansaku, L.G., Cohen, Eds. Berlin, Germany: Springer, 2011, pp. 3–18.
- [9] S. R. Soekadar, M. Witkowski, N. Vitiello, and N. Birbaumer, "An EEG/EOG-based hybrid brain-neural computer interaction (BCNI) system to control an exoskeleton for the paralyzed hand," *Biomed. Eng.*, vol. 60, no. 3, pp. 199–205, Jun. 2015, doi: [10.1515/BMFT-2014-0126](https://doi.org/10.1515/BMFT-2014-0126).
- [10] M. Witkowski, M. Cortese, M. Cempini, J. Mellinger, N. Vitiello, and S. R. Soekadar, "Enhancing brain-machine interface (BMI) control of a hand exoskeleton using electrooculography (EOG)," *J. Neuroeng. Rehabil.*, vol. 11, no. 1, Dec. 2014, Art. no. 165, doi: [10.1186/1743-0003-11-165](https://doi.org/10.1186/1743-0003-11-165).
- [11] S. R. Soekadar, M. Witkowski, J. Mellinger, A. Ramos, N. Birbaumer, and L. G. Cohen, "ERD-based online brain-machine interfaces (BMI) in the context of neurorehabilitation: optimizing BMI learning and performance," *IEEE Trans. Neural Syst. Rehabil. Eng.*, vol. 19, no. 5, pp. 542–549, Oct. 2011.
- [12] J. G. Colebatch and S. C. Gandevia, "The distribution of muscular weakness in upper motor neuron lesions affecting the arm," *Brain*, vol. 112, pp. 749–763, Jun. 1989, doi: [10.1093/brain/112.3.749](https://doi.org/10.1093/brain/112.3.749).
- [13] L. M. Pain, R. Baker, D. Richardson, and A. M. Agur, "Effect of trunk-restraint training on function and compensatory trunk, shoulder and elbow patterns during post-stroke reach: A systematic review," *Disability Rehabil.*, vol. 37, no. 7, pp. 553–562, 2015, doi: [10.3109/09638288.2014.932450](https://doi.org/10.3109/09638288.2014.932450).
- [14] S. Crea *et al.*, "Feasibility and safety of shared EEG/EOG and vision-guided autonomous whole-arm exoskeleton control to perform activities of daily living," *Sci. Rep.*, vol. 8, no. 1, Jul. 2018, Art. no. 10823, doi: [10.1038/s41598-018-29091-5](https://doi.org/10.1038/s41598-018-29091-5).
- [15] S. R. Soekadar *et al.*, "Restoration of finger and arm movements using hybrid brain/neural assistive technology in everyday life environments," in *Brain-Computer Interface Research. A State-of-the-Art Summary*, T. N. M.-K. Christoph Guger, B. Z. Allison, Eds. Berlin, Germany: Springer, 2019, ch. 5, pp. 53–61.
- [16] E. Trigili *et al.*, "Design and experimental characterization of a shoulder-elbow exoskeleton with compliant joints for post-stroke rehabilitation," *IEEE/ASME Trans. Mechatronics*, vol. 24, no. 4, pp. 1485–1496, Aug. 2019.
- [17] J. A. Diez, A. Blanco, J. M. Catalán, F. J. Badesa, L. D. Lledó, and N. Garcia-Aracil, "Hand exoskeleton for rehabilitation therapies with integrated optical force sensor," *Adv. Mech. Eng.*, vol. 10, no. 2, pp. 1–11, 2018.
- [18] G. Ercolini, E. Trigili, A. Baldoni, S. Crea, and N. Vitiello, "A novel generation of ergonomic upper-limb wearable robots: Design challenges and solutions," *Robotica*, vol. 37, no. 12, pp. 2056–2072, Aug. 2019.
- [19] S. Toyama, K. Takano, and K. Kansaku, "A non-adhesive solid-gel electrode for non-invasive brain-machine interface," (in English), *Frontiers Neurol.*, vol. 3, no. 114, Jul. 2012, pp. 1–8, doi: [10.3389/FNEUR.2012.00114](https://doi.org/10.3389/FNEUR.2012.00114).
- [20] G. Schalk, D. J. McFarland, T. Hinterberger, N. Birbaumer, and J. R. Wolpaw, "BCI2000: A general-purpose brain-computer interface (BCI) system," *IEEE Trans Biomed. Eng.*, vol. 51, no. 6, pp. 1034–1043, Jun. 2004.
- [21] D. J. McFarland, "The advantages of the surface Laplacian in brain-computer interface research," *Int. J. Psychophysiol.*, vol. 97, no. 3, pp. 271–276, Sep. 2015, doi: [10.1016/J.IJPYSCHO.2014.07.009](https://doi.org/10.1016/J.IJPYSCHO.2014.07.009).
- [22] G. Pfurtscheller and H. D. Lopes da Silva, "Event-related EEG/MEG synchronization and desynchronization: Basic principles," *Clin. Neurophysiol.*, vol. 110, no. 11, pp. 1842–1857, Nov. 1999, doi: [http://dx.doi.org/10.1016/S1388-2457\(99\)00141-8](https://doi.org/http://dx.doi.org/10.1016/S1388-2457(99)00141-8).
- [23] C. Lauretti *et al.*, "Learning by demonstration for motion planning of upper-limb exoskeletons," *Frontiers Neurorobot.*, vol. 12, 2018, pp. 1–14, doi: [10.3389/FBOT.2018.00005](https://doi.org/10.3389/FBOT.2018.00005).
- [24] A. J. Ijspeert, J. Nakanishi, H. Hoffmann, P. Pastor, and S. Schaal, "Dynamical movement primitives: Learning attractor models for motor behaviors," *Neural Comput.*, vol. 25, no. 2, pp. 328–373, 2013.
- [25] M. I. Lourakis, "A brief description of the Levenberg-Marquardt algorithm implemented by levmar," *Found. Res. Technol.*, vol. 4, no. 1, pp. 1–6, 2005.
- [26] C. D. Wolfe *et al.*, "Estimates of outcomes up to ten years after stroke: Analysis from the prospective South London Stroke Register," *PLoS Med.*, vol. 8, no. 5, May 2011, Art. no. e1001033, doi: [10.1371/JOURNAL.PMED.1001033](https://doi.org/10.1371/JOURNAL.PMED.1001033).
- [27] T. Ullberg, E. Zia, J. Petersson, and B. Norrving, "Changes in functional outcome over the first year after stroke: An observational study from the Swedish stroke register," *Stroke*, vol. 46, no. 2, pp. 389–394, Feb. 2015, doi: [10.1161/STROKEAHA.114.006538](https://doi.org/10.1161/STROKEAHA.114.006538).
- [28] W. Penfield and E. Boldrey, "Somatic motor and sensory representation in the cerebral cortex of man as studied by electrical stimulation," *Brain*, vol. 60, no. 4, pp. 389–443, 1937.
- [29] M. H. Schieber, "Constraints on somatotopic organization in the primary motor cortex," *J. Neurophysiol.*, vol. 86, no. 5, pp. 2125–2143, 2001.
- [30] A. Stancak, Jr., B. Feige, C. H. Lucking, and R. Kristeva-Feige, "Oscillatory cortical activity and movement-related potentials in proximal and distal movements," *Clin. Neurophysiol.*, vol. 111, no. 4, pp. 636–650, Apr. 2000, doi: [10.1016/S1388-2457\(99\)00310-7](https://doi.org/10.1016/S1388-2457(99)00310-7).
- [31] S. R. Soekadar, N. Birbaumer, M. W. Slutsky, and L. G. Cohen, "Brain-machine interfaces in neurorehabilitation of stroke," *Neurobiol. Disease*, vol. 83, pp. 172–179, Nov. 2015, doi: [10.1016/j.nbd.2014.11.025](https://doi.org/10.1016/j.nbd.2014.11.025).

- [32] J. Ushiba and S. R. Soekadar, "Brain-machine interfaces for rehabilitation of poststroke hemiplegia," *Prog. Brain Res.*, vol. 228, pp. 163–183, 2016, doi: [10.1016/bs.pbr.2016.04.020](https://doi.org/10.1016/bs.pbr.2016.04.020).
- [33] J. Clausen *et al.*, "Help, hope, and hype: Ethical dimensions of neuromodulation," *Science*, vol. 356, no. 6345, pp. 1338–1339, Jun. 2017, doi: [10.1126/science.aam7731](https://doi.org/10.1126/science.aam7731).
- [34] J. Iivanainen, M. Stenroos, and L. Parkkonen, "Measuring MEG closer to the brain: Performance of on-scalp sensor arrays," *NeuroImage*, vol. 147, pp. 542–553, Feb. 2017, doi: [10.1016/j.neuroimage.2016.12.048](https://doi.org/10.1016/j.neuroimage.2016.12.048).
- [35] E. Boto *et al.*, "Moving magnetoencephalography towards real-world applications with a wearable system," *Nature*, vol. 555, no. 7698, pp. 657–661, Mar. 2018, doi: [10.1038/nature26147](https://doi.org/10.1038/nature26147).
- [36] M. A. Cervera *et al.*, "Brain-computer interfaces for post-stroke motor rehabilitation: A meta-analysis," *Ann. Clin. Translational Neurol.*, vol. 5, no. 5, pp. 651–663, May 2018, doi: [10.1002/acn3.544](https://doi.org/10.1002/acn3.544).
- [37] A. Cavallo *et al.*, "Minimizing bio-signal recording sites for noninvasive hybrid brain/neural control," *IEEE Syst. J.*, to be published, doi: [10.1109/SYST.2020.3021751](https://doi.org/10.1109/SYST.2020.3021751).
- [38] L. N. Awad *et al.*, "A soft robotic exosuit improves walking in patients after stroke," *Sci. Translational Med.*, vol. 9, no. 400, Jul. 2017, pp. 2182–2197, doi: [10.1126/scitranslmed.aai9084](https://doi.org/10.1126/scitranslmed.aai9084).
- [39] M. Coscia *et al.*, "Neurotechnology-aided interventions for upper limb motor rehabilitation in severe chronic stroke," *Brain*, vol. 142, no. 8, pp. 2182–2197, Aug. 2019, doi: [10.1093/brain/awz181](https://doi.org/10.1093/brain/awz181).
- [40] S. Hazubski, S. R. Soekadar, H. Hoppe, and A. Otte, "Neuroprosthetics 2.0," *EBioMed*, vol. 48, Oct. 2019, Art. no. 22, doi: [10.1016/j.ebiom.2019.09.036](https://doi.org/10.1016/j.ebiom.2019.09.036).

2.3 Feasibility and safety of bilateral hybrid EEG/EOG brain/neural-machine interaction

Nann, M., Peekhaus, N., Angerhöfer, C., Soekadar, S. R. (2020). Feasibility and Safety of Bilateral Hybrid EEG/EOG Brain/Neural-Machine Interaction. *Frontiers in Human Neuroscience*, 14(521), 580105.



Feasibility and Safety of Bilateral Hybrid EEG/EOG Brain/Neural–Machine Interaction

Marius Nann^{1,2}, Niels Peekhaus^{1,2}, Cornelius Angerhöfer^{1,2} and Surjo R. Soekadar^{1,2*}

¹ Clinical Neurotechnology Lab, Charité – University Medicine Berlin, Berlin, Germany, ² Applied Neurotechnology Lab, University Hospital Tübingen, Tübingen, Germany

OPEN ACCESS

Edited by:

Cuntai Guan,
Nanyang Technological University,
Singapore

Reviewed by:

Ashraf S. Gorgey,
Hunter Holmes McGuire VA Medical
Center, United States
Jianjun Meng,
Shanghai Jiao Tong University, China

*Correspondence:

Surjo R. Soekadar
surjo.soekadar@charite.de

Specialty section:

This article was submitted to
Brain-Computer Interfaces,
a section of the journal
Frontiers in Human Neuroscience

Received: 06 July 2020

Accepted: 09 November 2020

Published: 09 December 2020

Citation:

Nann M, Peekhaus N,
Angerhöfer C and Soekadar SR
(2020) Feasibility and Safety
of Bilateral Hybrid EEG/EOG
Brain/Neural–Machine Interaction.
Front. Hum. Neurosci. 14:580105.
doi: 10.3389/fnhum.2020.580105

Cervical spinal cord injuries (SCIs) often lead to loss of motor function in both hands and legs, limiting autonomy and quality of life. While it was shown that unilateral hand function can be restored after SCI using a hybrid electroencephalography/electrooculography (EEG/EOG) brain/neural hand exoskeleton (B/NHE), it remained unclear whether such hybrid paradigm also could be used for operating two hand exoskeletons, e.g., in the context of bimanual tasks such as eating with fork and knife. To test whether EEG/EOG signals allow for fluent and reliable as well as safe and user-friendly bilateral B/NHE control, eight healthy participants (six females, mean age 24.1 ± 3.2 years) as well as four chronic tetraplegics (four males, mean age 51.8 ± 15.2 years) performed a complex sequence of EEG-controlled bilateral grasping and EOG-controlled releasing motions of two exoskeletons visually presented on a screen. A novel EOG command performed by prolonged horizontal eye movements (>1 s) to the left or right was introduced as a reliable switch to activate either the left or right exoskeleton. Fluent EEG control was defined as average “time to initialize” (TTI) grasping motions below 3 s. Reliable EEG control was assumed when classification accuracy exceeded 80%. Safety was defined as “time to stop” (TTS) all unintended grasping motions within 2 s. After the experiment, tetraplegics were asked to rate the user-friendliness of bilateral B/NHE control using Likert scales. Average TTI and accuracy of EEG-controlled operations ranged at 2.14 ± 0.66 s and $85.89 \pm 15.81\%$ across healthy participants and at 1.90 ± 0.97 s and $81.25 \pm 16.99\%$ across tetraplegics. Except for one tetraplegic, all participants met the safety requirements. With $88 \pm 11\%$ of the maximum achievable score, tetraplegics rated the control paradigm as user-friendly and reliable. These results suggest that hybrid EEG/EOG B/NHE control of two assistive devices is feasible and safe, paving the way to test this paradigm in larger clinical trials performing bimanual tasks in everyday life environments.

Keywords: bilateral exoskeleton control, bimanual tasks, EEG, EOG, brain-computer interface, BCI, brain-machine (computer) interface

INTRODUCTION

Cervical spinal cord injuries (SCIs) often result in loss of motor function in all four extremities. According to the National Spinal Cord Injury Statistical Center (NSCISC), 41.1% of all SCIs lead to complete or incomplete tetraplegia (National Spinal Cord Injury Statistical Center, 2019). While the inability to walk is usually sufficiently compensated by use of a wheelchair (Rushton et al., 2010),

restoration of hand and arm function is still insufficiently solved. Therefore, restoration of hand and arm function is of highest priority in this patient population (Anderson, 2004; Snock et al., 2004; Lo et al., 2016). Depending on the SCI's location, the degree of impairment and related motor abilities can vary substantially. In particular, injuries between the spinal motion sections C5 and C7 are characterized by some remaining motor function in the shoulder and arm but absence of movements in the wrist and fingers (Ahuja et al., 2017). For these cases, restoration of hand function would be an important goal to regain autonomy and to improve quality of life (Campbell et al., 1999).

To date, the most common methods for restoration of upper limb motor function are surgical interventions (Bunketorp-Käll et al., 2017). To a certain degree, upper limb reconstructive surgeries, such as tendon transfers or tenodesis (Bednar and Woodside, 2018), can restore arm and hand function in SCI. However, besides the risks associated with surgery, tendon transfer strongly depends on the availability and quality of tendons and muscles suitable for transfer. While tenodesis enables tetraplegics to passively grasp objects through extension of the wrist (termed tenodesis grasp), the resulting grasping force is often insufficient to perform basal activities of daily living (ADLs), e.g., lifting up a water bottle, zipping a jacket, or reliably holding cutlery for eating (Dunn et al., 2016).

As an alternative to surgical interventions, recent advancements in neurotechnology and robotics opened up new possibilities to restore hand and arm function after cervical SCI (Soekadar et al., 2016) or stroke (Soekadar et al., 2008, 2015a; Nann et al., 2020). It was shown that exoskeletons or functional electrical stimulation (FES) of paralyzed muscles can enhance grasping force and improve hand function in tetraplegics (Ragnarsson, 2008; Ho et al., 2014; Yun et al., 2017; Cappello et al., 2018). A very intuitive way to control such assistive devices can be achieved by using a brain-computer interface (BCI; Wolpaw et al., 2002; Collinger et al., 2013a). BCIs translate electric, magnetic, or metabolic brain activity, e.g., associated with motor imagery (MI) or the attempt to move the paralyzed fingers, into control signals of digital devices, e.g., a robotic arm (Hochberg et al., 2012; Collinger et al., 2013b), exoskeleton (Soekadar et al., 2016; Tang et al., 2016; Frolov et al., 2017; Benabid et al., 2019), or FES device (Osuagwu et al., 2016; Vidaurre et al., 2016). Besides providing assistance, it was shown that repeated BCI use following SCI can also trigger neural recovery (Donati et al., 2016). Several studies showed that BCI-controlled FES can restore hand movement (Bouton et al., 2016; Vidaurre et al., 2016; Ajiboye et al., 2017). However, it is noteworthy that persons with SCI can develop upper extremity spasticity (Holtz et al., 2017; Gohritz and Fridén, 2018). In such cases, effective restoration of hand function via FES may not be successful due to increased muscle tone and tendon contractures. In contrast, a BCI-controlled hand exoskeleton, which actively opens and closes the affected hand, can overcome such limitations and may, thus, be superior to BCI-controlled FES. Within the last years, several robotic devices have entered the commercial market including three exoskeletons that were specifically designed for SCI patients (Mekki et al., 2018). Although still rather cost-intensive, new

3D-printed designs may yield low-cost hand exoskeletons in the near future (Yoo et al., 2019).

The most common approach for non-invasive brain/neural control of an exoskeleton uses modulation of sensorimotor rhythms (SMRs, 8–12 Hz) quantified as event-related desynchronization (ERD; SMR-ERD; Pfurtscheller and da Silva, 1999; Soekadar et al., 2011). SMR-ERD modulations related to MI or attempted finger movements are most prominent over the hand knob area of the contralateral primary motor cortex. Using electroencephalography (EEG), the optimal position to record SMR-ERD is typically at electrode positions C3 or C4 (according to the international 10/20 system; Neuper et al., 2006). Recently, it was demonstrated that a SMR-based brain/neural hand exoskeleton (B/NHE) can fully restore unilateral hand function in tetraplegics in an everyday life environment, e.g., to eat and drink in an outside restaurant (Soekadar et al., 2016). To deal with the inherent low signal-to-noise ratio of EEG recordings in everyday life environments, a hybrid EEG/electrooculography (EEG/EOG) brain/neural-machine interaction (B/NMI) system has been successfully introduced (Soekadar et al., 2015b, 2016; Creel et al., 2018; Nann et al., 2020). To enhance BCI control in everyday life environments, maximal horizontal oculoversions (HOVs) assessed by EOG were integrated as an additional control signal to reduce false classifications (Witkowski et al., 2014; Soekadar et al., 2015b). While exoskeleton closing motions were controlled by SMR-ERD related to intended grasping movements, HOVs were translated into opening motions or veto commands to interrupt unintended closing motions.

To date, the majority of studies in clinical settings have mainly focused on the restoration of *unilateral* motor function (Alam et al., 2016; Carvalho et al., 2019; Coscia et al., 2019). Most ADLs, however, involve *bilateral* motor function, e.g., eating with fork and knife, opening a water bottle, or a bag of potato chips. While, for example, a unilateral B/NHE might be sufficient to restore bimanual ADLs in hemiplegic stroke patients, patients suffering from tetraplegia depend on mobilization of both hands and arms to execute bimanual tasks. Therefore, a reliable and safe control paradigm allowing intuitive operation of bilateral hand exoskeletons would be very desirable.

The goal of such a bilateral control paradigm is to reliably detect the user's attempt to operate either the left or right exoskeleton, both exoskeletons simultaneously, or none of them. This results in a four-class classification problem. The simplest approach to deal with such a multiclass problem is to implement a single classifier that differentiates between left and right hemispheric SMR-ERD (Meng et al., 2016; León, 2017; Lotte et al., 2018). Although Meng et al. (2016) demonstrated that this kind of classification method is feasible in principle, it requires sufficient lateralization of SMR-ERD to C3 and C4. Given that chronic tetraplegics often do not show such lateralization (Osuagwu et al., 2016; Dahlberg et al., 2018), such approach may not be suitable for reliable exoskeleton control in SCI. A possible solution to overcome the lack of lateralization in SCI patients is to introduce a reliable switch to activate either the left or right exoskeleton.

Here, we introduce a novel EOG command performed by prolonged HOV (>1 s; **Figure 3**) to the left or right and

tested whether use of such new command allows for reliable control of two hand exoskeletons. The prolonged HOV is not in conflict with the already established hybrid EEG/EOG paradigm according to Soekadar et al. (2016), where a *short* HOV (<1 s; **Figure 3**) is used to veto an ongoing exoskeleton opening or closing. To test the feasibility and safety of such novel bilateral EEG/EOG-based B/NMI control, eight healthy participants as well as four chronic tetraplegics performed a neurofeedback paradigm consisting of a complex sequence of bilateral grasping and releasing motions of two exoskeletons visually presented on a screen. In the following work, feasibility was defined as fluency and accuracy of bilateral EEG/EOG B/NHE control. While fluent control was defined as “time to initialize” (TTI) EEG-controlled operations in average below 3 s (i.e., valid SMR-ERDs were detected in average within 3 s; Crea et al., 2018), reliable control was defined as average classification accuracy above 80%, following the recommendation of Vidaurre and Blankertz (2010) and Ortner et al. (2015), e.g., when benchmarking common spatial patterns (CSPs). Safety requirements were met when all unintended closing motions were interrupted by using short HOV before the exoskeleton was fully closed. This means the “time to stop” (TTS) all unintended closing motions ranged within 2 s, the time of a full exoskeleton closing motion. Moreover, user-friendliness of bilateral control was assessed among tetraplegics by using a Likert scale.

MATERIALS AND METHODS

Participants

Eight BCI-naïve healthy participants (six females, mean age 24.1 ± 3.2 years) and four BCI-naïve chronic tetraplegics (four males, mean age 51.8 ± 15.2 years, time since injury > 2 years) with complete ($n = 2$; American Spinal Injury Association (ASIA), grade A) and incomplete ($n = 2$, ASIA grades B and C) SCI (injury location between C5 and C7) were invited to a single-session experiment at the University Hospital of Tübingen, Germany. Before entering the study, all participants provided written informed consent. The study protocol complied with the Declaration of Helsinki and was approved by University of Tübingen's local ethics committee (registration code of ethical approval: 201/2018BO1).

Experimental Setup and Biosignal Online Processing

Electroencephalography was recorded from nine conventional recording sites (F3, T3, C3, P3, F4, T4, C4, P4, and Cz) according to the international 10/20 system; **Figure 1**). Two additional EOG electrodes were placed laterally to the outer canthi of the left and right eye to assess HOVs (**Figures 1, 2**; Heide et al., 1999). A reference electrode was symmetrically placed over the sagittal midline at FCz to avoid biased electrical potentials toward one hemisphere (**Figure 1**). The ground electrode was located at Fpz (**Figure 1**). All biosignals were sampled at 1 kHz and amplified by a wireless active-electrode EEG system (actiCAP®, LiveAmp®, Brain Products GmbH, Gilching, Germany; **Figure 1**). To ensure high signal quality, all impedances were kept below $25\text{ k}\Omega$.

For online processing and classification, the BCI2000 software platform was used (Schalk et al., 2004). In order to attenuate eye blinks and other bihemispheric artifacts, bipolar EOG signal was calculated by subtracting left from right EOG. To remove low-frequency drifts as well as high-frequency noise, the bipolar EOG signal was then band-pass filtered with a first-order Butterworth filter at 0.02–3 Hz. To reduce the relatively long settling time that the low high-pass corner frequency at 0.02 Hz would have caused (>50 s), the band-pass filter was initialized with the mean value of the first processed sample block of the bipolar EOG signal. Such filter initialization drastically reduced the settling time to be applicable in online settings. The very low frequency content in the EOG signal allows to extract the quasi-rectangular curve shapes resulting from HOVs and thus ensures reliable detection of prolonged HOVs (i.e., threshold was exceeded for >1 s; **Figure 3**). EEG signals were first band-pass filtered with a first-order Butterworth filter at 1–30 Hz to remove baseline drifts and high-frequency noise. Afterward, surface Laplacian filters were applied to increase signal-to-noise ratio of the target electrodes at C3 and C4, respectively, (McFarland, 2015). A surface Laplacian filter was shown to be effective in detecting motor-specific SMR-ERD especially in online settings while suppressing distant sources (e.g., eye blinks) without the need for complex models, e.g., accounting for volume conduction. Subsequently, the power spectra of Laplace-filtered C3 and C4 EEG signals were estimated online from 500 ms moving

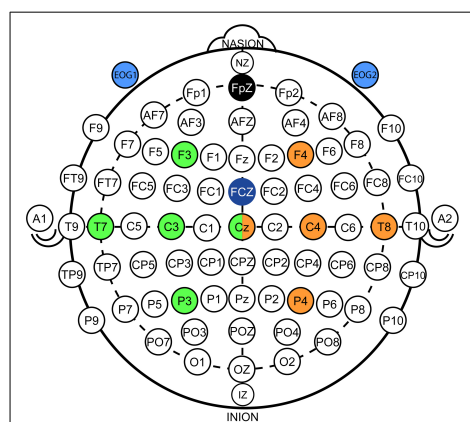
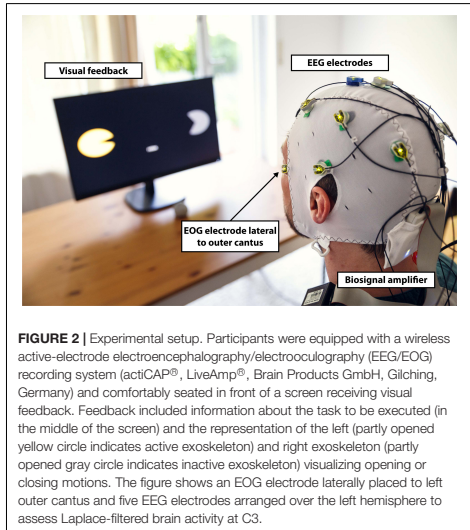


FIGURE 1 | Electroencephalography/electrooculography (EEG/EOG) electrode setup. EEG setup: Nine conventional EEG recording sites were used in accordance to the international 10/20 system. Five electrodes on each hemisphere were applied that were centered around C3 (green color coding) and C4 (orange color coding). Signals from Cz were used for both hemispheres. EOG setup: Two EOG electrodes (light blue color coding) were placed laterally to the outer canthi of the left and right eye to assess horizontal oculoversions (HOVs) based on the bipolar EOG signal (i.e., difference between EOG1 and EOG2). Ground and reference electrodes were placed at Fpz (black color coding) and FCz (dark blue color coding), respectively.



windows based on an autoregressive model of order 100 (Burg algorithm; Soekadar et al., 2011). Dependent on the optimal SMR frequency showing the largest modulation between 8 and 13 Hz during motor imagination/attempted finger movements vs. rest, the accumulated power of a 3-Hz bin around that modulation frequency [frequency of interest (FOI) \pm 1.5 Hz] was extracted. Lastly, SMR-ERD related to imagined or attempted right- or left-hand movements was computed according to the power method described by Pfurtscheller and Aranibar (1979):

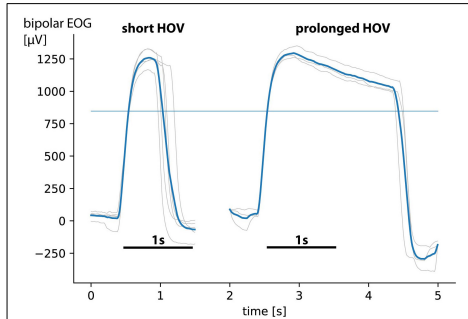
$$RV = \frac{1}{|T_{ref}|} \sum_{t \in T_{ref}} P_t \quad (1)$$

$$ERD(t) = \frac{P_t - RV}{RV} \times 100\% \quad (2)$$

where P_t is the estimated power of the 3-Hz-wide bin at every sample block t . RV is the reference value to normalize power P_t to receive the instantaneous $ERD(t)$ at every sample block t . Notably, to receive ERD related to Laplace-filtered C3 (C3-ERD) and C4 (C4-ERD) EEG signals, two identical SMR-ERD processing pipelines were implemented in parallel for online calculation.

Brain–Computer Interface Calibration and Familiarization

To calibrate HOV detection thresholds for each side, participants were instructed to perform 5 *short* as well as 3 *prolonged* HOVs to each side, respectively. HOV detection thresholds were set at $\pm 70\%$ of median single-trial EOG maxima and minima (median was selected to receive a more robust



estimation; **Figure 3**). To determine the C3- as well as C4-ERD detection thresholds, two calibration runs were conducted. During the first run, participants were instructed to either imagine (healthy participants)/attempt (tetraplegics) left or right finger movements (active phases) or to relax (rest phases) according to 20 externally paced randomized visual cues lasting 5 s each. After each active or rest phase, an intertrial interval (ITI) with a randomized length of 4–6 s followed. After the first run, FOI was set to the optimal SMR frequency, and RVs for C3 and C4 were determined as average power of the entire run including all active and rest phases as well as all ITIs. During the second run, which consisted of the same 20 visual cues, participants received online visual feedback based on their elicited SMR-ERD at C3 and C4. Finally, individual SMR-ERD detection thresholds were set to the average C3- and C4-ERD elicited within all active phases, respectively. After successful calibration, several familiarization runs were performed until the participant felt comfortable with all control commands.

Electroencephalography/Electrooculography-Based Bilateral Control Paradigm

The EEG/EOG-based bilateral control paradigm was implemented as a hierarchical classifier with two sequential binary classification stages. This is a common approach to decompose the multiclass classification problem into several binary classification problems (Lotte et al., 2018). At the first stage, a linear classifier detected *prolonged* HOVs either to the left or to the right to activate the respective exoskeleton. As soon as the HOV detection threshold was exceeded for longer than 1 s, the classifier recognized this as a volitional laterality switch and enabled the specific classifier at the second stage. Dependent on the selected exoskeleton, either C3- or C4-ERD was then continuously analyzed and translated

into closing motions as long as the laterality-specific ERD detection threshold was exceeded. The principle of this two-stage EEG/EOG-based hierarchical classifier is illustrated in **Figure 4A**. To open the closed exoskeleton or to interrupt (veto) an unintended closing motion, a *short* HOV to any direction reset the exoskeleton again. A *short* HOV was classified when HOV detection threshold was exceeded less than 1 s (see **Figure 3** for differences in HOV type). Such hybrid *short* EOG/EEG-based paradigm was already successfully applied in tetraplegics during unilateral hand exoskeleton control

(Soekadar et al., 2016). To ensure safety, *short* HOV commands had the highest priority to veto any ongoing action in case two EEG/EOG-based features were detected at the same time (see priority order in **Table 1**).

Study Protocol and Audiovisual Online Feedback

To test for feasibility and safety of the novel EEG/EOG-based bilateral control paradigm, healthy participants as well

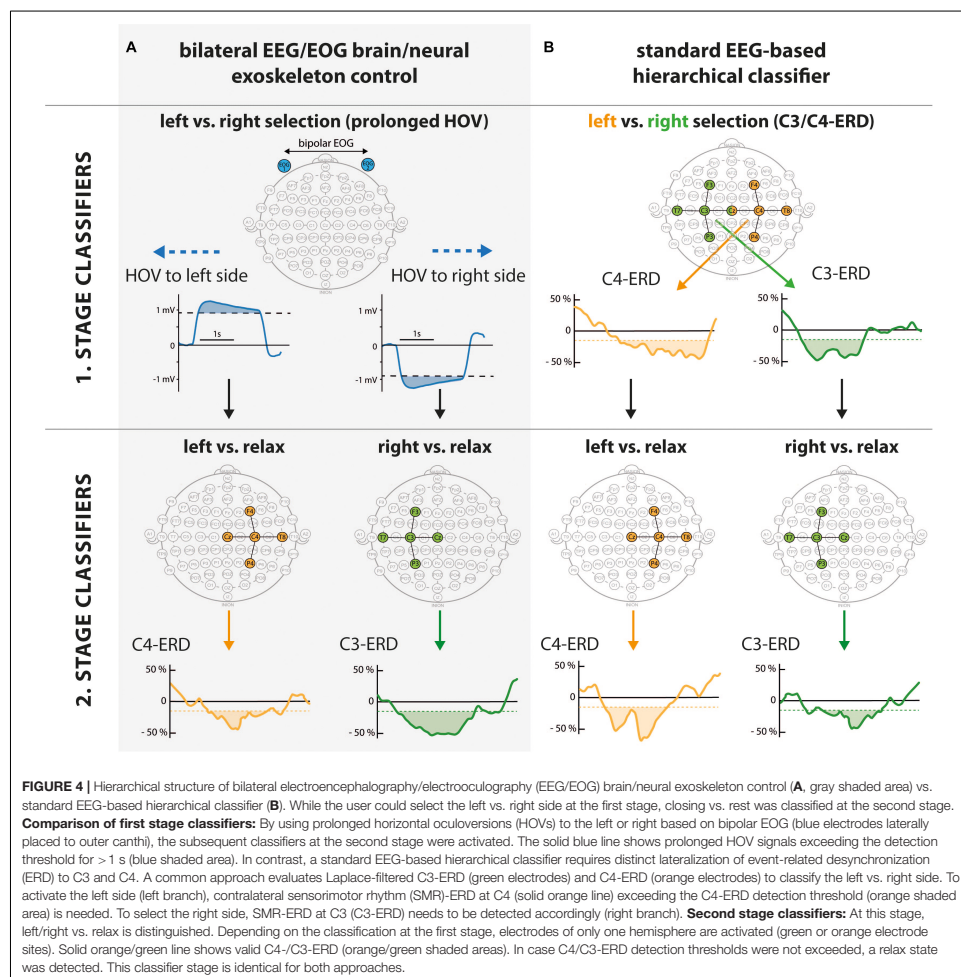
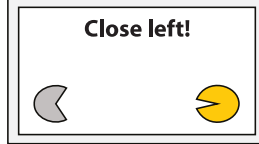
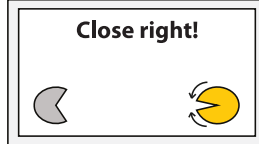


TABLE 1 | Overview of brain/neural-machine interface (B/NMI) control commands.

B/NMI control command	EEG/EOG-based feature	Respective task instruction with visual feedback
Interrupt closing motion	Short HOV toward any side Example: Short HOV to any side to interrupt (veto) the left ongoing exoskeleton motion	 
Open exoskeleton	Short HOV toward the direction of activated exoskeleton Example: Short HOV to the left to open left closed exoskeleton	 
Switch active exoskeleton	Prolonged HOV (> 1 s) toward desired hand exoskeleton Example: Before execute task instruction "Close left," prolonged HOV to the left is required to activate left exoskeleton	 
Close exoskeleton	SMR-ERD of contralateral motor cortex (C3- or C4-ERD) Example: C3-ERD required to close right exoskeleton	
Rest	No action required.	

The first column lists all possible commands for controlling each side. Importantly, the order of control commands listed in the table defines priority in case that two electroencephalography/electrooculography (EEG/EOG)-based features are detected at the same time starting with the highest priority at the top. The second column shows EEG/EOG-based features including examples for specific task instructions depicted in the third column. In the last column, visual feedback including exoskeleton motions for specific task instructions is illustrated. Yellow color coding indicates the active exoskeleton; gray color coding, the inactive exoskeleton. Only one possible instruction is illustrated for each control command. ERD, event-related desynchronization; HOV, horizontal oculoversion; SMR, sensorimotor rhythm.

as tetraplegics performed a pseudo-randomized sequence of $2 \times$ approximately 40 subtasks consisting of all B/NMI control commands required for bimanual operation of the two visual exoskeletons (Table 1). The sequence included subtasks to close one of the exoskeletons (requiring C4- or C3-ERD), to open them again, or to stop (veto) an ongoing closing motion as fast as possible to simulate for unintended hand exoskeleton motions or unexpected incidents (the latter two required both

short HOVs). In case a subtask required to close an exoskeleton, which had not been activated yet, participants first had to perform a prolonged HOV to the respective side before closing of the exoskeleton could be performed. To test for false positives, intervals to rest were randomly built in, in which the participants were instructed to avoid any action. A detailed overview on the bilateral B/NMI control commands, their corresponding EEG/EOG-based features, and their respective visual feedback

are summarized in **Table 1**. To enhance reliable distinction of *short* vs. *prolonged* HOV, an auditory feedback with two different sounds was provided to confirm successful HOV execution. The time between subtasks varied randomly between 5 and 7 s. Each sequence lasted approximately 5 min. In case no SMR-ERD was elicited, subtasks were aborted after 10 s. The total number of HOV-based subtasks being executed slightly varied depending on the users' previous SMR-ERD performance. For example, in case the user was not able to elicit ERD during a closing task, there was no need to reopen the exoskeleton again and was thus not requested. At the end of the session, tetraplegics rated user-friendliness of B/NMI control by using a five-level Likert-scale questionnaire. To account for the special needs of the tetraplegics, study protocols slightly differed between healthy participants and the patients. To reduce the overall session length, only six instead of eight rest phases were included. Moreover, the veto instructions were not randomly interspersed within the main study protocol but evaluated in a preceding pure EOG-based sequence. This was done to not overstrain the capabilities of the tetraplegic participants, since it was just a one-session study without any additional training day.

Outcome Measures and Offline Data Analysis

Feasibility and safety of the novel EEG/EOG-based control paradigm were assessed according to the following outcome measures. Feasibility was defined as *fluency* and *accuracy* of EEG-controlled operations. Fluency of control was evaluated as time from appearance of task instruction until exceedance of the SMR-ERD detection threshold. In case a laterality switch was required, timer count started just after successful activation of the exoskeleton (by performing a *prolonged* HOV). Fluent control was assumed when the average TTI such EEG-controlled operations ranged below 3 s (Cres et al., 2018). To assess the accuracy of bilateral control, the two-stage classifier performance was evaluated. At the first stage, exoskeleton selection was considered valid when successful *prolonged* HOV was performed. At the second stage, a trial was counted as successful when a full exoskeleton closing motion was conducted requiring the side-specific SMR-ERD detection threshold to be exceeded by a minimum of 2 s in total. Accurate bilateral control was assumed when the accuracy of all classifiers exceeded 80% in average. Due to the fact that the sequence can contain different numbers of subtasks, the balanced accuracy was applied to account for a potential bias toward the more frequent class (Brodersen et al., 2010). The balanced accuracy is given by $\frac{1}{2} \left(\frac{TP}{P} + \frac{TN}{N} \right)$ weighting the true-positive and true-negative rate equally. Since classification stages were built up as binary classifiers, chance level ranged at 50%. To compare the presented hybrid EEG/EOG-based classifier accuracy with an implementation, which was built up with EEG-based binary classifiers only, an offline data analysis was performed. The different implementation methods at the first stage are illustrated in **Figure 4**. Unlike the online implementation, in which prolonged HOV (first stage) and side-specific ERD (second stage) were used, offline classification was only based on the recorded

side-specific ERD (second stage of online paradigm) for both stages, since this was the classification while imagined/attempted finger movements were performed. This allowed comparison of the two approaches without the need to conduct two separate online sessions. Consequently, side-specific C3- and C4-ERDs were both classified depending on the instructed task. In case a left side closing was instructed, closing motions >2 s of the right or both exoskeletons or no movement were classified as false-negative events, whereas closing motion >2 s of the left exoskeleton was classified as a true-positive event. For the instruction to close the right side, the opposite events were classified: Movement of the right exoskeleton was classified as a true-negative event, while all other events were considered as false positives. To test for differences in average classification accuracy, a mixed-design analysis with "group" (healthy participants, tetraplegics) as between-group variable and "classification approach" (hybrid EEG/EOG brain/neural control, standard EEG-based hierarchical classifier) as repeated-measures variable was performed. To account for the limited number of data samples, bootstrapping was applied (Wilcox, 2011). Significance level was defined at $p < 0.05$. Safety was assumed when the TTS an unintended closing motion was interrupted within 2 s, meaning that closing motions were aborted before the exoskeleton was fully closed. Moreover, user-friendliness was met when the majority of tetraplegics rated EEG/EOG-based bilateral control as comfortable and easy to apply.

RESULTS

Feasibility

Average TTI [mean TTI \pm standard deviation (SD)] all EEG-controlled visual closing motions ranged at 2.14 ± 0.66 s across healthy participants and at 1.90 ± 0.97 s across tetraplegics, documenting *fluent* bilateral B/NMI control. **Figures 5A, 6A** show the individual TTI distribution for each participant. Only one healthy participant exceeded the fluency criterion (P04: 3.25 ± 2.65 s).

Average accuracy (mean \pm SD) for bilateral EEG/EOG brain/neural exoskeleton control ranged across all classifiers (i.e., including 1. stage classifier: prolonged HOV, and 2. stage classifier: C3-/C4-ERD) at $85.89 \pm 9.47\%$ across healthy participants and at $81.25 \pm 5.84\%$ across tetraplegics (**Figure 4A**). For the standard EEG-based hierarchical classifier, average accuracy declined across all classifiers to $71.33 \pm 17.21\%$ among healthy participants and to $58.68 \pm 10.62\%$ among tetraplegics (**Figure 4B**). There was a significant main effect of "classification approach" ($\Psi = -17.23, p < 0.001$), confirming superiority of the novel bilateral EEG/EOG brain/neural control for both healthy participants as well as tetraplegics. There was no main effect of "group" ($\Psi = 6.04, p = 0.419$) and no interaction between "classification approach" and "group" ($\Psi = 4.88, p = 0.449$). **Tables 2, 3** list individual accuracy rates for each healthy participant and tetraplegic as well as present accuracy results of all classifiers at every hierarchical classification stage. Chance level of binary classifiers ranged at 50%. Importantly, due to the novel implementation (compare **Figure 4A**), *prolonged* HOVs to

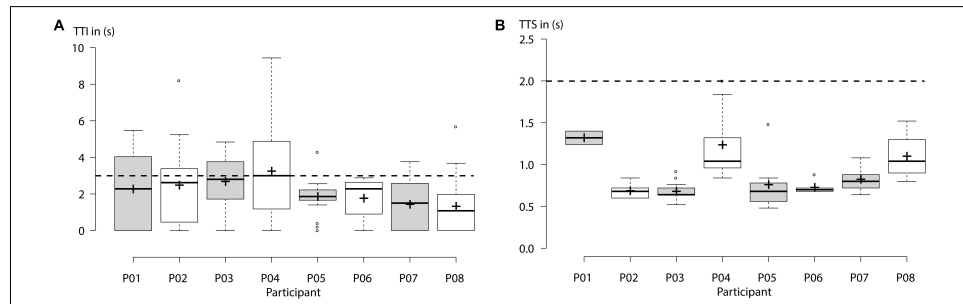


FIGURE 5 | Healthy participants: **(A)** “Time to initialize” (TTI) electroencephalography (EEG)-controlled closing motions of the left- or right-hand exoskeleton for each participant. Horizontal dashed line indicates the threshold for fluency criterion set at 3 s. Average TTI across all subjects ranged below 3 s, documenting fluent control. **(B)** “Time to stop” (TTS) an ongoing closing motion by using short horizontal oculoversions (HOVs). Horizontal dashed line indicates the threshold for safety criterion set at 2 s. Centerlines of boxplot show the median, while crosses show the mean. Box limits indicate the 25th and 75th percentiles.

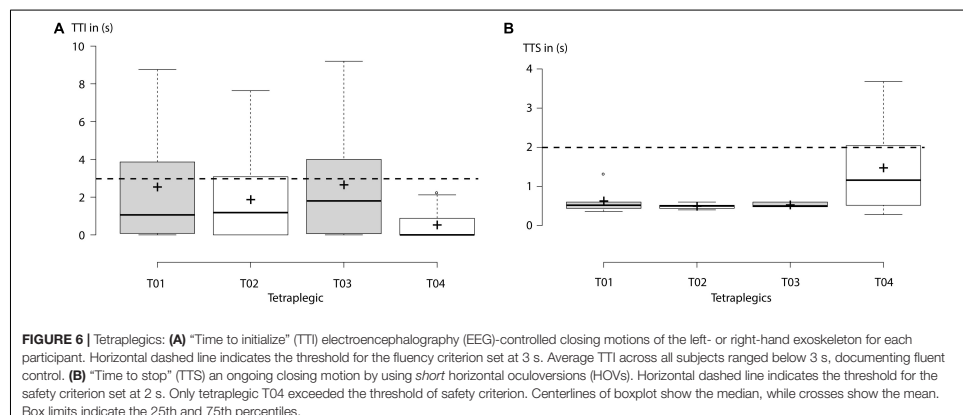


FIGURE 6 | Tetraplegics: **(A)** “Time to initialize” (TTI) electroencephalography (EEG)-controlled closing motions of the left- or right-hand exoskeleton for each participant. Horizontal dashed line indicates the threshold for the fluency criterion set at 3 s. Average TTI across all subjects ranged below 3 s, documenting fluent control. **(B)** “Time to stop” (TTS) an ongoing closing motion by using short horizontal oculoversions (HOVs). Horizontal dashed line indicates the threshold for the safety criterion set at 2 s. Only tetraplegic T04 exceeded the threshold of safety criterion. Centerlines of boxplot show the median, while crosses show the mean. Box limits indicate the 25th and 75th percentiles.

activate either the right or left exoskeleton at the first stage were classified in 100% of the cases.

Safety

Average TTS (mean TTS \pm SD) ongoing closing motions using short HOVs ranged at 0.92 ± 0.26 s across healthy participants and at 0.78 ± 0.46 s across tetraplegics. Figures 5B, 6B show the individual TTS distribution for each participant. Only one tetraplegic did not meet safety requirements while requiring more than 2 s to stop ongoing closing motions in some of the trials (T04: average TTS \pm SD ranged at 1.47 ± 1.24 s; Figure 6B).

User-Friendliness

With $88 \pm 11\%$ (mean \pm SD) of the maximum achievable score, tetraplegics rated the novel bilateral EEG/EOG-based control paradigm as user-friendly and reliable. More specifically, all tetraplegics answered that they did not experience any side effects or discomfort, that the calibration/control instructions

were easy to follow, and that the overall control was reliable and practical. Notably, all tetraplegics stated that the novel HOV-based control was easy to learn and that HOV control was comfortable. Importantly, three out of four tetraplegics would use the presented control to operate real hand exoskeletons bilaterally (Figure 7).

DISCUSSION

The presented study demonstrates feasibility and safety of a novel EEG/EOG-based B/NMI control paradigm for operating two hand exoskeletons. While feasibility was defined as fluency and accuracy of operation, safety was assumed when unintended closing motions could be aborted. We showed that eight healthy participants as well as four chronic tetraplegics were able to perform a complex sequence of subtasks mimicking bimanual tasks in daily life using four EEG/EOG-based control

TABLE 2 | Accuracy of bilateral electroencephalography/electrooculography (EEG/EOG) brain/neural exoskeleton control.

No.	Healthy participants			Tetraplegics			Total	
	1. stage		Total	1. stage		Total		
	Left/Right	Left/Rest	Right/Rest	Left/Right	Left/Rest	Right/Rest		
1	100.00	65.60	67.90	77.83	100.00	58.30	66.70	75.00
2	100.00	78.40	74.00	84.13	100.00	70.80	75.00	81.93
3	100.00	65.20	80.00	81.73	100.00	83.30	54.20	79.17
4	100.00	42.00	68.30	70.10	100.00	91.70	75.00	88.90
5	100.00	89.70	91.90	93.87				
6	100.00	94.40	100.00	98.13				
7	100.00	96.90	87.50	94.80				
8	100.00	78.40	81.20	86.53				
Mean	100.00	76.33	81.35	85.89	100.00	76.03	67.73	81.25
SD	0.00	18.34	11.36	9.47	0.00	14.61	9.83	5.84

Mean values with standard deviation (SD) are provided in bold.

TABLE 3 | Accuracy of standard electroencephalography (EEG)-based hierarchical classifier.

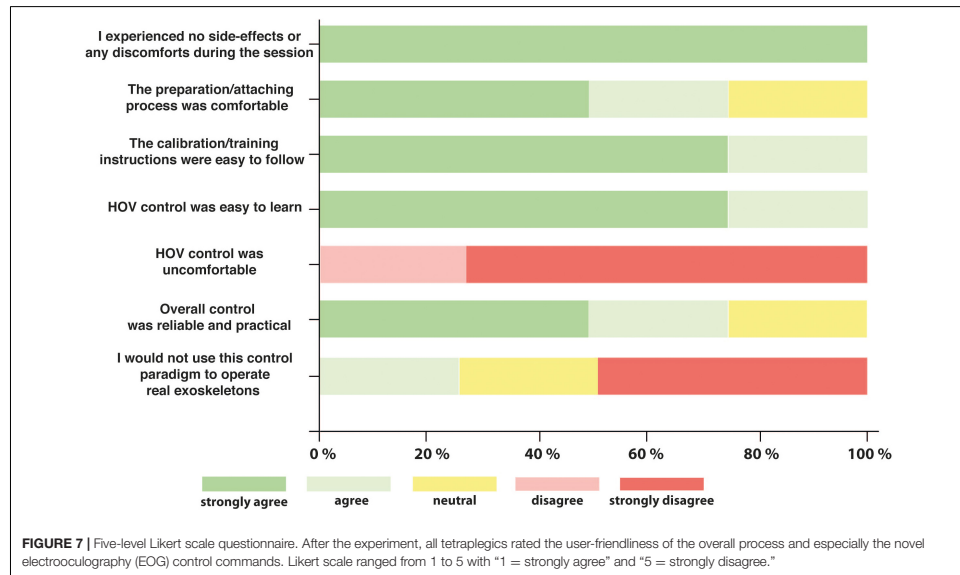
No.	Healthy participants			Tetraplegics			Total	
	1. stage		Total	1. stage		Total		
	Left/Right	Left/Rest	Right/Rest	Left/Right	Left/Rest	Right/Rest		
1	59.80	53.10	55.40	56.10	33.30	50.00	45.80	43.03
2	73.20	69.00	74.00	72.07	54.20	66.70	66.70	62.53
3	75.70	65.20	80.00	73.63	54.20	83.30	50.00	62.50
4	42.20	38.90	68.30	49.80	62.50	75.00	62.50	66.67
5	92.90	89.70	91.90	91.50				
6	83.30	94.40	100.00	92.57				
7	77.30	96.90	75.00	83.07				
8	27.30	59.70	68.80	51.93				
Mean	66.46	70.86	76.68	71.33	51.05	68.75	56.25	58.68
SD	22.03	20.99	14.05	17.21	12.46	14.22	9.94	10.62

Mean values with standard deviation (SD) are provided in bold.

commands [i.e., side-specific SMR-ERD at C3 or C4, as well as *prolonged* (>1 s) and *short* HOVs; **Table 1**]. Fluent control was documented by an average TTI EEG-controlled operations below 3 s (2.14 ± 0.66 s across healthy participants and 1.90 ± 0.97 s across tetraplegics). These results are comparable to those of previous studies, in which a unilateral whole-arm exoskeleton was controlled by healthy participants (Crea et al., 2018) or stroke survivors (Nann et al., 2020). Accurate control was confirmed by an average classification accuracy exceeding 80% ($85.89 \pm 15.81\%$ across healthy participants and $81.25 \pm 16.99\%$ across tetraplegics). Except for one tetraplegic, the TTS all ongoing motions were below 2 s (in average 0.92 ± 0.26 s across healthy participants and 0.78 ± 0.46 s across tetraplegics) underlining the system's safety. Finally, user-friendliness among tetraplegics was proven by stating no discomfort and ease of use in controlling the B/NMI system for bilateral operation with $88 \pm 11\%$ of the maximal achievable scores.

These results demonstrate for the first time that the presented hybrid EEG/EOG-based B/NMI control paradigm can be used for reliable and safe operation of two hand exoskeletons, e.g., to perform bimanual tasks.

Control of two exoskeletons requires classification of more than two classes (multiclass classification). This problem can be solved either by directly applying multiclass methods, such as naive Bayesian classifiers (Suk and Lee, 2012; Zhang et al., 2015) or multilayer perceptrons (Balakrishnan and Puthusserpady, 2005), or, as more commonly used, by decomposing the problem into several binary classifications (Lotte et al., 2018). There are different possible decomposition methods, e.g., pairwise classification (Vuckovic et al., 2018) or by hierarchical classification (Dong et al., 2017; Gundelakh et al., 2018). However, all studies have relatively low binary classification accuracies in common ranging from 50 to 70%. To achieve a higher control accuracy, fusion of EOG- and EEG-based features



was suggested and implemented in the presented bilateral control paradigm. A decisive step was to use a highly reliable EOG-based feature at safety-critical positions in the hierarchical classifier structure (Figure 4).

Fusing EEG with other biosignals like EOG is a well-established approach in the BCI field (Pfurtscheller et al., 2010). Soekadar et al. (2016) showed that such a hybrid EEG/EOG-based B/NHE fully restored hand function after SCI. Tetraplegics could eat and drink in a noisy outside restaurant by opening up the exoskeleton with *short* HOVs. This principle was now extended toward bilateral hand exoskeleton control introducing *prolonged* HOV. The advantage of this implementation was shown in the comparative offline analysis, where classification accuracy declined by 14.6% in healthy participants and by 22.6% in tetraplegics. The substantial decline in classification accuracy in tetraplegics compared to healthy participants underlines the need to compensate for the lack of lateralization in SCI by a reliable EOG-based switch between the two actuators.

One healthy participant (P04) did not meet the fluency criterion by 0.25 s in average, and one tetraplegic (T04) exceeded the safety criterion in some of the trials. However, in both cases, the unusually large SDs of 2.65 s for P04 and 1.24 s of T04 indicate that either the calibration threshold was not optimal or the participant did not attend to the task. Moreover, T04 was the only participant who stated that he would not want to use this paradigm in real life underpinning the previous assumptions.

Since EEG-based B/NMI control is generally more effortful than using other biosignals, e.g., electromyography (EMG) or HOV, one could argue that all exoskeleton movements could

be controlled by HOV. However, contrary to eye movements, EEG-based control was shown to be more intuitive since exoskeleton closing motions are directly linked to imagining or attempting to move the paralyzed fingers (Soekadar et al., 2016).

Moreover, there is increasing evidence that repeated brain/neural control of exoskeletons can trigger neural recovery (Donati et al., 2016; Wagner et al., 2018). Therefore, a combination of both operational purposes, i.e., *assistive* and *restorative* use, was suggested (Soekadar et al., 2019; Soekadar and Nann, 2020). Here, the assistive neural exoskeleton is used as a technical aid for the physiotherapist to train the patient in performing ADLs. This hybrid approach promises to facilitate generalization of learned skills to real-life environments and may increase the impact of the rehabilitation treatment. The proposed B/NMI control paradigm paves the way toward implementation of such hybrid approach for restoration of bimanual ADLs.

Besides extending the existing EEG/EOG B/NMI control paradigm toward bilateral hand exoskeleton control, minimizing electrode biosignal recording sites constitutes another important step for everyday life applicability (Cavallo et al., 2020). Moreover, considering that the high classification accuracy (>80%) was achieved with a minimalistic setup of only nine EEG recording sites, this opens up new opportunities for an easy applicable EEG headset system without the need for time-consuming whole-head EEG recordings, which is usually needed for advanced CSP algorithms, achieving comparable classification results.

To reliably detect prolonged HOVs (>1 s), bipolar EOG signals have to contain low-frequency information. Therefore, a high-pass filter (lower cutoff frequency at 0.02 Hz) has to be used.

As low-frequency bands are prone to be susceptible to movement artifacts, e.g., related to head movements, it needs to be tested whether the proposed approach for bilateral brain/neural exoskeleton control can be applied under less controlled and very noisy conditions (e.g., in an outside restaurant). Here, using other EOG signal features that are less dependent on information in the lower frequency bands could overcome this issue.

Larger clinical studies are needed to investigate whether these results can be generalized toward a broader spectrum of SCI patients. While all participants rated the brain/neural control paradigm as fluent, further increasing fluency would be desirable. In this context, taking advantage of lateralized brain activity [e.g., in the form of lateralized potential shifts preceding voluntary movements, the so-called Bereitschaftspotential or BP (Nann et al., 2019), or movement-related cortical potentials (MRCPs; Schwarz et al., 2020)] may contribute toward such aim. Since it was shown that SMR-ERDs are more pronounced over the contralateral hemisphere (Nikulin et al., 2008), it might be possible using advanced signal-processing tools to determine the side of the intended movement by assessing such lateralized activity only.

DATA AVAILABILITY STATEMENT

The raw data supporting the conclusions of this article will be made available by the authors, without undue reservation.

REFERENCES

- Ahuja, C. S., Wilson, J. R., Nori, S., Kotter, M. R. N., Druschel, C., Curt, A., et al. (2017). Traumatic spinal cord injury. *Nat. Rev. Dis. Primers* 3:17018. doi: 10.1038/nrdp.2017.18
- Ajiboye, A. B., Willett, F. R., Young, D. R., Memberg, W. D., Murphy, B. A., Miller, J. P., et al. (2017). Restoration of reaching and grasping movements through brain-controlled muscle stimulation in a person with tetraplegia: a proof-of-concept demonstration. *Lancet* 389, 1821–1830. doi: 10.1016/S0140-6736(17)30601-3
- Alam, M., Rodrigues, W., Pham, B. N., and Thakor, N. V. (2016). Brain-machine interface facilitated neurorehabilitation via spinal stimulation after spinal cord injury: recent progress and future perspectives. *Brain Res.* 1646, 25–33. doi: 10.1016/j.brainres.2016.05.039
- Anderson, K. D. (2004). Targeting recovery: priorities of the spinal cord-injured population. *J. Neurotrauma* 21, 1371–1383. doi: 10.1089/neur.2004.21.1371
- Balakrishnan, D., and Puthuserypady, S. (2005). "Multilayer perceptrons for the classification of brain computer interface data," in *Proceedings of the IEEE 31st Annual Northeast Biomedical Engineering Conference, 2005 IEEE*, Hoboken, NJ, 118–119.
- Bednar, M. S., and Woodside, J. C. (2018). Management of upper extremities in tetraplegia: current concepts. *JAAOS J. Am. Acad. Orthopaedic Surg.* 26, e333–e341. doi: 10.5435/jaaos-d-15-00465
- Benabid, A. L., Costealde, T., Eliseyev, A., Charvet, G., Verney, A., Karakas, S., et al. (2019). An exoskeleton controlled by an epidural wireless brain-machine interface in a tetraplegic patient: a proof-of-concept demonstration. *Lancet Neurol.* 18, 1112–1122. doi: 10.1016/s1474-4422(19)30321-7
- Bouton, C. E., Shaikhouni, A., Annetta, N. V., Bockbrader, M. A., Friedenberg, D. A., Nielson, D. M., et al. (2016). Restoring cortical control of functional movement in a human with quadriplegia. *Nature* 533, 247–250. doi: 10.1038/nature17435
- Brodersen, K. H., Ong, C. S., Stephan, K. E., and Buhmann, J. M. (2010). "The balanced accuracy and its posterior distribution," in *Proceedings of the 2010 20th International Conference on Pattern Recognition: IEEE*, Istanbul, 3121–3124.
- Bunketorp-Käll, L., Wangdell, J., Reinholdt, C., and Fridén, J. (2017). Satisfaction with upper limb reconstructive surgery in individuals with tetraplegia: the development and reliability of a Swedish self-reported satisfaction questionnaire. *Spinal Cord* 55, 664–671. doi: 10.1038/sc.2017.12
- Campbell, M. L., Sheets, D., and Strong, P. S. (1999). Secondary health conditions among middle-aged individuals with chronic physical disabilities: implications for unmet needs for services. *Assist. Technol.* 11, 105–122. doi: 10.1080/10400435.1999.10131995
- Cappello, L., Meyer, J. T., Galloway, K. C., Peisner, J. D., Granberry, R., Wagner, D. A., et al. (2018). Assisting hand function after spinal cord injury with a fabric-based soft robotic glove. *J. Neuroeng. Rehabil.* 15, 59–59. doi: 10.1186/s12984-018-0391-x
- Carvalho, R., Dias, N., and Cerqueira, J. J. (2019). Brain-machine interface of upper limb recovery in stroke patients rehabilitation: a systematic review. *Physiother. Res. Int.* 24:e1764. doi: 10.1002/pri.1764
- Cavallo, A., Roth, V., Haslacher, D., Nann, M., and Soekadar, S. R. (2020). Minimizing biosignal recording sites for noninvasive hybrid brain/neural control. *IEEE Syst. J.* 1–7. doi: 10.1109/JSYST.2020.3021751
- Collinger, J. L., Boninger, M. L., Bruns, T. M., Curley, K., Wang, W., and Weber, D. J. (2013a). Functional priorities, assistive technology, and brain-computer interfaces after spinal cord injury. *J. Rehabil. Res. Dev.* 50:145. doi: 10.1682/jrrd.2011.11.0213
- Collinger, J. L., Wodlinger, B., Downey, J. E., Wang, W., Tyler-Kabara, E. C., Weber, D. J., et al. (2013b). High-performance neuroprosthetic control by an individual with tetraplegia. *Lancet* 381, 557–564. doi: 10.1016/S0140-6736(12)61816-9
- Coscia, M., Wessel, M. J., Chaudary, U., Millán, J. D. R., Micera, S., Guggisberg, A., et al. (2019). Neurotechnology-aided interventions for upper limb motor rehabilitation in severe chronic stroke. *Brain* 142, 2182–2197. doi: 10.1093/brain/awz181
- Crea, S., Nann, M., Trigili, E., Cordella, F., Baldoni, A., Badesa, F. J., et al. (2018). Feasibility and safety of shared EEG/EOG and vision-guided autonomous whole-arm exoskeleton control to perform activities of daily living. *Sci. Rep.* 8:10823. doi: 10.1038/s41598-018-29091-5

ETHICS STATEMENT

The studies involving human participants were reviewed and approved by the Ethics Commission at the Medical Faculty of the Eberhard Karls University and the University Hospital Tübingen. The patients/participants provided their written informed consent to participate in this study.

AUTHOR CONTRIBUTIONS

MN and NP designed the study. NP collected the data of the healthy participants. MN, NP, and CA collected the data of the tetraplegics. MN and NP analyzed the data. MN, NP, CA, and SS interpreted the data and performed the literature search. MN, NP, CA, and SS wrote the manuscript. All authors contributed to the article and approved the submitted version.

FUNDING

This research was supported by the Baden-Württemberg Stiftung (NEU007/1), the European Research Council (ERC-2017-STG-759370), and the Einstein Foundation Berlin. We acknowledge support from the German Research Foundation (DFG) and the Open Access Publication Fund of Charité-Universitätsmedizin Berlin.

- Dahlberg, L. S., Becerra, L., Borsook, D., and Linnman, C. (2018). Brain changes after spinal cord injury, a quantitative meta-analysis and review. *Neurosci Biobehav. Rev.* 90, 272–293. doi: 10.1016/j.neubiorev.2018.04.018
- Donati, A. R., Shokur, S., Morya, E., Campos, D. S., Moioli, R. C., Gitti, C. M., et al. (2016). Long-term training with a brain-machine interface-based gait protocol induces partial neurological recovery in paraplegic patients. *Sci. Rep.* 6:30383. doi: 10.1038/srep30383
- Dong, E., Li, C., Li, L., Du, S., Belkacem, A. N., and Chen, C. (2017). Classification of multi-class motor imagery with a novel hierarchical SVM algorithm for brain-computer interfaces. *Med. Biol. Eng. Comput.* 55, 1809–1818. doi: 10.1007/s11517-017-1611-4
- Dunn, J. A., Sinnott, K. A., Rothwell, A. G., Mohammed, K. D., and Simcock, J. W. (2016). Tendon transfer surgery for people with tetraplegia: an overview. *Arch. Phys. Med. Rehabil.* 97, S75–S80.
- Frolow, A. A., Mokienko, O., Lyukmanov, R., Biryukova, E., Kotov, S., Turbina, L., et al. (2017). Post-stroke rehabilitation training with a motor-imagery-based brain-computer interface (BCI)-controlled hand exoskeleton: a randomized controlled multicenter trial. *Front. Neurosci.* 11:400. doi: 10.3389/fnins.2017.00400
- Gohritz, A., and Fréder, J. (2018). Management of spinal cord injury-induced upper extremity spasticity. *Hand Clin.* 34, 555–565. doi: 10.1016/j.hcl.2018.07.001
- Gundelakh, F., Stankevich, L., and Sonkin, K. (2018). “Mobile robot control based on noninvasive brain-computer interface using hierarchical classifier of imagined motor commands,” in *Proceedings of the MATEC Web of Conferences*, (Les Ulis: EDP Sciences), 03003. doi: 10.1051/matecconf/20181603003
- Heide, W., Koenig, E., Trillenberg, P., Kompf, D., and Zee, D. S. (1999). Electroencephalography: technical standards and applications. The International Federation of Clinical Neurophysiology. *Electroencephalogr. Clin. Neurophysiol. Suppl.* 52, 223–240.
- Ho, C. H., Triolo, R. J., Elias, A. L., Kilgore, K. L., Dimarco, A. F., Bogie, K., et al. (2014). Functional electrical stimulation and spinal cord injury. *Phys. Med. Rehabil. Clin.* 25, 631–654.
- Hochberg, L. R., Bacher, D., Jarosiewicz, B., Masse, N. Y., Simeral, J. D., Vogel, J., et al. (2012). Reach and grasp by people with tetraplegia using a neurally controlled robotic arm. *Nature* 485, 372–375. doi: 10.1038/nature11076
- Holtz, K. A., Lipson, R., Noonan, V. K., Kwon, B. K., and Mills, P. B. (2017). Prevalence and effect of problematic spasticity after traumatic spinal cord injury. *Arch. Phys. Med. Rehabil.* 98, 1132–1138. doi: 10.1016/j.apmr.2016.09.124
- León, C. L. (2017). *Multilabel Classification of EEG-based Combined Motor Imageries Implemented for the 3D Control of a Robotic Arm*. Nancy: University of Lorraine.
- Lo, C., Tran, Y., Anderson, K., Craig, A., and Middleton, J. (2016). Functional priorities in persons with spinal cord injury: using discrete choice experiments to determine preferences. *J. Neurotrauma* 33, 1958–1968. doi: 10.1089/neu.2016.4423
- Lotte, F., Bougrain, L., Cichocki, A., Clerc, M., Congedo, M., Rakotomamonjy, A., et al. (2018). A review of classification algorithms for EEG-based brain-computer interfaces: a 10 year update. *J. Neural Eng.* 15:031005. doi: 10.1088/1741-2552/ab2f2
- McFarland, D. J. (2015). The advantages of the surface Laplacian in brain-computer interface research. *Int. J. Psychophysiol.* 97, 271–276. doi: 10.1016/j.ijpsycho.2014.07.009
- Mekki, M., Delgado, A. D., Fry, A., Putrino, D., and Huang, V. (2018). Robotic rehabilitation and spinal cord injury: a narrative review. *Neurotherapeutics* 15, 604–617.
- Meng, J., Zhang, S., Bekyo, A., Olson, J., Baxter, B., and He, B. (2016). Noninvasive electroencephalogram based control of a robotic arm for reach and grasp tasks. *Sci. Rep.* 6:38565.
- Nann, M., Cohen, L. G., Deecke, L., and Soekadar, S. R. (2019). To jump or not to jump—the Bereitschaftspotential required to jump into 192-meter abyss. *Sci. Rep.* 9:2243. doi: 10.1038/s41598-018-38447-w
- Nann, M., Cordella, F., Trigili, E., Lauretti, C., Bravi, M., Miccinilli, S., et al. (2020). Restoring activities of daily living using an EEG/EOG-controlled semi-autonomous and mobile whole-arm exoskeleton in chronic stroke. *IEEE Syst. J.* 1–8. doi: 10.1109/JSYST.2020.3021485
- National Spinal Cord Injury Statistical Center (2019). *National Spinal Cord Injury Statistical Center Annual Statistical Report*. Birmingham, AL: University of Alabama at Birmingham.
- Neuper, C., Wortz, M., and Pfurtscheller, G. (2006). ERD/ERS patterns reflecting sensorimotor activation and deactivation. *Prog. Brain Res.* 159, 211–222. doi: 10.1016/S0079-6123(06)59014-4
- Nikulin, V. V., Hohlfeld, F. U., Jacobs, A. M., and Curio, G. (2008). Quasi-movements: a novel motor-cognitive phenomenon. *Neuropsychologia* 46, 727–742. doi: 10.1016/j.neuropsychologia.2007.10.008
- Ortner, R., Schäringer, J., Lechner, A., and Guger, C. (2015). “How many people can control a motor imagery based BCI using common spatial patterns?” in *Proceedings of the 2015 7th International IEEE/EMBS Conference on Neural Engineering (NER)*. IEEE, Montpellier, 202–205.
- Osuagwu, B. C., Wallace, L., Fraser, M., and Vuckovic, A. (2016). Rehabilitation of hand in subacute tetraplegic patients based on brain computer interface and functional electrical stimulation: a randomised pilot study. *J. Neural Eng.* 13:065002. doi: 10.1088/1741-2560/13/6/065002
- Pfurtscheller, G., Allison, B. Z., Brunner, C., Bauernfeind, G., Solis-Escalante, T., Scherer, R., et al. (2010). The hybrid BCI. *Front. Neurosci.* 4:30. doi: 10.3389/fnpro.2010.00003
- Pfurtscheller, G., and Aranibar, A. (1979). Evaluation of event-related desynchronization (ERD) preceding and following voluntary self-paced movement. *Electroencephalogr. Clin. Neurophysiol.* 46, 138–146. doi: 10.1016/0013-4694(79)90063-4
- Pfurtscheller, G., and da Silva, F. H. L. (1999). Event-related EEG/MEG synchronization and desynchronization: basic principles. *Clin. Neurophysiol.* 110, 1842–1857. doi: 10.1016/S1388-2457(99)00141-8
- Ragnarsson, K. (2008). Functional electrical stimulation after spinal cord injury: current use, therapeutic effects and future directions. *Spinal Cord* 46, 255–274. doi: 10.1038/sj.sc.3102091
- Rushton, P. W., Miller, W. C., Mortenson, W. B., and Garden, J. (2010). Satisfaction with participation using a manual wheelchair among individuals with spinal cord injury. *Spinal Cord* 48, 691–696. doi: 10.1038/sc.2009.197
- Schalk, G., McFarland, D. J., Hinterberger, T., Birbaumer, N., and Wolpaw, J. R. (2004). BC12000: a general-purpose brain-computer interface (BCI) system. *IEEE Trans. Biomed. Eng.* 51, 1034–1043. doi: 10.1109/TBME.2004.827072
- Schwarz, A., Pereira, J., Kobler, R., and Müller-Putz, G. R. (2020). Unimanual and bimanual reach-and-grasp actions can be decoded from human EEG. *IEEE Trans. Biomed. Eng.* 67, 1684–1695. doi: 10.1109/TBME.2019.2942974
- Snoek, G. J., Mij, I. J., Hermans, H. J., Maxwell, D., and Biering-Sørensen, F. (2004). Survey of the needs of patients with spinal cord injury: impact and priority for improvement in hand function in tetraplegics. *Spinal Cord* 42, 526–532. doi: 10.1038/sj.sc.3101638
- Soekadar, S. R., Cohen, L. G., and Birbaumer, N. (2015a). “Clinical brain-machine interfaces,” in *Cognitive Plasticity in Neurologic Disorders*, eds J. I. Tracy and B. M. Hampshire (Oxford: Oxford University Press), 347–363.
- Soekadar, S. R., Haagen, K., and Birbaumer, N. (2008). “Brain-computer interfaces (BCI): restoration of movement and thought from neuroelectric and metabolic brain activity,” in *Coordination: Neural, Behavioral and Social Dynamics*, eds A. Fuchs and V. K. Jirsa (Berlin: Springer). doi: 10.1007/978-3-540-74479-5_11
- Soekadar, S. R., and Nann, M. (2020). “Neural-gesteuerte robotik für assistenz und rehabilitation im alltag,” in *Mensch-Roboter-Kollaboration*, ed. H. J. Buxbaum (Wiesbaden: Springer), 117–131. doi: 10.1007/978-3-658-28307-0_8
- Soekadar, S. R., Nann, M., Crea, S., Trigili, E., Gómez, C., Opisso, E., et al. (2019). “Restoration of finger and arm movements using hybrid brain/neural assistive technology in everyday life environments,” in *Brain-Computer Interface Research, A State-of-the-Art Summary 7*, eds N. M.-K. Christoph Guger and B. Z. Allison (Berlin: Springer International Publishing), 53–61. doi: 10.1007/978-3-030-05668-1_5
- Soekadar, S. R., Witkowski, M., Mellinger, J., Ramos, A., Birbaumer, N., and Cohen, L. G. (2016). Hybrid EEG/EOG-based brain/neural hand exoskeleton restores fully independent daily living activities after quadriplegia. *Sci. Robot.* 1:eag3296. doi: 10.1126/scirobotics.aag3296
- Soekadar, S. R., Witkowski, M., Mellinger, J., Ramos, A., Birbaumer, N., and Cohen, L. G. (2011). ERD-based online brain-machine interfaces (BMI) in the context of neurorehabilitation: optimizing BMI learning and performance. *IEEE Trans. Neural Syst. Rehabil. Eng.* 19, 542–549. doi: 10.1109/TNSRE.2011.2166809

- Soekadar, S. R., Witkowski, M., Vitiello, N., and Birbaumer, N. (2015b). An EEG/EOG-based hybrid brain-neural computer interaction (BCNI) system to control an exoskeleton for the paralyzed hand. *Biomed. Tech.* 60, 199–205. doi: 10.1515/bmrt-2014-0126
- Suk, H.-I., and Lee, S.-W. (2012). A novel Bayesian framework for discriminative feature extraction in brain-computer interfaces. *IEEE Trans. Pattern Anal. Machine Intell.* 35, 286–299. doi: 10.1109/tpami.2012.69
- Tang, Z., Sun, S., Zhang, S., Chen, Y., Li, C., and Chen, S. (2016). A brain-machine interface based on ERD/ERS for an upper-limb exoskeleton control. *Sensors* 16:2050. doi: 10.3390/s16122050
- Vidaurre, C., and Blankertz, B. (2010). Towards a cure for BCI illiteracy. *Brain Topogr.* 23, 194–198. doi: 10.1007/s10548-009-0121-6
- Vidaurre, C., Klauer, C., Schauer, T., Ramos-Murguialday, A., and Müller, K.-R. (2016). EEG-based BCI for the linear control of an upper-limb neuroprosthesis. *Med. Eng. Phys.* 38, 1195–1204. doi: 10.1016/j.medengphy.2016.06.010
- Vuckovic, A., Pangaro, S., and Finska, P. (2018). Unimanual versus bimanual motor imagery classifiers for assistive and rehabilitative brain computer interfaces. *IEEE Trans. Neural Syst. Rehabil. Eng.* 26, 2407–2415. doi: 10.1109/tnsre.2018.2877620
- Wagner, F. B., Mignardot, J. B., Le Goff-Mignardot, C. G., Demesmaeker, R., Komi, S., Capogrosso, M., et al. (2018). Targeted neurotechnology restores walking in humans with spinal cord injury. *Nature* 563, 65–71. doi: 10.1038/s41586-018-0649-2
- Wilcox, R. R. (2011). *Introduction to Robust Estimation and Hypothesis Testing*. Cambridge, MA: Academic press.
- Witkowski, M., Cortese, M., Cempini, M., Mellinger, J., Vitiello, N., and Soekadar, S. R. (2014). Enhancing brain-machine interface (BMI) control of a hand exoskeleton using electrooculography (EOG). *J. Neuroeng. Rehabil.* 11:165. doi: 10.1186/1743-0003-11-165
- Wolpaw, J. R., Birbaumer, N., Mcfarland, D. J., Pfurtscheller, G., and Vaughan, T. M. (2002). Brain-computer interfaces for communication and control. *Clin. Neurophysiol.* 113, 767–791. doi: 10.1016/s1388-2457(02)00057-3
- Yoo, H.-J., Lee, S., Kim, J., Park, C., and Lee, B. (2019). Development of 3D-printed myoelectric hand orthosis for patients with spinal cord injury. *J. Neuro Eng. Rehabil.* 16:162.
- Yun, Y., Dancause, S., Esmatloo, P., Serrato, A., Merring, C. A., Agarwal, P., et al. (2017). “Maestro: an EMG-driven assistive hand exoskeleton for spinal cord injury patients,” in *Proceedings of the 2017 IEEE International Conference on Robotics and Automation (ICRA)*. IEEE, Singapore, 2904–2910.
- Zhang, Y., Zhou, G., Jin, J., Zhao, Q., Wang, X., and Cichocki, A. (2015). Sparse Bayesian classification of EEG for brain–computer interface. *IEEE Trans. Neural Netw. Learn. Syst.* 27, 2256–2267. doi: 10.1109/tnnls.2015.2476656

Conflict of Interest: The authors declare that the research was conducted in the absence of any commercial or financial relationships that could be construed as a potential conflict of interest.

Copyright © 2020 Nann, Peekhaus, Angerhofer and Soekadar. This is an open-access article distributed under the terms of the Creative Commons Attribution License (CC BY). The use, distribution or reproduction in other forums is permitted, provided the original author(s) and the copyright owner(s) are credited and that the original publication in this journal is cited, in accordance with accepted academic practice. No use, distribution or reproduction is permitted which does not comply with these terms.

2.4 Heart rate variability predicts decline in sensorimotor rhythm control

Nann, M., Haslacher, D., Colucci, A., Eskofier, B., von Tscharner, V., Soekadar, S.R. (2021). Heart Rate Variability Predicts Decline in Sensorimotor Rhythm Control. *Journal of Neural Engineering*, 18(4), 0460b5.

Journal of Neural Engineering



PAPER

OPEN ACCESS

RECEIVED
23 December 2020REVISED
15 June 2021ACCEPTED FOR PUBLICATION
6 July 2021PUBLISHED
23 July 2021

Original content from
this work may be used
under the terms of the
Creative Commons
Attribution 4.0 licence.

Any further distribution
of this work must
maintain attribution to
the author(s) and the title
of the work, journal
citation and DOI.



Heart rate variability predicts decline in sensorimotor rhythm control

Marius Nann^{1,2}, David Haslacher², Annalisa Colucci², Bjoern Eskofier³, Vinzenz von Tscharner⁴ and Surjo R Soekadar^{2,*}

¹ Applied Neurotechnology Lab, Department of Psychiatry and Psychotherapy, University Hospital of Tübingen, Tübingen, Germany
² Clinical Neurotechnology Lab, Neuroscience Research Center (NWFZ), Department of Psychiatry and Psychotherapy, Charité - University Medicine Berlin, Berlin, Germany

³ Machine Learning and Data Analytics Lab, Department of Computer Science, Friedrich-Alexander University Erlangen-Nürnberg (FAU), Erlangen, Germany
⁴ Human Performance Lab, University of Calgary, Calgary, Canada

* Author to whom any correspondence should be addressed.

E-mail: surjo.soekadar@charite.de

Keywords: sensorimotor rhythms, SMR, brain-computer interface, BCI, heart rate variability, HRV, Granger causality

Abstract

Objective. Voluntary control of sensorimotor rhythms (SMRs, 8–12 Hz) can be used for brain–computer interface (BCI)-based operation of an assistive hand exoskeleton, e.g. in finger paralysis after stroke. To gain SMR control, stroke survivors are usually instructed to engage in motor imagery (MI) or to attempt moving the paralyzed fingers resulting in task- or event-related desynchronization (ERD) of SMR (SMR-ERD). However, as these tasks are cognitively demanding, especially for stroke survivors suffering from cognitive impairments, BCI control performance can deteriorate considerably over time. Therefore, it would be important to identify biomarkers that predict decline in BCI control performance within an ongoing session in order to optimize the man–machine interaction scheme. **Approach.** Here we determine the link between BCI control performance over time and heart rate variability (HRV). Specifically, we investigated whether HRV can be used as a biomarker to predict decline of SMR-ERD control across 17 healthy participants using Granger causality. SMR-ERD was visually displayed on a screen. Participants were instructed to engage in MI-based SMR-ERD control over two consecutive runs of 8.5 min each. During the 2nd run, task difficulty was gradually increased. **Main results.** While control performance ($p = .18$) and HRV ($p = .16$) remained unchanged across participants during the 1st run, during the 2nd run, both measures declined over time at high correlation (performance: $-0.61\%/10\text{ s}$, $p = 0$; HRV: $-0.007\text{ ms}/10\text{ s}$, $p < .001$). We found that HRV exhibited predictive characteristics with regard to within-session BCI control performance on an individual participant level ($p < .001$). **Significance.** These results suggest that HRV can predict decline in BCI performance paving the way for adaptive BCI control paradigms, e.g. to individualize and optimize assistive BCI systems in stroke.

1. Introduction

Besides serving as a powerful tool to improve understanding of brain oscillatory activity (Schultze-Kraft *et al* 2016), brain–computer interface (BCI) systems play an increasing role in the medical field, e.g. to operate a hand exoskeleton to restore lost hand function in finger paralysis after stroke or spinal cord injury (Ang *et al* 2011, Soekadar *et al* 2016). The best established method for such clinical application

utilizes voluntary control of sensorimotor-rhythms (SMRs, 8–12 Hz) recorded by electroencephalography (EEG) (Birbaumer and Cohen 2007). To gain control, stroke survivors are usually instructed to engage in motor imagery (MI) or to attempt moving the paralyzed fingers resulting in task- or event-related desynchronization (ERD) of SMR (SMR-ERD). Besides assistance, there is increasing evidence that repeated BCI use can trigger neural recovery leading to improved hand motor function

(Ramos *et al* 2013, Ang *et al* 2015, Frolov *et al* 2017a, Cervera *et al* 2018, Bai *et al* 2020). However, optimal frequency, dose and intensity of BCI training to maximize the rehabilitation effect remains unclear (Soekadar *et al* 2015, Young *et al* 2015, Lang *et al* 2016). Recently, it was proposed that merging both strategies, i.e. introducing assistance to perform bimanual activities of daily living (ADL) in the context of stroke rehabilitation protocols, may substantially increase the impact of BCI technology and broaden its use in the medical field (Soekadar *et al* 2019, Soekadar 2020, Soekadar and Nann 2020).

However, BCI control tasks, e.g. performing repetitive MI of grasping movements, are cognitively demanding. As a consequence, decline in concentration and attention due to mental fatigue can negatively affect BCI control performance (Curran and Stokes 2003, Myrden and Chau 2015). Especially stroke survivors suffering from cognitive impairments including post-stroke fatigue (Christensen *et al* 2008, Acciaresi *et al* 2014) have a limited capacity to maintain reliable BCI control over a longer period of time (Frolov *et al* 2017b). Current research showed that subjective fatigue and inattention correlated with diminished BCI performance (Foong *et al* 2019). This does not only reduce applicability of BCIs for assistance but also for triggering motor recovery, e.g. after stroke, because decline in attention was shown to negatively affect cortical plasticity (Stefan *et al* 2004).

Despite extensive research efforts to identify predictive performance markers across subjects (Blankertz *et al* 2010, Hammer *et al* 2012), there is currently no adaptive control paradigm applied in BCI neurorehabilitation in which within-session decline in SMR-based BCI performance becomes predicted on an individual level. Avoiding such performance decline would be critical to sustain high control performance during assistance and to optimize efficacy of rehabilitation protocols. Also, maintaining optimal BCI control performance would be highly relevant for the management of the patient's motivation to engage in regular use (Hammer *et al* 2012), and to prevent overtraining in terms of dose and intensity (Soekadar *et al* 2015). However, tracking negative trends in BCI performance over the course of a training session is difficult due to large trial-to-trial variations within each individual user (Grosseg-Wentrup and Schölkopf 2012). Moreover, given that the long-term goal is to apply BCI systems in everyday life environments, e.g. during ADLs (Soekadar *et al* 2016), the required self-paced BCI protocol further impedes detection of a negative performance trend. It would be thus important to identify sensitive biomarkers that predict decline in BCI performance at a point at which optimization of the patient-machine interaction scheme can yield stable control performance.

Recently, neuroadaptive human-computer interaction systems gained interest as they allow for passive

cognitive monitoring without interfering with active voluntary control commands (Zander and Kothe 2011, Gerjets *et al* 2014). For instance, a neuroadaptive control paradigm has been developed to classify and adapt to the cognitive state of pilots during demanding flight simulations to increase their task accuracy (Klaproth *et al* 2020). Neuroadaptive technology has been widely used to discriminate between and adapt for different levels of workload during cognitive tasks, e.g. during a working memory task (Hogervorst *et al* 2014). While cortical features are commonly used for classification, e.g. changes in the alpha (8–12 Hz) or theta (4–8 Hz) power band (Klimesch 1999), also peripheral physiological measures as heart rate (HR), heart rate variability (HRV), respiration rate or skin conductance were shown to be suitable for discrimination (Hogervorst *et al* 2014).

Unlike EEG-based classification approaches that commonly require a high number of electrodes and sophisticated analysis methods (Faller *et al* 2019), peripheral physiological measures like HR or respiration rate are straightforward to record and less complex in analysis. Already over 150 years ago, Claude Bernard discovered the close interaction between the brain and the heart (Thayer and Lane 2009). Cortical control of cardiac activity is mediated by the joint activity of sympathetic and parasympathetic (vagus) nerves (Levy 1990). Especially the vagus nerve originating from the brain and directly innervating the heart muscle has an important control function in slowing down pulse and HR (countering the sympathetic innervation, which accelerates the pulse) to continuously adapt to physiological processes and account for changes in physical and/or cognitive demands. The strongest vagally-mediated adaptation process constitutes the adjustment of the HR to breathing, also called respiratory sinus arrhythmia (RSA). Since breathing induces unintended changes in blood pressure, HR needs to be constantly adapted for pressure stabilization (Aasman *et al* 1987). Besides cortical control of cardiac activity via efferent nerves, i.e. top-down control, there are also afferent nerve fibers for bottom-up control (Cameron 2001). For instance, mechanosensory and chemosensory neurons forward important information from the heart to the brain to obtain a robust control loop. Thus, there is a complex bidirectional brain-heart interaction that allows for constant adaptation to changing physiological demands (Shaffer *et al* 2014).

To quantify the activity of the parasympathetic system, analysis of HRV is broadly applied. More specifically, there is strong evidence that particularly the high-frequency (HF)-HRV component in the range of 0.15–0.4 Hz reflects the modulation of vagus nerve activity (Malik and Camm 1993, Berntson *et al* 1997). In addition to physiological adaptation processes, numerous studies have shown that vagal activity is also sensitive to cognitive processes and attenuates

during cognitively demanding tasks, e.g. during driving (Stuiver *et al* 2014) and aviation simulation (Rowe *et al* 1998, Muth *et al* 2012), visual attention test (Duschek *et al* 2009) or a sustained perceptual attention task (Overbeek *et al* 2014). Suppression of vagal activity induced by high cognitive demand results in lower adaptation to variations in blood pressure and thus reduced HRV (Hogervorst *et al* 2014).

However, despite extensive research in the field of psychophysiology, it is unknown to what extend voluntary control of SMR in the context of BCI control impacts vagal activity. Moreover, it is unknown whether HF-HRV can be used as a biomarker to predict decline in BCI control performance. Hence, understanding this relationship is an important prerequisite for the development of HRV-based neuroadaptive BCI systems to optimize control performance and stroke neurorehabilitation protocols.

A driving simulator study showed that measures of the autonomous system like HR can reflect cognitive demand linked to driving performance (Mehler *et al* 2009). It was also shown that HF-HRV can reflect cognitive demand (Muth *et al* 2012) suggesting that HF-HRV might predict BDI performance.

Although there are studies indicating that resting-state HF-HRV recorded before the actual task can contain predictive information, e.g. for P300 BCI performance (Kaufmann *et al* 2012) or for cooperative behavior in a hawk-dove game (Beffara *et al* 2016), such approach does not provide time-resolved information on within-session BCI performance. Given that detection of such trends are rather difficult to detect due to large trial-to-trial variations over the course of a BCI control session within each individual user (Grosse-Wentrup and Schölkopf 2012), the 1st objective (O1) was to evaluate specificity of HRV decline for BCI control performance using linear regression analyses based on multilevel models. The 2nd objective (O2) was then to test whether HF-HRV predicts average BCI control performance on a participant level within a single run consisting of 50 BCI control trials. For this, we performed a Granger causality analysis to investigate the predictive characteristics of HRV. Granger causality, introduced by Clive Granger in 1969 (Granger 1969), is a statistical hypothesis test and has been widely applied in economic science as a forecasting method, e.g. of two stock market time series. In short, a variable X (here HRV) Granger-causes a 2nd variable Y (here BCI control performance), when prediction of Y is better including information of X than without (Wiener 1956). This is done by a series of F -tests on lagged values. It is important to note that the Granger causality analysis does not necessarily provide evidence for a causal relationship in a more general sense between X and Y , but rather shows a statistical relationship indicating that past information of X improves prediction of Y (Maziarz 2015). Recently, Granger causality has

gained broad interest and various applications in the field of neuroscience (Seth *et al* 2015).

2. Methods

2.1. Participants

Twenty-four able-bodied participants (seven females, mean age 33 ± 12 years) were invited to the University Hospital of Tübingen, Germany, for a familiarization and experimental session on two consecutive days. During the familiarization session, all participants gave written informed consent and were pre-screened whether they were able to elicit detectable SMR-ERD and whether they showed a normal heartbeat pattern to allow for HRV analysis. In case of regular medication intake (e.g. beta blocker) or neurological diseases (e.g. neuropathy due to diabetes mellitus), participants were excluded from the study. After successful pre-screening, 17 participants were invited to the experimental session on the following day. The study protocol was in line with the Declaration of Helsinki and was approved by the local ethics committee at the University of Tübingen (registration code of ethical approval: 201/2018BO1).

2.2. Task description and study design

The participants were instructed to engage in MI of left or right grasping movements and received visual feedback based on SMR-ERD modulations presented on a screen in front of them. Participants performed two consecutive runs with 50 trials each resulting in an overall duration of 500 s (8.5 min) per run. A run consisted of a pseudorandomized and externally paced sequence of MI and relax tasks with participants instructed to blank their minds and rest. Both tasks had a length of 5 s and were separated by intertrial intervals (ITIs) with a randomized duration of 4–6 s.

The study followed a within-participant repeated measures one-factor design with task difficulty as independent variable. To increase task difficulty between runs, SMR-ERD detection threshold as well as ratio in number of MI to relax tasks were manipulated. During the 1st run, SMR-ERD detection threshold was kept constant and task ratio was balanced (task difficulty: ‘normal’). To increase task difficulty during the 2nd run (task difficulty: ‘hard’), SMR-ERD detection threshold was gradually lowered by -20% relative to the individual SMR-ERD detection threshold determined during calibration every 100 s. In contrast, detection threshold for the relax tasks, in which participants should stay above that threshold (i.e. true negative rate), was kept constant. We reasoned that changing this threshold could be perceived as very frustrating, because feedback gradually would indicate that participants cannot reach a relaxed state which would introduce even more stress. Moreover, task ratio was unbalanced with 60%

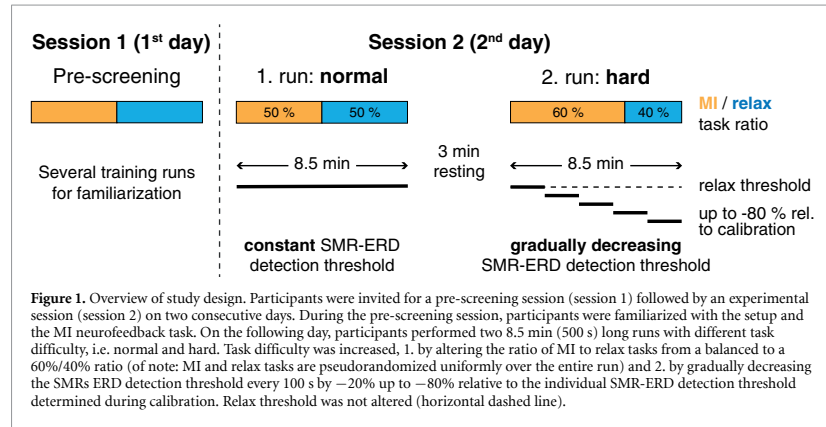


Figure 1. Overview of study design. Participants were invited for a pre-screening session (session 1) followed by an experimental session (session 2) on two consecutive days. During the pre-screening session, participants were familiarized with the setup and the MI neurofeedback task. On the following day, participants performed two 8.5 min (500 s) long runs with different task difficulty, i.e. normal and hard. Task difficulty was increased, 1. by altering the ratio of MI to relax tasks from a balanced to a 60%/40% ratio (of note: MI and relax tasks are pseudorandomized uniformly over the entire run) and 2. by gradually decreasing the SMRs ERD detection threshold every 100 s by –20% up to –80% relative to the individual SMR-ERD detection threshold determined during calibration. Relax threshold was not altered (horizontal dashed line).

MI to 40% relax tasks (overview of study design see figure 1). The increase in task difficulty during the 2nd run was not communicated to the participants to avoid biasing their motivational state or influence their expectations.

2.3. BCI control

EEG was recorded from 22 conventional recording sites (Fp1, Fp2, AFz, F3, Fz, F4, T7, C3, Cz, C4, T8, CPz, P7, P3, Pz, P4, P8, POz, O1, O2, M1, and M2 according to the international 10/20 system) and referenced to FCz. Ground electrode was placed at Fpz. Dependent on the selected laterality of the imagined grasping movements, either C3 for the right hand or C4 for the left hand together with the respective four nearest electrodes for Laplacian filtering were selected for further signal processing (McFarland 2015). Two additional channels were used to assess the HR for offline HRV analysis (see section 2.4). All biosignals were amplified with a wireless saline-based EEG system (smarting®, mBrainTrain®, Belgrade, Serbia, in combination with a customized GT Gelfree-S3 EEG cap, Wuhan Greentek Pty Ltd, Wuhan, China) and sampled at 500 Hz. All impedances were kept below 10 kΩ. To provide visual online feedback of participant's voluntary SMR control, the BCI2000 software platform was used for real time processing and classification (Schalk et al 2004).

First, EEG signals at C3 or C4 (dependent on the imagined hand) were bandpass-filtered at 1–30 Hz as well as Laplace-filtered to increase signal-to-noise ratio (McFarland 2015, Soekadar et al 2016). Afterwards, instantaneous SMR power amplitude of a 3 Hz wide bin around the frequency of interest (FOI ± 1.5 Hz) was estimated from a 400 ms moving window based on an autoregressive model of order 50 according to the Burg algorithm (Soekadar et al 2011). FOI was individually determined during calibration and was set to the frequency showing

the largest SMR power downmodulation during MI. Lastly, SMR-ERD was calculated according to the power method of Pfurtscheller and Aranibar (1979).

BCI online control required individual calibration before the two experimental runs. Therefore, participants performed three short calibration runs in which they followed 20 externally paced visual cues instructing them to either engage in MI or to relax. Based on the 1st run in absence of online feedback, individual average power was estimated to normalize instantaneous power for SMR-ERD computation. This means that the individual average power (also termed reference value, RV) (Soekadar et al 2011) of the 1st run is used as reference time period for the computation of SMR-ERD for the following runs, thus following the design of an asynchronous BCI (Soekadar et al 2016). During the following two calibration runs, an individual SMR-ERD detection threshold was determined to provide meaningful online feedback. Detection threshold was set to the average of elicited SMR-ERD across all MI tasks (Soekadar et al 2016, Nann et al 2020). The resulting calibration parameters, i.e. RV and detection threshold, were used as input parameters for the two subsequent task runs and remained unaltered.

2.4. Analysis of HRV

For the analysis of HRV, a one-lead electrocardiography (ECG) was derived with disposable Ag-AgCl electrodes (COVIDIEN plc, Dublin, Ireland) from the outer clavicles according to Mason and Likar (1966). ECG was lowpass-filtered at 130 Hz including removal of 50 Hz line noise. Interbeat intervals (IBIs) were extracted and corrected, in case IBIs exceeded the average IBI value of a window comprising 20 previous and 20 following beats by 30% (von Tscharner and Zandiye 2017). Cleaned IBIs were resampled at 4 Hz by using a modified Akima cubic interpolation to obtain equidistant time series

(Camm *et al* 1996, Berntson *et al* 1997, Singh *et al* 2004). The resampled IBI time series was bandpass-filtered at 0.15–0.4 Hz resulting in a time series that only contained the HF-HRV component, which was found to reflect modulation in vagal tone (Malik and Camm 1993). To receive the final HRV outcome measure, standard deviation of the filtered IBI time series was computed. Similar to the Porges-Bohrer method (Lewis *et al* 2012), only variance of the frequency band of spontaneous breathing (HF band: 0.15–0.4 Hz) is evaluated. This has the advantage that other distracting sources of variance like blood pressure modulation (low-frequency band: 0.04–0.15 Hz) and non-stationary aperiodic trends (ultra-low-frequency band: <0.04 Hz) are removed resulting in increased signal-to-noise ratio. According to recent recommendations, no correction for respiration rate was performed since spontaneous breathing was present throughout the entire experiment (Thayer *et al* 2011, Laborde *et al* 2017). Since inter-individual distribution of HRV measures are usually strongly positively skewed, HRV values are ln-transformed to regain normal distribution for further parametric statistical analysis (Riniolo and Porges 2000).

2.5. Outcome measures

To capture temporal HRV changes within each experimental run (run length equals 500 s), HRV measures were computed based on overlapping 100 s windows iteratively shifted by 10 s. This results in a HRV time series with 41 data points per run. Estimating HRV measures on the basis of such relatively short observation windows (called ultra-short-term HRV measures) recently gained interest as it allows to study HRV changes with a higher temporal resolution compared to standard window lengths (5 min or 24 h) (Shaffer and Ginsberg 2017). There is growing evidence that such ultra-short-term HRV measures, especially the ones that are processed within the time-domain, e.g. the standard deviation of heart fluctuations, correlate with the clinically accepted short-term measures computed over a standard window length of 5 min (Muñoz *et al* 2015, Shaffer and Ginsberg 2017, Castaldo *et al* 2019).

The outcome measure for BCI performance was defined as the percentage of time the SMR-ERD detection threshold was exceeded during the MI task and not exceeded during the relax task relative to trial length. For offline SMR-ERD computation, the normalized instantaneous power modulation recorded during the online session was used (see section 2.3). To obtain the equal 100 s window length as for HRV data analysis, BCI performance measures were averaged across ten tasks (on average a task and a ITI resulted in 10 s duration). Shifting this window iteratively by 10 s results in a time series of 41 data points per run, equal to the length of the HRV time series.

For multilevel model analyses (see section 2.6) and plotting, both outcome measures were expressed as difference scores where values are subtracted from the 1st computed value of each run (representing difference to 1st 100 s) (Overbeek *et al* 2014). Looking at HRV reactivity instead of absolute values reveals within-participant short-term changes in each run and reduces undesired inter-individual variations, e.g. as age, gender or disease-related effects on HRV (Quintana and Heathers 2014, Laborde *et al* 2017).

2.6. Offline analysis

2.6.1. Multilevel model analysis

To investigate whether BCI performance as well as HRV changed over time and task difficulty, two separate multilevel models for each outcome measure were applied (Snijders and Bosker 1999, Raudenbush and Bryk 2002) using the package ‘nlme’ in R (Pinheiro *et al* 2013). Multilevel modeling is an extension of the linear regression analysis and constitutes a powerful and flexible method to analyze hierarchical and repeated-measures data (Muth *et al* 2012). In our study, the dependent variables ‘BCI performance’ and ‘HRV’ as outcome measures (level 1) were nested within ‘participants’ and ‘task difficulty’ residing at level 2. In addition, the predictor variables ‘time’ (41 continuous data points) and ‘task difficulty’ (two categorical levels: normal, hard) resided at level 1. Multilevel modeling can account for the lack of independence of the outcome measures within participants and is thus well suitable for a repeated-measures design. Additionally, unlike a repeated-measures ANOVA, the assumption of sphericity can be neglected. To account for the high autocorrelation of both outcome time series, which was caused by the moving windows, a 1st-order autoregressive covariance structure was modeled (Field *et al* 2012). Normality of residuals was checked by visual inspection with quantile-quantile plots (Q-Q plots) and scatter plots of fits vs residuals. To test for an overall effect of predictor variables onto the response variable, the model was compared with the baseline model (i.e. no predictors at levels 1 or 2) using a chi-square likelihood ratio test.

2.6.2. Granger-causality analysis

To test whether HRV predicted BCI control performance, Granger causality analysis was applied (Granger 1969). We tested whether the null hypothesis H_0 (HRV does not Granger-cause BCI control performance) could be rejected. However, Granger causality analysis can indicate spurious causality when one or both time series are non-stationary (He and Maekawa 2001). Since both outcome measures were assumed to change over time, i.e. they show a trend, non-stationarity of time series was presumed. Toda and Yamamoto (1995) introduced a method, which allows to test for Granger causality on non-stationary time series. This method is based on augmented vector autoregression (VAR) modeling and a modified

Wald test statistic and was shown to be superior to the original Granger test (R packages ‘vars’ and ‘aod’). The Toda–Yamamoto implementation to test for Granger causality was applied on time series on single participant level. To combine test statistics of all participants, Fisher’s combined probability test (Fisher’s method) was applied to perform a meta-analysis of *p*-values (Fisher 1925) (R package ‘metap’). Significance threshold for all statistical tests was assumed at *p* = .05.

3. Results

3.1. Changes of BCI performance over time

The comparison with the baseline model revealed a significant effect of ‘time’ and ‘task difficulty’ on ‘BCI performance’ ($\chi^2(2) = 401.60, p < .0001$). While there was no overall main effect of ‘time’ on ‘BCI performance’ ($b = -0.087$ [95% CI: −0.202, 0.029], $t(1324) = -1.47, p = 0.142$), there was a significant interaction of ‘time’ and ‘task difficulty’ ($b = -0.523$, [95% CI: −0.686, −0.359], $t(1324) = -6.27, p = 0$), indicating that ‘task difficulty’ affects the relationship between ‘time’ and ‘BCI performance’. To investigate the effect over ‘time’ for each run individually, interaction was resolved by conducting separate multilevel models for normal and hard ‘task difficulty’. The models were identical to the main model but excluded the main effect and interaction term of ‘task difficulty’. These analyses showed that during the normal run, there was no change in BCI performance over time ($b = -0.087$ [95% CI: −0.212, 0.039], $t(662) = -1.36, p = .176$). However, during the hard run, there was a strong decline in BCI performance over time ($b = -0.614$ [95% CI: −0.723, −0.504], $t(662) = -10.97, p = 0$). The gradient of the regression line implies an average decline in BCI performance of −0.6% per 10 s, which accumulates to an overall drop of −24% at the end of the hard run (compared to a non-significant decrease of −3.5% in total during the normal run, figure 2).

3.2. Changes of HRV over time

Equal to the analysis of BCI performance, there was a significant effect of ‘time’ and ‘task difficulty’ on ‘HRV’ ($\chi^2(2) = 94.71, p < .0001$), but no overall main effect of ‘time’ was found ($b = -0.002$ [95% CI: −0.006, 0.001], $t(1324) = -1.30, p = 0.193$). Even though not significant, there was a trend for ‘task difficulty’ affecting the relationship between ‘time’ and ‘HRV’ ($b = -0.004$ [95% CI: −0.009, 0.001], $t(1324) = -1.76, p = .079$). Therefore, interaction was again resolved to investigate effects over time for both levels of ‘task difficulty’. These analyses revealed that during the normal run, there was no change in HRV ($b = -0.002$ [95% CI: −0.005, 0.001], $t(662) = -1.42, p = 0.157$). During the hard run, however, HRV declined over time ($b = -0.007$

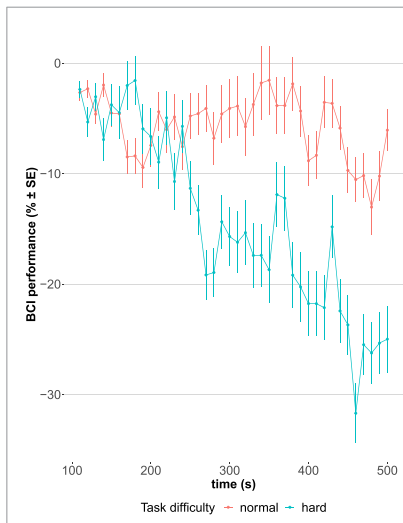


Figure 2. Change in BCI performance over time during runs with normal (red) and hard (blue) task difficulty level. Every run had a length of 500 s. Each point represents an average value (with error bars showing standard error, SE) across participants based on a 100 s window. Time series was generated by moving windows iteratively shifted by 10 s. First value of time series was computed based on the 1st 100 s and utilized as reference value for difference score calculation (i.e. subsequent values are subtracted from the 1st computed value).

[95% CI: −0.01, −0.003], $t(662) = -3.40, p < .001$, figure 3). Thus, HRV shows the same behavior over time as BCI performance indicating that decline in HRV is specific to a decline in BCI performance.

3.3. Time series prediction

Test statistic based on the Fisher’s method showed that HRV Granger-caused BCI control performance considering all participants including both levels of task difficulty ($\chi^2(68) = 997.9, p < .0001$). All *p*-values except one were highly significant according to the Toda–Yamamoto implementation. Figure 4 shows the time series of HRV and BCI performance of one participant exemplarily. Only results for one participant did not reject the null hypothesis during a run with normal task difficulty (*p* = .22). In 30 out of 34 runs, the lag was determined at lag = 1 indicating that HRV precedes BCI control performance by 10 s. In only four cases lags were larger with up to 70 s. However, it should be noted that 10 s was the lowest resolvable time interval as duration of one task trial (5 s) in combination with a subsequent ITI (randomized between 4 and 6 s) was on average 10 s long. Therefore, windows were shifted by 10 s each and thus determined the respective time resolution.

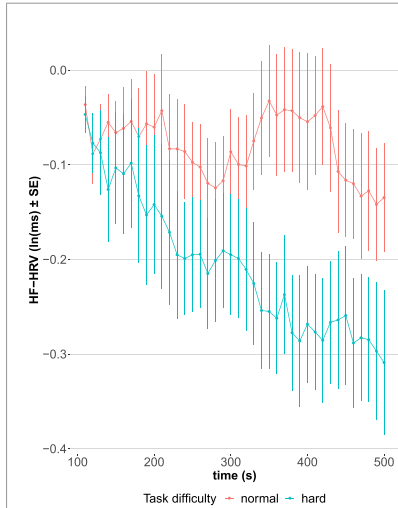


Figure 3. Change in natural logarithm (ln)-transformed HF-HRV over time during runs with normal (red) and hard (blue) task difficulty level. Every run had a length of 500 s. Each point represents an average value (with error bars showing SE) across participants based on a 100 s window. Time series was generated by moving windows iteratively shifted by 10 s. First value of time series was computed based on the 1st 100 s and utilized as reference value for difference score calculation (i.e. subsequent values are subtracted from the 1st computed value).

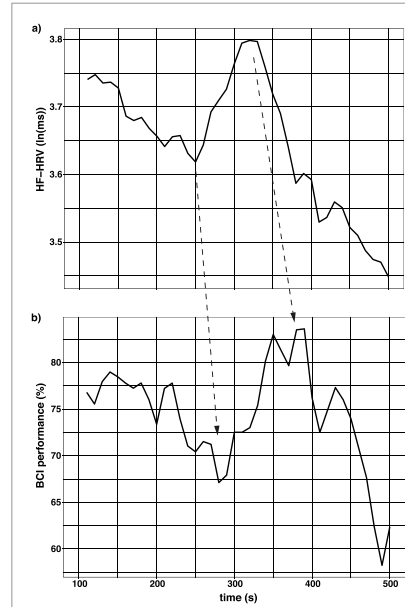


Figure 4. Time series of: (a) HF-HRV and (b) BCI performance of one participant. Dashed arrows highlight fiducial turning points, where predictive characteristics of HRV is apparent.

4. Discussion

It was shown that SMR-ERD-based brain/neural hand exoskeletons are promising tools to trigger neural recovery after stroke or spinal cord injury. However, BCI control tasks, e.g. MI or attempting to move the paralyzed fingers, are cognitively demanding and can thus lead to inattention and fatigue, especially in stroke survivors suffering from cognitive impairments and post-stroke fatigue. As a consequence, BCI performance deteriorates over time causing frustration and reduced motivation to engage BCI control on a regular basis. Currently, there is no standardized strategy in the BCI field to anticipate decline in SMR-ERD BCI control performance online and to adapt the control paradigm accordingly. Even though numerous studies have shown that changes in HRV are closely linked to cognitive processes (Thayer *et al* 2009, Overbeek *et al* 2014, Stuiver *et al* 2014), it was unknown whether HRV can predict BCI control performance within a single session.

We found that during the 1st run with normal task difficulty, BCI performance over time remained unchanged ($p = .176$). However, there was a decline by $-0.6\%/10$ s ($p = 0$) during the 2nd, more difficult run (task difficulty gradually increased,

figure 2). Since only healthy and well-performing participants were selected in a pre-screening process (see section 2.1), a decline in performance during the 1st run, e.g. due to fatigue, was not expected. However, the slight trend ($-0.09\%/10$ s) indicates that prolonged use would most likely lead to a significant decrease, too. The strong decline in the 2nd run confirms sufficient gradual decrease of SMR-ERD detection threshold. Of course, such extreme increase in task difficulty does not reflect a normal BCI training situation, but should simulate a state of increasing exhaustion, which stroke survivors often experience during cognitive tasks due to post-stroke fatigue. The reported performance drop of $\sim 24\%$ at the end of the hard run is comparable to studies that investigated critical declines in BCI performance. For instance, Vourvopoulos *et al* (2019) reported a decrease of up to $\sim 37\%$ in a virtual reality-based MI-BCI study with chronic stroke survivors and Käthner *et al* (2014) presented a study, in which manipulation of task difficulty resulted in an average decrease in BCI performance of up to $\sim 30\%$ in healthy subjects. Equal to the results of BCI performance, HRV was unaltered during the normal run ($p = .157$) but attenuated almost linearly within the 2nd run ($p < .001$, figure 3). These results demonstrate the specificity of HRV changes relative to BCI performance.

Further, causality analysis revealed that HRV Granger-causes BCI performance ($p < .001$) for both levels of task difficulty. The results suggest that HRV is a specific biomarker to predict decline in BCI performance. Our results show, for the 1st time, that HRV has predictive value to forecast within-session decline in BCI control performance.

In this context, it should be noted that Granger causality does not proof causality in the more general sense (Bunge 2017); i.e. that a decline in HRV directly causes a decline in BCI performance.

Even though this study cannot proof causality, our findings suggest a relationship in line with the Yerkes–Dodson law (Yerkes and Dodson 1908). Our results suggest that increased cognitive demand due to increased task difficulty result in decreased vagal activity preceding decline in BCI performance. Changes in HRV were likely mediated by top-down control of efferent neurons linked to decreased parasympathetic activation relative to a normal baseline (Shaffer *et al* 2014). Subsequent performance decline might be explained by bottom-up control via afferent neurons. Involving the locus coeruleus (LC), which is known to be linked with the vagus nerve (Mather *et al* 2017) and the anterior cingulate cortex (ACC) (Aston-Jones and Cohen 2005), Tervo *et al* (2014) showed that depending on the LC input to ACC, cognitive control strategies might be switched from a strategic mode based on learned models to a stochastic exploitative mode exploring new models. The potential bottom-up mechanism including a switch in behavioral modes might be an explanation why vagal suppression preceded decline in SMR control performance.

Besides these potential mechanisms, it cannot be excluded that change in HRV had also a direct impact on brain dynamics influencing SMR control as it was shown that HRV biofeedback or training can influence EEG power spectra (Reid *et al* 2013, Dassy *et al* 2020). After it was shown that mindfulness meditation can increase BCI performance (Tan *et al* 2014), it seems likely that interoception plays an important role for SMR control, or potentially any form of self-regulation. To untangle the causal relationship between HRV, interoception and SMR control, further studies are necessary that purposefully modulate afferent input, e.g. using vagus nerve stimulation.

Our findings have substantial implications on novel neuroadaptive control paradigms to individualize and optimize stroke neurorehabilitation protocols. HRV as potential control parameter for adaptation has several advantages. In contrast to EEG-based monitoring, e.g. for workload, heartbeat analysis is very simple to record and to analyze. While EEG measures usually require a time-consuming calibration to account for inter-individual variations in topographical and frequency representations of

fatigue, heartbeat and for HRV analysis relevant R-peaks detection equals among all humans. To utilize this measure for individual adaptions, a baseline in HRV can easily be determined by expressing the measure as ratio score relative to task onset and define a critical linear threshold, e.g. -5% to task onset. Hence, no time-intensive calibration is necessary. A shortcoming of this study was that ECG was recorded according to the standard lead I representation of Einthoven and is, thus, not optimal for daily home use. However, since heartbeat is one of the strongest biosignals in the human body, it is very easy to record this measure with wearables at well accessible positions, e.g. at the wrist or even at the head, e.g. by using EEG headsets with integrated ECG recording channels (Ahn *et al* 2019, Rosenberg *et al* 2016, von Rosenberg *et al* 2017).

Closed-loop neuroadaptive technology was shown to improve user performance in demanding human–computer interaction tasks. Faller *et al* (2019) showed that flight duration in a boundary-avoidance task was prolonged when dynamically adjusted EEG-based auditory neurofeedback reduced individual's arousal state. They argued that a reduction in arousal improves performance according to the right side of the Yerkes and Dodson law (Yerkes and Dodson 1908). Importantly, the study showed that HRV increased again when arousal was downregulated by the user based on individual neurofeedback. While in our open-loop study, the opposite effect on the right side of the Yerkes and Dodson law was investigated, i.e. decrease in performance and HRV, Faller's study indicates that HRV is suitable for closed-loop applications as HRV recovered instantaneously when arousal was reduced (Lehrer and Gevirtz 2014, Faller *et al* 2019).

Further studies are needed to investigate how to use and process predictive HRV information. One possibility is an open-loop system to simply interrupt or stop the BCI training as soon as the user exceeds a predefined critical HRV attenuation threshold. This would avoid frustrating and enhance rewarding experiences, e.g. to increase motivation for further training sessions. Another possibility is a closed-loop system where the BCI control paradigm is dynamically adapted. Several approaches for adaption are conceivable: adjusting classification thresholds, recalibrating the BCI system on the fly, or applying external stimuli. It was shown, for example, that vibro-tactile feedback time-locked to heartbeat has a calming effect and might help to stabilize BCI performance (Azevedo *et al* 2017). Nevertheless, both methods, open-loop or closed-loop, are promising to individualize BCI stroke training.

It should be noted that only the right side of the Yerkes and Dodson law was investigated. This means the behavior of HRV was only evaluated when BCI performance decreased. This was achieved

by the pre-screening procedure ensuring to have a homogenous group of relatively good performers who decline in control performance over time. Contrary to this, it would be very interesting to look at the left side of the inverted u-shape, expecting that low arousal, e.g. boredom or no engagement during the task at all, also reduces performance output. Thus, a slight reduction in HRV, which was often associated with mental effort (Aasman *et al* 1987), could be interpreted as task motivation and linked with a positive rewarding feedback to the user. Another possible limitation of an HRV-adaptive closed-loop system could relate to be the altered autonomic nervous system after stroke (Dorrance and Fink 2011). It is unclear whether or to what extend our results can be generalized to patient populations. Stroke survivors, e.g. show cardiac abnormalities and have in general reduced HRV (Gujar *et al* 2004). To account for such low HRV, high ECG sampling rate is suggested (Berntson *et al* 1997). Further studies are needed to evaluate the implication of such pathophysiological effects and to validate our results in various patient populations. Moreover, also neuroethical dimensions of such integrated brain/neural interfaces should be considered (Clausen *et al* 2017), particularly, when advancing such systems towards hybrid minds that increasingly merge biological and artificial cognitive systems (Soekadar *et al* 2021).

5. Conclusion

The here presented study shows that HRV can predict decline in SMR-based BCI performance. The predictive characteristics of HRV is an important prerequisite for the development of neuro-adaptive BCI control paradigms, e.g. in stroke neurorehabilitation. Optimized BCI training based on individual changes in HRV can account for patient-dependent cognitive capabilities to potentially enhance rehabilitation efficacy. Moreover, it can contribute to sustain high levels of motivation during assistive BCI applications. Implementation and validation of such neuro-adaptive technology in an online BCI control paradigm is on the way.

Data availability statement

The data that support the findings of this study are available upon reasonable request from the authors.

Acknowledgments

This research was supported by the European Research Council (ERC-2017-STG-759370), the Einstein Foundation Berlin and the BMBF (NEO, 13GW0483C). The authors declare that the research was conducted in the absence of any commercial or financial relationships that could be construed as a potential conflict of interest.

Ethical statement

All able-bodied participants gave written informed consent before entering the study. The study protocol was in line with the Declaration of Helsinki and was approved by the local ethics committee at the University of Tübingen (registration code of ethical approval: 201/2018BO1).

ORCID iDs

- Marius Nann  <https://orcid.org/0000-0002-8936-944X>
 David Haslacher  <https://orcid.org/0000-0003-4380-3922>
 Bjoern Eskofier  <https://orcid.org/0000-0002-0417-0336>
 Vinzenz von Tscharner  <https://orcid.org/0000-0002-5779-6244>
 Surjo R Soekadar  <https://orcid.org/0000-0003-1280-5538>

References

- Aasman J, Mulder G and Mulder L J 1987 Operator effort and the measurement of heart-rate variability *Hum. Factors* **29** 161–70
 Acciaresi M, Bogousslavsky J and Paciaroni M 2014 Post-stroke fatigue: epidemiology, clinical characteristics and treatment *Eur. Neurol.* **72** 255–61
 Ahn J W, Ku Y and Kim H C 2019 A novel wearable EEG and ECG recording system for stress assessment *Sensors* **19** 1991
 Ang K K, Chua K S G, Phua K S, Wang C, Chin Z Y, Kuah C W K, Low W and Guan C 2015 A randomized controlled trial of EEG-based motor imagery brain-computer interface robotic rehabilitation for stroke *Clin. EEG Neurosci.* **46** 310–20
 Ang K K, Chua K S G, Chua K S G, Ang B T, Kuah C W K, Wang C, Phua K S, Chin Z Y and Zhang H 2011 A large clinical study on the ability of stroke patients to use an EEG-based motor imagery brain-computer interface *Clin. EEG Neurosci.* **42** 253–8
 Aston-Jones G and Cohen J D 2005 An integrative theory of locus coeruleus-norepinephrine function: adaptive gain and optimal performance *Annu. Rev. Neurosci.* **28** 403–50
 Azevedo T, Bennett R, Billicki N, Hooper A, Markopoulou J F and Tsakiris M 2017 The calming effect of a new wearable device during the anticipation of public speech *Sci. Rep.* **7** 2285
 Bai Z, Fong K N K, Zhang J J, Chan J and Ting K H 2020 Immediate and long-term effects of BCI-based rehabilitation of the upper extremity after stroke: a systematic review and meta-analysis *J. Neuroeng. Rehabil.* **17** 57
 Beffara B, Bret A G, Vermeulen N and Mermilliod M 2016 Resting high frequency heart rate variability selectively predicts cooperative behavior *Physiol. Behav.* **164** 417–28
 Berntson G G *et al* 1997 Heart rate variability: origins, methods, and interpretive caveats *Psychophysiology* **34** 623–48
 Birbaumer N and Cohen L G 2007 Brain-computer interfaces: communication and restoration of movement in paralysis *J. Physiol.* **579** 621–36
 Blankertz B, Sannelli C, Halder S, Hammer E M, Kübler A, Müller K-R, Curio G and Dickhaus T 2010 Neurophysiological predictor of SMR-based BCI performance *Neuroimage* **51** 1303–9
 Bunge M 2017 *Causality and Modern Science* (New York: Routledge) (<https://doi.org/10.4324/9781315081656>)
 Cameron O G 2001 *Visceral Sensory Neuroscience: Interception* (Oxford: Oxford University Press)

- Camm A J, Malik M, Bigger J T, Breithardt G, Cerutti S, Cohen R J, Coumel P, Fallen E L, Kennedy H I and Kleiger R 1996 Heart rate variability: standards of measurement, physiological interpretation and clinical use Task force of the European Society of Cardiology and the North American Society of Pacing and Electrophysiology
- Castaldo R, Montesinos L, Mellilo P, James C and Peccia L 2019 Ultra-short term HRV features as surrogates of short term HRV: a case study on mental stress detection in real life *BMC Med. Inform. Decis. Mak.* **19** 12
- Cervera M A, Soekadar S R, Ushiba J, Millan J D R, Liu M, Birbaumer N and Garipelli G 2018 Brain-computer interfaces for post-stroke motor rehabilitation: a meta-analysis *Ann. Clin. Transl. Neurol.* **5** 651–63
- Christensen D, Johnsen S P, Watt T, Harder I, Kirkevold M and Andersen G 2006 Dimensions of post-stroke fatigue: a two-year follow-up study *Cerebrovasc. Dis.* **26** 134–41
- Clausen J, Fetz E, Donoghue J, Ushiba J, Sporhusse U, Chandler J, Birbaumer N and Soekadar S R 2017 Help, hope, and hype: ethical dimensions of neuroprosthetics *Science* **356** 1338–9
- Curran E A and Stoke M J 2003 Learning to control brain activity: a review of the production and control of EEG components for driving brain-computer interface (BCI) systems *Brain Cogn.* **51** 326–36
- Dessy E, Mairesse O, van Puyvelde M, Cortoos A, Neyt X and Pattyn N 2020 Train your brain? Can we really selectively train specific EEG frequencies with neurofeedback training *Front. Hum. Neurosci.* **14** 22
- Dorrance A M and Fink G 2011 Effects of stroke on the autonomic nervous system *Compr. Physiol.* **5** 1241–63
- Duschek S, Muckenthaler M, Werner N and del Paso G A 2009 Relationships between features of autonomic cardiovascular control and cognitive performance *Biol. Psychol.* **81** 110–7
- Faller J, Cummings J, Saproo S and Sajda P 2019 Regulation of arousal via online neurofeedback improves human performance in a demanding sensory-motor task *Proc. Natl Acad. Sci. USA* **116** 6482–90
- Field A, Miles J and Field Z 2012 *Discovering Statistics Using R* (London: Sage Publications)
- Fisher R 1925 *Statistical Methods for Research Workers* (Edinburgh: Oliver and Boyd)
- Foong R, Ang K K, Quek C, Guan C, Phua K S, Kuah C W K, Deshmukh V A, Yam L H L, Rajeswaran D K and Tang N 2019 Assessment of the efficacy of EEG-based MI-BCI with visual feedback and EEG correlates of mental fatigue for upper-limb stroke rehabilitation *IEEE Trans. Biomed. Eng.* **67** 786–95
- Frolov A A, Hušek D A, Biryukova E V, Bobrov P D, Mokienko O A and Alexandrov A 2017a Principles of motor recovery in post-stroke patients using hand exoskeleton controlled by the brain-computer interface based on motor imagery *Neural Netw. World* **27** 107
- Frolov A A, Mokienko O, Lyukmanov R, Biryukova E, Kotov S, Turbin I, Nadareishvily G and Bushkova Y 2017b Post-stroke rehabilitation training with a motor-imagery-based brain-computer interface (BCI)-controlled hand exoskeleton: a randomized controlled multicenter trial *Front. Neurosci.* **11** 400
- Gerjets P, Walter C, Rosentiel W, Bogdan M and Zander T O 2014 Cognitive state monitoring and the design of adaptive instruction in digital environments: lessons learned from cognitive workload assessment using a passive brain-computer interface approach *Front. Neurosci.* **8** 385
- Granger C W 1969 Investigating causal relations by econometric models and cross-spectral methods *Econ. J. Econ. Soc.* **37** 424–38
- Grosse-Wentrup M and Schölkopf B 2012 High gamma-power predicts performance in sensorimotor-rhythm brain-computer interfaces *J. Neural Eng.* **9** 046001
- Gujar A R, Sathyapraba T N, Nagaraja D, Thennarasu K and Pradhan N 2004 Heart rate variability and outcome in acute severe stroke *Neurocrit. Care* **1** 347–53
- Hammer E M, Halder S, Blankertz B, Sannelli C, Dickhaus T, Kleih S, Müller K-R and Kübler A 2012 Psychological predictors of SMR-BCI performance *Biol. Psychol.* **89** 80–6
- He Z and Maekawa K 2001 On spurious Granger causality *Econ. Lett.* **73** 307–13
- Hogervorst M A, Brouwer A-M and van Erp J B F 2014 Combining and comparing EEG, peripheral physiology and eye-related measures for the assessment of mental workload *Front. Neurosci.* **8** 322
- Kathine I, Wiessnegger S C, Müller-Putz G R, Kübler A and Halder S 2014 Effects of mental workload and fatigue on the P300, alpha and theta band power during operation of an ERP (P300) brain-computer interface *Biol. Psychol.* **102** 118–29
- Kaufmann T, Vogele C, Sutterlin S, Lukito S and Kubler A 2012 Effects of resting heart rate variability on performance in the P300 brain-computer interface *Int. J. Psychophysiol.* **83** 336–41
- Klaproth O W, Halbrügge M, Kröll L R, Vernaleken C, Zander T O and Russwinkel N 2020 A neuroadaptive cognitive model for dealing with uncertainty in tracing pilots' cognitive state *Top. Cogn. Sci.* **12** 1012–29
- Klimesch W 1999 EEG alpha and theta oscillations reflect cognitive and memory performance: a review and analysis *Brain Res. Rev.* **29** 169–95
- Laborde S, Mosley E and Thayer J F 2017 Heart rate variability and cardiac vagal tone in psychophysiological research—recommendations for experiment planning, data analysis, and data reporting *Front. Psychol.* **8** 213
- Lang C E, Strube M J, Bland M D, Waddell K J, Cherry-Allen K M, Nudo R J, Dromerick A W and Birkemeier R L 2016 Dose response of task-specific upper limb training in people at least 6 months poststroke: a phase II, single-blind, randomized, controlled trial *Ann. Neurol.* **80** 342–54
- Lehrer P M and Gevirtz R 2014 Heart rate variability biofeedback: how and why does it work? *Front. Psychol.* **5** 756
- Levy M N 1990 Autonomic interactions in cardiac control a *Ann. New York Acad. Sci.* **601** 209–21
- Lewis G F, Furman S A, McCool M F and Porges S W 2012 Statistical strategies to quantify respiratory sinus arrhythmia: are commonly used metrics equivalent? *Biol. Psychol.* **89** 349–64
- Malik M and Camm A J 1993 Components of heart rate variability—what they really mean and what we really measure? *Am. J. Cardiol.* **72** 821–2
- Mason R E and Likar I 1966 A new system of multiple-lead exercise electrocardiography *Am. Heart J.* **71** 196–205
- Mather M, Yoo J O O, Clewett H, Lee D V, Greening T-H, Ponzig S G, Min A J and Thayer J F 2017 Higher locus coeruleus MRI contrast is associated with lower parasympathetic influence over heart rate variability *NeuroImage* **150** 329–35
- Maziarz M 2015 A review of the Granger-causality fallacy *J. Phil. Econ. Reflections Econ. Soc. Issues* **8** 86–105
- McFarland D J 2015 The advantages of the surface Laplacian in brain-computer interface research *Int. J. Psychophysiol.* **97** 271–6
- Mehler B, Reimer B, Coughlin J F and Dusek J A 2009 Impact of incremental increases in cognitive workload on physiological arousal and performance in young adult drivers *Transp. Res. Rec.* **2138** 6–12
- Munoz M L et al 2015 Validity of (ultra-)short recordings for heart rate variability measurements *PLoS One* **10** e0138921
- Muth E R, Moss J D, Rosopa P J, Salley J N and Walker A D 2012 Respiratory sinus arrhythmia as a measure of cognitive workload *Int. J. Psychophysiol.* **83** 96–101
- Myrdén A and Chau T 2015 Effects of user mental state on EEG-BCI performance *Front. Hum. Neurosci.* **9** 308
- Nann M, Peekhaus N, Angerhöfer C and Soekadar S R 2020 Feasibility and safety of bilateral hybrid EEG/EOG brain/neural-machine interaction *Front. Hum. Neurosci.* **14** 580105

- Overbeek T J, van Boxtel A and Westerink J H 2014 Respiratory sinus arrhythmia responses to cognitive tasks: effects of task factors and RSA indices *Biol. Psychol.* **99** 1–14
- Pfurtscheller G and Aranibar A 1979 Evaluation of event-related desynchronization (ERD) preceding and following voluntary self-paced movement *Electroencephalogr. Clin. Neurophysiol.* **46** 138–46
- Pinheiro J, Bates D, Debray S, Sarkar D and Team R C 2013 nlme: linear and nonlinear mixed effects models *R Package Version 3*, 111
- Quintana D S and Heathers J A J 2014 Considerations in the assessment of heart rate variability in biobehavioral research *From Psychol.* **5** 805
- Ramos-Murgulday A, Broetz D, Rea M, Laer L and Yilmaz O et al 2013 Brain–computer interface (BCI) in chronic stroke: a controlled study *Ann Neurol.* **74** 100–8
- Raudenbush S W and Bryk A S 2002 *Hierarchical Linear Models: Applications and Data Analysis Methods* (Thousand Oaks: Sage)
- Reid A, Nihon S, Thompson L and Thompson M 2013 The effects of heart rate variability training on sensorimotor rhythm: a pilot study *J. Neurother.* **17** 43–8
- Riniolo T C and Porges S W 2000 Evaluating group distributional characteristics why psychophysiologicalists should be interested in qualitative departures from the normal distribution? *Psychophysiology* **37** 21–8
- Rosenberg V O N, Chanwimalueang W, Goverdovsky T, Looney V, Sharp D and Mandic D P 2016 Smart helmet: wearable multichannel ECG and EEG *IEEE J. Transl. Eng. Health Med.* **4** 2700111
- Rowe D W, Silbert J and Irwin D 1998 Heart rate variability: indicator of user state as an aid to human–computer interaction *Proc. SIGCHI Conf. on Human Factors in Computing Systems* (ACM Press/Addison-Wesley Publishing Co) pp 480–7
- Schalk G, McFarland D J, Hinterberger T, Birbaumer N and Wolpaw J R 2004 BCI2000: a general-purpose brain–computer interface (BCI) system *IEEE Trans. Biomed. Eng.* **51** 1034–43
- Schultze-Kraft M, Birman D, Rusconi M, Allefeld C, Gorgen K, Dahne S, Blankertz B and Haynes J D 2016 The point of no return in vetoing self-initiated movements *Proc. Natl Acad. Sci. USA* **113** 1080–5
- Seth A K, Barrett A B and Barnett L 2015 Granger causality analysis in neuroscience and neuroimaging *J. Neurosci.* **35** 3293–7
- Shaffer F and Ginsberg J P 2017 An overview of heart rate variability metrics and norms *Front. Public Health* **5** 258
- Shaffer F, McCraty R and Zerr C L 2014 A healthy heart is not a metronome: an integrative review of the heart's anatomy and heart rate variability *Front. Psychol.* **5** 1040
- Singh D, Vinod K and Saxena S C 2004 Sampling frequency of the RR interval time series for spectral analysis of heart rate variability *J. Med. Eng. Technol.* **28** 263–72
- Snijders T A and Bosker R J 1999 *An Introduction to Basic and Advanced Multilevel Modeling* (London: Sage)
- Wong G Y and Mason W M 1985 The hierarchical logistic regression. Model for multilevel analysis *J. Am. Stat. Assoc.* **80** 13–524
- Sockadar S R et al 2016 Hybrid EEG/EOG-based brain/neural hand exoskeleton restores fully independent daily living activities after quadriplegia *Sci. Robot.* **1** eaag3296
- Sockadar S R 2020 Gehirn-computer Schnittstellen zur Verbesserung von Lebensqualität und sozialer Teilhabe *Altern: Biologie Und Chancen* ed A Ho (Berlin: Springer)
- Sockadar S R, Birbaumer N, Slutsky M W and Cohen L G 2015 Brain–machine interfaces in neurorehabilitation of stroke *Neurobiol. Dis.* **83** 172–9
- Sockadar S R, Chandler J, Ienca M and Bublitz C 2021 On the verge of the hybrid mind *Morals Mach.* **1** 30–43
- Sockadar S R, Nann M, Cres S, Trigili E, Gómez C, Opisso E, Cohen L G, Birbaumer N and Vitello N 2019 Restoration of finger and arm movements using hybrid brain/neural assistive technology in everyday life environments *Brain–Computer Interface Research, A State-of-the-Art Summary* 7 ed C Guger, N M K Brendan and Z Allison (Cham: Springer International Publishing) (https://doi.org/10.1007/978-3-030-05668-1_5)
- Sockadar S R, Witkowski M, Mellinger J, Ramos A, Birbaumer N and Cohen L G 2011 ERD-based online brain–machine interfaces (BMI) in the context of neurorehabilitation: optimizing BMI learning and performance *IEEE Trans. Neural. Syst. Rehabil. Eng.* **19** 542–9
- Sockadar S and Nann M 2020 Neural-gesteuerte robotik für assistenz und rehabilitation im alltag *Mensch-Roboter-Kollaboration* ed H J Buxbaum (Wiesbaden: Springer Gabler)
- Stefan K, Wyćisło M and Classen J 2004 Modulation of associative human motor cortical plasticity by attention *J. Neurophysiol.* **92** 66–72
- Stuiver A, Brookhuis K A, de Waard D and Mulder B 2014 Short-term cardiovascular measures for driver support: increasing sensitivity for detecting changes in mental workload *Int. J. Psychophysiol.* **92** 35–41
- Tan L-F, Dienes Z, Jansari A and Goh S-Y 2014 Effect of mindfulness meditation on brain–computer interface performance *Conscious. Cogn.* **23** 12–21
- Tervo D R, Proskurnin M, Manakov M, Kabra M, Vollmer A, Branson K and Karpova A Y 2014 Behavioral variability through stochastic choice and its gating by anterior cingulate cortex *Cell* **159** 21–32
- Thayer J F, Hansen A L, Saus-Rose E and Johnsen B H 2009 Heart rate variability, prefrontal neural function, and cognitive performance: the neurovisceral integration perspective on self-regulation, adaptation, and health *Ann. Behav. Med.* **37** 141–53
- Thayer J F and Lane R D 2009 Claude Bernard and the heart–brain connection: further elaboration of a model of neurovisceral integration *Neurosci. Biobehav. Rev.* **33** 81–8
- Thayer J F, Loerbroks A and Sternberg E M 2011 Inflammation and cardiorespiratory control: the role of the vagus nerve *Respir. Physiol. Neurobiol.* **178** 387–94
- Toda H Y and Yamamoto T 1995 Statistical inference in vector autoregressions with possibly integrated processes *J. Econom.* **66** 225–50
- von Rosenberg W, Chanwimalueang T, Goverdovsky V, Peters N S, Papavassiliou C and Mandic D P 2017 Hearables: feasibility of recording cardiac rhythms from head and in-ear locations *R. Soc. Open Sci.* **4** 171214
- von Tscharner V and Zandiyeh P 2017 Multi-scale transitions of fuzzy sample entropy of RR-intervals and their phase-randomized surrogates: a possibility to diagnose congestive heart failure *Biomed. Signal Process. Control* **31** 350–6
- Vourvopoulos A, Pardo O M, Lefebvre S, Neureither M, Saldana D, Jahng E and Liew S-L 2019 Effects of a brain–computer interface with virtual reality (VR) neurofeedback: a pilot study in chronic stroke patients *Front. Hum. Neurosci.* **13** 210
- Wiener N 1956 The Theory of Prediction *Modern Mathematics for Engineers Beckbeck E F* New York: McGraw-Hill
- Yerkes R M and Dodson J D 1908 The relation of strength of stimulus to rapidity of habit formation *J. Comparative Neurol. Psychol.* **18** 459–82
- Young B M et al 2015 Dose-response relationships using brain–computer interface technology impact stroke rehabilitation *Front. Hum. Neurosci.* **9** 361
- Zander T O and Kothe C 2011 Towards passive brain–computer interfaces: applying brain–computer interface technology to human–machine systems in general *J. Neural Eng.* **8** 025005

3. Discussion

Brain-controlled assistive neurotechnology promise substantial enhancements in severe and chronic upper limb paralysis after stroke or cervical SCI, because no standardized therapy is currently available for those cases, i.e., approximately one third of all stroke survivors (Ullberg et al., 2015; Wolfe et al., 2011) and almost all tetraplegics (Aarabi et al., 2021). For these individuals, conventional rehabilitation methods are neither applicable nor effective, because the required residual motor capabilities are lacking. However, before novel assistive neurotechnology can be broadly utilized as alternative treatment approach in clinical settings or even for in-home use, important prerequisites have to be achieved. Therefore, this doctoral thesis deals with the scientific question how brain/neural-machine interfaces (B/NMI) for upper limb motor restoration can be improved in terms of applicability, reliability and robustness towards a broad use for assistive and rehabilitative purposes. Thereon, three specific objectives were derived.

First, we investigated whether B/NMI whole-arm exoskeleton control in severe hemiplegia after chronic stroke is intuitive, feasible and safe. Control of whole-arm exoskeletons with several degree of freedoms requires usually a large amount of control commands. To compensate for the limited bandwidth of non-invasive B/NMI, a shared control was introduced merging the EEG/EOG-based B/NMI control with context-aware (vision-guided) robotics. With this approach we could show that naïve able-bodied users as well as hemiplegic stroke survivors were able to control a whole-arm exoskeleton while successfully conducting a drinking task, which was exemplarily implemented as an important basal ADL (Crea et al., 2018; Marius Nann et al., 2021). These studies documented feasibility and safety of such EEG/EOG-controlled semiautonomous whole-arm exoskeleton in chronic stroke.

The implemented shared control based on a finite state machine divides an ADL in meaningful and purposeful sub-tasks allowing each of them to be individually initialized as well as aborted with EEG/EOG-based control commands. This approach, a trade-off between automation and control, fosters

self-efficacy and user acceptance, in particular, by giving the users the opportunity to always abort/veto an ongoing movement (Clausen et al., 2017). This is a crucial advantage in contrast to similar approaches. For instance, Barsotti et al. (2015) presented a SMR-based whole-arm exoskeleton control, but used volitional SMR modulation only to once initially trigger an entirely predefined sequence of exoskeleton movements without any subsequent control/abort possibilities for the user.

The modular setup of the suggested approach allows to implement all kinds of further ADLs including a different functional link of EEG/EOG control commands. In the presented studies, EEG-based volitional SMR modulation was assigned to grasping and releasing motions of the hand exoskeleton, whereas EOG-based horizontal eye movements initiated reaching as well as placing back movements of the shoulder/elbow exoskeleton. We reasoned that this is a good trade-off between intuitiveness and ease of use as well as considerations related to source location of electric brain activity specific to motor related SMR modulations. It was shown that hand muscles over the motor cortex are larger and more lateralized represented than shoulder and upper-arm muscles (Penfield & Boldrey, 1937; Schieber, 2001; Stancak et al., 2000). This fact facilitated reliable detection of hand movement intention.

However, before the presented control approach can be generalized and applied to various ADL scenarios, whole-arm exoskeletons need to be further technically improved. Current systems have still a limited working area, which means that objects have to be placed close to the user limiting the implementation of more complex ADL tasks. Recently, new exoskeletons have entered the commercial market, but were mainly developed for weak or flaccid spasticity, e.g., like after SCI (Mekki et al., 2018). Active motorized devices that are explicitly designed for severe chronic spasticity in the upper limb after stroke are still not commercially available, and can only be found as prototypes in research.

Nevertheless, our modular control approach is a multi-purpose interface, which can be coupled to all kind of different and possible in future available assistive whole-arm exoskeletons.

As second objective, we investigated whether bilateral B/NMI control after cervical SCI is feasible and safe. In contrast to stroke survivors, hand motor function in tetraplegia is absent at both upper extremities. Therefore, unilateral restoration of hand function after SCI is insufficient as most activities of daily living involve bimanual manipulation, e.g., to eat with fork and knife or to open the lid of a bottle. While many classification algorithms were developed to classify multiple states mainly in offline settings, e.g., to distinguish all four extremities against each other (Lotte et al., 2018), these classifiers have been rarely applied in clinically relevant online applications. A possible reason could be that classification accuracies still ranged insufficiently low in such online settings and thus limited purposeful use. Another issue among SCI survivors is that they often show less lateralization (Dahlberg et al., 2018; Osuagwu et al., 2016), so that classification algorithms relying on lateralized brain activity are unsuitable, e.g., to distinguish left or right motor activity.

The novelty of our approach was to complement the established EEG-based grasping and EOG-based releasing or stop commands (Soekadar et al., 2016) with a novel EOG command, a prolonged horizontal eye movement (>1 s) to the left or to the right, reliably switching laterality to activate either the left or right exoskeleton. With this method, we documented fluent initialization of grasping motions in healthy subjects and tetraplegics, as well as safe use as unintended grasping could be stopped before a full motion was conducted. Novel bilateral control showed an increased accuracy by approximately 20 % compared to a standard bilateral classification without prolonged EOG command in tetraplegics (Nann et al., 2020). This result confirms the effectiveness of the novel bilateral B/NMI control paradigm and underlines the necessity to account for the reduced lateralization in brain activity after SCI.

A major limitation of the study was that participants performed the complex bimanual sequence only with two virtual exoskeletons receiving online visual feedback on a screen because two equally-built hand exoskeletons for the left and right hand were not available at the time of the experiment. Nevertheless, the significance of the study is not mitigated by this circumstance.

The implemented threshold-based detection method for the prolonged horizontal eye movements requires very low-frequency information (<0.02 Hz) of the used bipolar EOG signal. This limits to a certain extend the daily life applicability as such low-frequency signals are prone to be susceptible for movement artefacts, e.g., induced by head movements. To overcome this issue, new EOG features could be implemented that do not depend on this low frequency band. Another strategy could be to integrate more intelligence into the hand exoskeletons by integrating an automatic object recognition in each hand. This means that activation of left or right exoskeleton is done by context-aware sensorics. Thanks to the modularity of the suggested B/NMI control paradigm, such alternative setups could be easily implemented.

As last objective, we investigated whether heart rate variability (HRV) is applicable as biomarker to predict declining SMR control performance. The goal was to find a biomarker that reflects a negative overall trend in performance within an ongoing session irrespective of variations from trial to trial (Grosse-Wentrup & Schölkopf, 2012). A decline in performance should be avoided, especially when developing a system for stroke survivors. This group often experience rapidly evolving fatigue that is accompanied with a substantial decline in BCI control performance. A larger study reported fatigue in post-stroke users after 20-30 min of BCI training and was even more pronounced by factors like insomnia in the night before training, depressive symptoms, or general weakness (Frolov et al., 2017).

In our study involving healthy participants, we successfully showed that HRV is specific as well as predictive to a decrease in SMR control performance (M. Nann et al., 2021). Notably, specificity and prediction characteristics of HRV are independent to ongoing trial-to-trial variations. To reveal whether HRV is predictive, Granger-causality analysis was applied (Granger, 1969). It is worth noting, that Granger-causality does not describe a causal link but allows to derive the conclusion that prediction of BCI control performance is better when information of HRV is included against a prediction with performance information only.

Grosse-Wentrup and Schölkopf (2012) postulated already in 2012 that there is a need for performance prediction within an ongoing session, which is independent on trial-to-trial variations. They could show that high gamma power predicts SMR control performance. However, EEG recordings with good quality in the high gamma band (70-80 Hz) are challenging as the gamma band is susceptible to muscle artifacts (Muthukumaraswamy, 2013). To minimize such artifacts, EEG recordings need to be highly controlled in lab environments and, thus, contradicts to applications in everyday life environments. In contrast, HRV is very easy to record, because the heart beat signal is one of the strongest biosignals in the human body.

As a next step, reliable prediction of SMR performance can be utilized to develop adaptive and personalized BCI/BMI control paradigms. Such open- or closed-loop paradigms based on individual HRV changes within an ongoing training session might optimize learning and thus promotes neuroplasticity and Hebbian-based motor recovery (Remsik et al., 2016; Soekadar et al., 2015b; Soekadar et al., 2015c). Moreover, dose, intensity and frequency of BCI training could be individualized. Additionally, avoiding a decline in SMR performance would simply reduce frustration during BCI/BMI training sessions and thus foster the motivation for further trainings.

In conclusion, all results of the here presented studies contribute to an improved applicability of assistive B/NMI systems. We could successfully show feasibility and safety of B/NMI whole-arm exoskeleton and bilateral control for stroke and SCI survivors, respectively. Moreover, we paved the way for neuro-adaptive BCI/BMI control paradigms based on individual changes in HRV by revealing a specific and predictive link between HRV and SMR control performance.

As already introduced, besides enhancing B/NMI control for assistive purposes, there is growing evidence that repeated BCI use triggers neural recovery (restorative BCIs/BMIs) (Biasiucci et al., 2018; Donati et al., 2016; Ramos-Murguialday et al., 2013). Importantly, motor function improved only when training was linked to relevant activities of daily living (ADL). Hence, it was

suggested to merge these two approaches of assistive and rehabilitative use to obtain long-lasting improvements in motor function to promote B/NMI systems as a standard therapy in upper limb paralysis after brain and spinal cord lesions (Soekadar et al., 2015b).

Even though BCI-triggered rehabilitation effects have been mainly investigated after stroke, there were also several promising results after incomplete SCI showing restoration of walking to a certain degree (Donati et al., 2016; Wagner et al., 2018). While in complete SCI with complete destruction of corticospinal pathways there is no prospect of recovery, Aarabi et al. (2021) presented an encouraging trend in demographics that incomplete injuries significantly increased whereas complete injuries decreased. This means that an increasing number of SCI survivors might potentially benefit from future rehabilitation treatment strategies based on neural-controlled assistive technology.

The overarching goal is to broaden the use of B/NMI systems in clinical and in-home environments. Therefore, applicability and reliability of such systems need to be as sophisticated as possible that individuals are intrinsically motivated to use them. This would allow to systematically investigate long-lasting effects of ADL-linked B/NMI training within larger clinical studies in rehabilitation facilities or everyday life environments.

4. Summary

Operation of assistive exoskeletons based on voluntary control of sensorimotor rhythms (SMR, 8-12 Hz) enables intuitive control of finger or arm movements in severe paralysis after chronic stroke or cervical spinal cord injury (SCI). To improve reliability of such systems outside the laboratory, in particular when brain activity is recorded non-invasively with scalp electroencephalography (EEG), a hybrid EEG/electrooculography (EOG) brain/neural-machine interface (B/NMI) was recently introduced. Besides providing assistance, recent studies indicate that repeated use of such systems can trigger neural recovery.

However, important prerequisites have to be achieved before broader use in clinical settings or everyday life environments is feasible. Current B/NMI systems predominantly restore hand function, but do not allow simultaneous control of more proximal joints for whole-arm motor coordination as required for most stroke survivors suffering from paralysis in the entire upper limb. Besides paralysis, cognitive impairments including post-stroke fatigue due to the brain lesion reduce the capacity to maintain effortful B/NMI control over a longer period of time. This impedes the applicability in daily life assistance and might even limit the efficacy of neurorehabilitation training. In contrast to stroke survivors, tetraplegics due to cervical SCI lack motor function in both hands. Given that most activities of daily living (ADL) involve bimanual manipulation, e.g., to open the lid of a bottle, bilateral exoskeleton control is required but was not shown yet in tetraplegics.

To further enhance B/NMI systems, we first investigated whether B/NMI whole-arm exoskeleton control in hemiplegia after chronic stroke is feasible and safe. In contrast to simple grasping, control of more complex tasks involving the entire upper limb was not feasible with established B/NMIs because high-dimensionality of such multiple joint systems exceeds the bandwidth of these interfaces. Thus, we blended B/NMI control with vision-guidance to receive a semiautonomous whole-arm exoskeleton control. Such setup allowed to divide ADL tasks into a sequence of EEG/EOG-triggered sub-tasks reducing complexity for the user. While, for instance, a drinking task was resolved into EOG-induced reaching, lifting and placing back the cup, grasping and releasing movements were based on intuitive SMR control. Feasibility of such shared vision-guided

B/NMI control was assumed when executions were initialized within 3 s (fluent control) and a minimum of 75 % of subtasks were executed within that time (reliable control). We showed feasibility in healthy subjects as well as stroke survivors without report of any side effects documenting safe use.

Similarly, feasibility and safety of bilateral B/NMI control after cervical SCI was evaluated. To enable bilateral B/NMI control, established EEG-based grasping and EOG-based releasing or stop commands were complemented with a novel EOG command allowing to switch laterality by performing prolonged horizontal eye movements (>1 s) to the left or to the right. Study results with healthy subjects and tetraplegics document fluent initialization of grasping motions below 3 s as well as safe use as unintended grasping could be stopped before a full motion was conducted. Superiority of novel bilateral control was documented by a higher accuracy of up to 22 % in tetraplegics compared to a bilateral control without prolonged EOG command.

Lastly, as reliable B/NMI control is cognitively demanding, e.g., by imagining or attempting the desired movements, we investigated whether heart rate variability (HRV) can be used as biomarker to predict declining control performance, which is often reported in stroke survivors due to their cognitive impairments. Referring to the close brain-heart connection, we showed in healthy subjects that a decline in HRV is specific as well as predictive to a decline in B/NMI control performance within a single training session. The predictive link was revealed by a Granger-causality analysis.

In conclusion, we could demonstrate important enhancements in B/NMI control paradigms including complex whole-arm exoskeleton control as well as individual performance monitoring within a training session based on HRV. Both achievements contribute to broaden the use as a standard therapy in stroke neurorehabilitation. Especially the predictive characteristic of HRV paves the way for adaptive B/NMI control paradigms to account for individual differences among impaired stroke survivors. Moreover, we also showed feasibility and safety of a novel implementation for bilateral B/NMI control, which is necessary for reliable operation of two hand-exoskeletons for bimanual ADLs after SCI.

5. Bibliography

- Aarabi, B., Albrecht, J. S., Simard, J. M., Chryssikos, T., Schwartzbauer, G., Sansur, C. A., et al. (2021). Trends in demographics and markers of injury severity in traumatic cervical spinal cord Injury. *Journal of neurotrauma*, 38(6), 756-764.
- Acciarresi, M., Bogousslavsky, J., Paciaroni, M. (2014). Post-stroke fatigue: epidemiology, clinical characteristics and treatment. *European neurology*, 72(5-6), 255-261.
- Ahuja, C. S., Wilson, J. R., Nori, S., Kotter, M. R. N., Druschel, C., Curt, A., et al. (2017). Traumatic spinal cord injury. *Nat Rev Dis Primers*, 3, 17018.
- Amiri, S., Fazel-Rezai, R., Asadpour, V. (2013). A review of hybrid brain-computer interface systems. *Advances in Human-Computer Interaction*, 2013.
- Babiloni, C., Carducci, F., Cincotti, F., Rossini, P. M., Neuper, C., Pfurtscheller, G., et al. (1999). Human movement-related potentials vs desynchronization of EEG alpha rhythm: a high-resolution EEG study. *Neuroimage*, 10(6), 658-665.
- Barsotti, M., Leonardis, D., Loconsole, C., Solazzi, M., Sotgiu, E., Procopio, C., et al. (2015). *A full upper limb robotic exoskeleton for reaching and grasping rehabilitation triggered by MI-BCI*. Paper presented at the 2015 IEEE international conference on rehabilitation robotics (ICORR).
- Bednar, M. S., Woodside, J. C. (2018). Management of Upper Extremities in Tetraplegia: Current Concepts. *JAAOS - Journal of the American Academy of Orthopaedic Surgeons*, 26(16), e333-e341.
- Berntson, G. G., Bigger, J. T., Jr., Eckberg, D. L., Grossman, P., Kaufmann, P. G., Malik, M., et al. (1997). Heart rate variability: origins, methods, and interpretive caveats. *Psychophysiology*, 34(6), 623-648.
- Biasiucci, A., Leeb, R., Iturrate, I., Perdikis, S., Al-Khadairy, A., Corbet, T., et al. (2018). Brain-actuated functional electrical stimulation elicits lasting arm motor recovery after stroke. *Nature communications*, 9(1), 1-13.
- Birbaumer, N., Ghanayim, N., Hinterberger, T., Iversen, I., Kotchoubey, B., Kubler, A., et al. (1999). A spelling device for the paralysed. *Nature*, 398(6725), 297-298.
- Blankertz, B., Sannelli, C., Halder, S., Hammer, E. M., Kübler, A., Müller, K.-R., et al. (2010). Neurophysiological predictor of SMR-based BCI performance. *Neuroimage*, 51(4), 1303-1309.
- Buch, E., Weber, C., Cohen, L. G., Braun, C., Dimyan, M. A., Ard, T., et al. (2008). Think to move: a neuromagnetic brain-computer interface (BCI) system for chronic stroke. *Stroke*, 39(3), 910-917.
- Bunketorp-Käll, L., Wangdell, J., Reinholdt, C., Fridén, J. (2017). Satisfaction with upper limb reconstructive surgery in individuals with tetraplegia: the development and reliability of a Swedish self-reported satisfaction questionnaire. *Spinal Cord*, 55(7), 664-671.
- Campbell, M. L., Sheets, D., Strong, P. S. (1999). Secondary health conditions among middle-aged individuals with chronic physical disabilities: implications for unmet needs for services. *Assist Technol*, 11(2), 105-122.

- Cempini, M., Cortese, M., Vitiello, N. (2015). A Powered Finger-Thumb Wearable Hand Exoskeleton With Self-Aligning Joint Axes. *IEEE/ASME Transactions on Mechatronics*, 20(2), 705-716.
- Center, N. S. C. I. S. (2019). National Spinal Cord Injury Statistical Center Annual Statistical Report. *Birmingham, AL, University of Alabama at Birmingham*.
- Chowdhury, A., Raza, H., Dutta, A., Prasad, G. (2017). EEG-EMG based hybrid brain computer interface for triggering hand exoskeleton for neuro-rehabilitation *Proceedings of the Advances in Robotics* (pp. 1-6).
- Christensen, D., Johnsen, S. P., Watt, T., Harder, I., Kirkevold, M., Andersen, G. (2008). Dimensions of post-stroke fatigue: a two-year follow-up study. *Cerebrovasc Dis*, 26(2), 134-141.
- Clausen, J., Fetz, E., Donoghue, J., Ushiba, J., Sporhase, U., Chandler, J., et al. (2017). Help, hope, and hype: Ethical dimensions of neuroprosthetics. *Science*, 356(6345), 1338-1339.
- Colebatch, J. G., Gandevia, S. C. (1989). The distribution of muscular weakness in upper motor neuron lesions affecting the arm. *Brain*, 112 (Pt 3), 749-763.
- Collaborators, G. B. D. S. (2019). Global, regional, and national burden of stroke, 1990-2016: a systematic analysis for the Global Burden of Disease Study 2016. *Lancet Neurol*, 18(5), 439-458.
- Collinger, J. L., Wodlinger, B., Downey, J. E., Wang, W., Tyler-Kabara, E. C., Weber, D. J., et al. (2013). High-performance neuroprosthetic control by an individual with tetraplegia. *Lancet*, 381(9866), 557-564.
- Coscia, M., Wessel, M. J., Chaudary, U., Millan, J. D. R., Micera, S., Guggisberg, A., et al. (2019). Neurotechnology-aided interventions for upper limb motor rehabilitation in severe chronic stroke. *Brain*, 142(8), 2182-2197.
- Crea, S., Nann, M., Trigili, E., Cordella, F., Baldoni, A., Badesa, F. J., et al. (2018). Feasibility and safety of shared EEG/EOG and vision-guided autonomous whole-arm exoskeleton control to perform activities of daily living. *Sci Rep*, 8(1), 10823.
- Curran, E. A., Stokes, M. J. (2003). Learning to control brain activity: a review of the production and control of EEG components for driving brain-computer interface (BCI) systems. *Brain Cogn*, 51(3), 326-336.
- Dahlberg, L. S., Becerra, L., Borsook, D., Linnman, C. (2018). Brain changes after spinal cord injury, a quantitative meta-analysis and review. *Neuroscience & Biobehavioral Reviews*, 90, 272-293.
- Donati, A. R., Shokur, S., Morya, E., Campos, D. S., Moioli, R. C., Gitti, C. M., et al. (2016). Long-Term Training with a Brain-Machine Interface-Based Gait Protocol Induces Partial Neurological Recovery in Paraplegic Patients. *Sci Rep*, 6, 30383.
- Farwell, L. A., Donchin, E. (1988). Talking off the top of your head: toward a mental prosthesis utilizing event-related brain potentials. *Electroencephalogr Clin Neurophysiol*, 70(6), 510-523.
- Foong, R., Ang, K. K., Quek, C., Guan, C., Phua, K. S., Kuah, C. W. K., et al. (2019). Assessment of the efficacy of EEG-based MI-BCI with visual feedback and EEG correlates of mental fatigue for upper-limb stroke

- rehabilitation. *IEEE Transactions on Biomedical Engineering*, 67(3), 786-795.
- Frisoli, A., Loconsole, C., Leonardis, D., Banno, F., Barsotti, M., Chisari, C., et al. (2012). A new gaze-BCI-driven control of an upper limb exoskeleton for rehabilitation in real-world tasks. *IEEE Transactions on Systems, Man, and Cybernetics, Part C (Applications and Reviews)*, 42(6), 1169-1179.
- Frolov, A. A., Mokienko, O., Lyukmanov, R., Biryukova, E., Kotov, S., Turbina, L., et al. (2017). Post-stroke Rehabilitation Training with a Motor-Imagery-Based Brain-Computer Interface (BCI)-Controlled Hand Exoskeleton: A Randomized Controlled Multicenter Trial. *Front Neurosci*, 11, 400.
- Granger, C. W. (1969). Investigating causal relations by econometric models and cross-spectral methods. *Econometrica: journal of the Econometric Society*, 424-438.
- Grosse-Wentrup, M., Schölkopf, B. (2012). High gamma-power predicts performance in sensorimotor-rhythm brain-computer interfaces. *Journal of Neural Engineering*, 9(4), 046001.
- Grosse-Wentrup, M., Schölkopf, B. (2013). A review of performance variations in SMR-based Brain- Computer interfaces (BCIs) *Brain-Computer Interface Research* (pp. 39-51): Springer.
- Hammer, E. M., Halder, S., Blankertz, B., Sannelli, C., Dickhaus, T., Kleih, S., et al. (2012). Psychological predictors of SMR-BCI performance. *Biological Psychology*, 89(1), 80-86.
- Hatem, S. M., Saussez, G., Della Faille, M., Prist, V., Zhang, X., Dispa, D., et al. (2016). Rehabilitation of Motor Function after Stroke: A Multiple Systematic Review Focused on Techniques to Stimulate Upper Extremity Recovery. *Frontiers in human neuroscience*, 10, 442-442.
- Hazubski, S., Hoppe, H., Otte, A. (2020). Electrode-free visual prosthesis/exoskeleton control using augmented reality glasses in a first proof-of-technical-concept study. *Scientific Reports*, 10(1), 1-10.
- Hochberg, L. R., Bacher, D., Jarosiewicz, B., Masse, N. Y., Simeral, J. D., Vogel, J., et al. (2012). Reach and grasp by people with tetraplegia using a neurally controlled robotic arm. *Nature*, 485(7398), 372-375.
- Hogervorst, M. A., Brouwer, A. M., van Erp, J. B. (2014). Combining and comparing EEG, peripheral physiology and eye-related measures for the assessment of mental workload. *Front Neurosci*, 8(322), 322.
- Housman, S. J., Le, V., Rahman, T., Sanchez, R. J., Reinkensmeyer, D. J. (2007). *Arm-training with T-WREX after chronic stroke: preliminary results of a randomized controlled trial*. Paper presented at the 2007 IEEE 10th International Conference on Rehabilitation Robotics.
- Hull, J., Turner, R., Simon, A. A., Asbeck, A. T. (2020). A novel method and exoskeletons for whole-arm gravity compensation. *IEEE Access*, 8, 143144-143159.
- James, S. L., Theadom, A., Ellenbogen, R. G., Bannick, M. S., Montjoy-Venning, W., Lucchesi, L. R., et al. (2019). Global, regional, and national burden of traumatic brain injury and spinal cord injury, 1990–2016: a systematic analysis for the Global Burden of Disease Study 2016. *The Lancet Neurology*, 18(1), 56-87.

- Kawase, T., Sakurada, T., Koike, Y., Kansaku, K. (2017). A hybrid BMI-based exoskeleton for paresis: EMG control for assisting arm movements. *Journal of Neural Engineering*, 14(1), 016015.
- Lang, C. E., Strube, M. J., Bland, M. D., Waddell, K. J., Cherry-Allen, K. M., Nudo, R. J., et al. (2016). Dose response of task-specific upper limb training in people at least 6 months poststroke: A phase II, single-blind, randomized, controlled trial. *Annals of Neurology*, 80(3), 342-354.
- Laurent, K., De Sèze, M. P., Delleci, C., Koleck, M., Dehail, P., Orgogozo, J. M., et al. (2011). Assessment of quality of life in stroke patients with hemiplegia. *Annals of Physical and Rehabilitation Medicine*, 54(6), 376-390.
- León, C. L. (2017). *Multilabel classification of EEG-based combined motor imageries implemented for the 3D control of a robotic arm*.
- Liew, S. L., Rana, M., Cornelsen, S., Fortunato de Barros Filho, M., Birbaumer, N., Sitaram, R., et al. (2016). Improving Motor Corticothalamic Communication After Stroke Using Real-Time fMRI Connectivity-Based Neurofeedback. *Neurorehabilitation and Neural Repair*, 30(7), 671-675.
- Lincoln, N., Majid, M., Weyman, N. (2000). Cognitive rehabilitation for attention deficits following stroke. *Cochrane Database of Systematic Reviews*(4).
- Lotte, F., Bougrain, L., Cichocki, A., Clerc, M., Congedo, M., Rakotomamonjy, A., et al. (2018). A review of classification algorithms for EEG-based brain-computer interfaces: a 10 year update. *J Neural Eng*, 15(3), 031005.
- Lu, X., Battistuzzo, C. R., Zoghi, M., Galea, M. P. (2015). Effects of training on upper limb function after cervical spinal cord injury: a systematic review. *Clinical rehabilitation*, 29(1), 3-13.
- Marquez-Chin, C., Popovic, M. R. (2020). Functional electrical stimulation therapy for restoration of motor function after spinal cord injury and stroke: a review. *BioMedical Engineering OnLine*, 19, 1-25.
- Mates, J., Muller, U., Radil, T., Poppel, E. (1994). Temporal integration in sensorimotor synchronization. *J Cogn Neurosci*, 6(4), 332-340.
- McFarland, D. J., Neat, G. W., Read, R. F., Wolpaw, J. R. (1993). An EEG-based method for graded cursor control. *Psychobiology*, 21(1), 77-81.
- Mekki, M., Delgado, A. D., Fry, A., Putrino, D., Huang, V. (2018). Robotic rehabilitation and spinal cord injury: a narrative review. *Neurotherapeutics*, 15(3), 604-617.
- Meng, J., Zhang, S., Bekyo, A., Olsoe, J., Baxter, B., He, B. (2016). Noninvasive electroencephalogram based control of a robotic arm for reach and grasp tasks. *Scientific Reports*, 6, 38565.
- Molle Da Costa, R. D., Luvizutto, G. J., Martins, L. G., Thomaz De Souza, J., Regina Da Silva, T., Alvarez Sartor, L. C., et al. (2019). Clinical factors associated with the development of nonuse learned after stroke: a prospective study. *Topics in stroke rehabilitation*, 26(7), 511-517.
- Muth, E. R., Moss, J. D., Rosopa, P. J., Salley, J. N., Walker, A. D. (2012). Respiratory sinus arrhythmia as a measure of cognitive workload. *International Journal of Psychophysiology*, 83(1), 96-101.
- Muthukumaraswamy, S. D. (2013). High-frequency brain activity and muscle artifacts in MEG/EEG: a review and recommendations. *Front Hum Neurosci*, 7, 138.

- Myrden, A., Chau, T. (2015). Effects of user mental state on EEG-BCI performance. *Front Hum Neurosci*, 9, 308.
- Nann, M., Cordella, F., Trigili, E., Lauretti, C., Bravi, M., Miccinilli, S., et al. (2021). Restoring Activities of Daily Living Using an EEG/EOG-Controlled Semiautonomous and Mobile Whole-Arm Exoskeleton in Chronic Stroke. *IEEE Systems Journal*, 15(2), 2314-2321.
© 2021 IEEE. Reprinted, with permission, from Nann, M. et al., Restoring Activities of Daily Living Using an EEG/EOG-Controlled Semiautonomous and Mobile Whole-Arm Exoskeleton in Chronic Stroke, 09/2020.
- Nann, M., Haslacher, D., Colucci, A., Eskofier, B., von Tscharner, V., Soekadar, S. R. (2021). Heart rate variability predicts decline in sensorimotor rhythm control. *J Neural Eng*, 18(4), 0460b5.
- Nann, M., Peekhaus, N., Angerhofer, C., Soekadar, S. R. (2020). Feasibility and Safety of Bilateral Hybrid EEG/EOG Brain/Neural-Machine Interaction. *Front Hum Neurosci*, 14(521), 580105.
- Naseer, N., Hong, K.-S. (2015). fNIRS-based brain-computer interfaces: a review. *Frontiers in human neuroscience*, 9, 3.
- Osuagwu, B. C., Wallace, L., Fraser, M., Vuckovic, A. (2016). Rehabilitation of hand in subacute tetraplegic patients based on brain computer interface and functional electrical stimulation: a randomised pilot study. *J Neural Eng*, 13(6), 065002.
- Pain, L. M., Baker, R., Richardson, D., Agur, A. M. (2015). Effect of trunk-restraint training on function and compensatory trunk, shoulder and elbow patterns during post-stroke reach: a systematic review. *Disabil Rehabil*, 37(7), 553-562.
- Pedrocchi, A., Ferrante, S., Ambrosini, E., Gandolla, M., Casellato, C., Schauer, T., et al. (2013). MUNDUS project: Multimodal neuroprosthesis for daily upper limb support. *J Neuroeng Rehabil*, 10, 66.
- Penfield, W., Boldrey, E. (1937). Somatic motor and sensory representation in the cerebral cortex of man as studied by electrical stimulation. *Brain*, 60(4), 389-443.
- Peternel, L., Noda, T., Petrič, T., Ude, A., Morimoto, J., Babič, J. (2016). Adaptive control of exoskeleton robots for periodic assistive behaviours based on EMG feedback minimisation. *PLoS One*, 11(2), e0148942.
- Pfurtscheller, G., Allison, B. Z., Brunner, C., Bauernfeind, G., Solis-Escalante, T., Scherer, R., et al. (2010). The hybrid BCI. *Front Neurosci*, 4(3), 30.
- Pfurtscheller, G., Brunner, C., Schlogl, A., Lopes da Silva, F. H. (2006). Mu rhythm (de)synchronization and EEG single-trial classification of different motor imagery tasks. *Neuroimage*, 31(1), 153-159.
- Pfurtscheller, G., Muller, G. R., Pfurtscheller, J., Gerner, H. J., Rupp, R. (2003). 'Thought'--control of functional electrical stimulation to restore hand grasp in a patient with tetraplegia. *Neurosci Lett*, 351(1), 33-36.
- Pfurtscheller, G., Neuper, C. (1994). Event-related synchronization of mu rhythm in the EEG over the cortical hand area in man. *Neuroscience letters*, 174(1), 93-96.
- Pfurtscheller, G., Scherer, R., Neuper, C. (2008). EEG-based brain-computer interface. *OXFORD SERIES IN HUMAN-TECHNOLOGY INTERACTION*, 315.

- Poppel, E. (2004). Lost in time: a historical frame, elementary processing units and the 3-second window. *Acta neurobiologiae experimentalis*, 64(3), 295-302.
- Rahman, M. H., Ochoa-Luna, C., Saad, M., Archambault, P. (2015). EMG based control of a robotic exoskeleton for shoulder and elbow motion assist. *J Aut Con Eng*, 3(4).
- Rahman, M. H., Rahman, M. J., Cristobal, O., Saad, M., Kenné, J.-P., Archambault, P. S. (2015). Development of a whole arm wearable robotic exoskeleton for rehabilitation and to assist upper limb movements. *Robotica*, 33(1), 19-39.
- Ramos-Murguialday, A., Broetz, D., Rea, M., Laer, L., Yilmaz, O., Brasil, F. L., et al. (2013). Brain-machine interface in chronic stroke rehabilitation: a controlled study. *Ann Neurol*, 74(1), 100-108.
- Remsik, A., Young, B., Vermilyea, R., Kiekhoefer, L., Abrams, J., Evander Elmore, S., et al. (2016). A review of the progression and future implications of brain-computer interface therapies for restoration of distal upper extremity motor function after stroke. *Expert Rev Med Devices*, 13(5), 445-454.
- Ren, Y., Kang, S. H., Park, H.-S., Wu, Y.-N., Zhang, L.-Q. (2012). Developing a multi-joint upper limb exoskeleton robot for diagnosis, therapy, and outcome evaluation in neurorehabilitation. *IEEE Transactions on Neural Systems and Rehabilitation Engineering*, 21(3), 490-499.
- Rosamond, W., Flegal, K., Furie, K., Go, A., Greenlund, K., Haase, N., et al. (2008). American Heart Association Statistics Committee And Stroke Statistics Subcommittee. Disease and stroke statistics—2008 update: a report from the American Heart Association Statistics Committee and Stroke Statistics Subcommittee. *Circulation*, 117(4), e25-e146.
- Sakurada, T., Kawase, T., Takano, K., Komatsu, T., Kansaku, K. (2013). A BMI-based occupational therapy assist suit: asynchronous control by SSVEP. *Frontiers in neuroscience*, 7, 172.
- Sanchez, R., Wolbrecht, E., Smith, R., Liu, J., Rao, S., Cramer, S., et al. (2005). A pneumatic robot for re-training arm movement after stroke: Rationale and mechanical design. Paper presented at the Rehabilitation Robotics, 2005. ICORR 2005. 9th International Conference on.
- Schieber, M. H. (2001). Constraints on somatotopic organization in the primary motor cortex. *Journal of neurophysiology*, 86(5), 2125-2143.
- Sherwood, A. M., Dimitrijevic, M. R., McKay, W. B. (1992). Evidence of subclinical brain influence in clinically complete spinal cord injury: incomplete SCI. *Journal of the Neurological Sciences*, 110(1-2), 90-98.
- Soekadar, S. R., Birbaumer, N., Slutsky, M. W., Cohen, L. G. (2015a). Brain-machine interfaces in neurorehabilitation of stroke. *Neurobiol Dis*, 83, 172-179.
- Soekadar, S. R., Cohen, L. G., Birbaumer, N. (2015b). Clinical brain-machine interfaces. In J. I. Tracy, B. M. Hampstead, & S. K. (Eds.), *Cognitive Plasticity in Neurologic Disorders* (pp. 347-363): Oxford University Press.
- Soekadar, S. R., Kohl, S. H., Mihara, M., von Lüthmann, A. (2021). Optical brain imaging and its application to neurofeedback. *NeuroImage: Clinical*, 30, 102577.

- Soekadar, S. R., Witkowski, M., Birbaumer, N., Cohen, L. G. (2015c). Enhancing Hebbian Learning to Control Brain Oscillatory Activity. *Cereb Cortex*, 25(9), 2409-2415.
- Soekadar, S. R., Witkowski, M., Gómez, C., Opisso, E., Medina, J., Cortese, M., et al. (2016). Hybrid EEG/EOG-based brain/neural hand exoskeleton restores fully independent daily living activities after quadriplegia. *Science Robotics*, 1(1), eaag3296.
- Stancak, A., Jr., Feige, B., Lucking, C. H., Kristeva-Feige, R. (2000). Oscillatory cortical activity and movement-related potentials in proximal and distal movements. *Clin Neurophysiol*, 111(4), 636-650.
- Stuiver, A., Brookhuis, K. A., de Waard, D., Mulder, B. (2014). Short-term cardiovascular measures for driver support: Increasing sensitivity for detecting changes in mental workload. *Int J Psychophysiol*, 92(1), 35-41.
- Ullberg, T., Zia, E., Petersson, J., Norrving, B. (2015). Changes in functional outcome over the first year after stroke: an observational study from the Swedish stroke register. *Stroke*, 46(2), 389-394.
- Van Dokkum, L., Ward, T., Laffont, I. (2015). Brain computer interfaces for neurorehabilitation—its current status as a rehabilitation strategy post-stroke. *Annals of Physical and Rehabilitation Medicine*, 58(1), 3-8.
- Veerbeek, J. M., van Wegen, E., van Peppen, R., van der Wees, P. J., Hendriks, E., Rietberg, M., et al. (2014). What is the evidence for physical therapy poststroke? A systematic review and meta-analysis. *PLoS One*, 9(2), e87987.
- Vidal, J. J. (1973). Toward direct brain-computer communication. *Annual review of Biophysics and Bioengineering*, 2(1), 157-180.
- Vos, T., Lim, S. S., Abbafati, C., Abbas, K. M., Abbasi, M., Abbasifard, M., et al. (2020). Global burden of 369 diseases and injuries in 204 countries and territories, 1990–2019: a systematic analysis for the Global Burden of Disease Study 2019. *The Lancet*, 396(10258), 1204-1222.
- Wagner, F. B., Mignardot, J. B., Le Goff-Mignardot, C. G., Demesmaeker, R., Komi, S., Capogrosso, M., et al. (2018). Targeted neurotechnology restores walking in humans with spinal cord injury. *Nature*, 563(7729), 65-71.
- Wang, H., Li, Y., Long, J., Yu, T., Gu, Z. (2014). An asynchronous wheelchair control by hybrid EEG–EOG brain–computer interface. *Cognitive neurodynamics*, 8(5), 399-409.
- Wolf, S. L., Weinstein, C. J., Miller, J. P., Taub, E., Uswatte, G., Morris, D., et al. (2006). Effect of constraint-induced movement therapy on upper extremity function 3 to 9 months after stroke: the EXCITE randomized clinical trial. *Jama*, 296(17), 2095-2104.
- Wolfe, C. D., Crichton, S. L., Heuschmann, P. U., McKevitt, C. J., Toschke, A. M., Grieve, A. P., et al. (2011). Estimates of outcomes up to ten years after stroke: analysis from the prospective South London Stroke Register. *PLoS Med*, 8(5), e1001033.
- Wolpaw, J. R., Birbaumer, N., McFarland, D. J., Pfurtscheller, G., Vaughan, T. M. (2002). Brain-computer interfaces for communication and control. *Clin Neurophysiol*, 113(6), 767-791.

- Wyndaele, M., Wyndaele, J.-J. (2006). Incidence, prevalence and epidemiology of spinal cord injury: what learns a worldwide literature survey? *Spinal Cord*, 44(9), 523-529.
- Young, B. M., Nigogosyan, Z., Walton, L. M., Remsik, A., Song, J., Nair, V. A., et al. (2015). Dose-response relationships using brain-computer interface technology impact stroke rehabilitation. *Front Hum Neurosci*, 9, 361.
- Zander, T. O., Kothe, C. (2011). Towards passive brain-computer interfaces: applying brain-computer interface technology to human-machine systems in general. *J Neural Eng*, 8(2), 025005.

6. German summary

Assistive Exoskelette, die auf der willentlichen Steuerung von sensomotorischen Rhythmen (englisch: sensorimotor rhythms, SMR, 8-12 Hz) beruhen, ermöglichen eine intuitive Steuerung von Finger- oder Armbewegungen bei schweren Lähmungen, die nach (chronischem) Schlaganfall oder zervikaler Rückenmarksverletzung auftreten. Um die Zuverlässigkeit solcher Systeme außerhalb des Labors zu verbessern, wurde kürzlich eine neurale Gehirn-Maschine-Schnittstelle (englisch: brain/neural-machine interface, B/NMI), basierend auf Elektroenzephalographie (EEG) und Elektrookulographie (EOG), vorgestellt. Jüngste Studien deuten daraufhin, dass solche Systeme nicht nur eine Hilfestellung im Alltag bieten, sondern sich deren wiederholte Anwendung auch positiv auf die Neurorehabilitation auswirken kann.

Für den breiten Einsatz solcher Systeme im Alltag und klinischen Umfeld müssen allerdings noch wichtige Voraussetzungen erfüllt werden. Derzeitige B/NMI-Systeme wurden bisher überwiegend zur Wiederherstellung der Handfunktion entwickelt, erlauben dabei aber keine Mobilisierung der gesamten oberen Extremität. Die meisten Schlaganfallüberlebenden zeigen jedoch eine Lähmung der gesamten oberen Extremität, sodass dies dringlich erforderlich wäre. Des Weiteren reduzieren kognitive Beeinträchtigungen und die nach Schlaganfall auftretende Müdigkeit (englisch: post-stroke fatigue) die Fähigkeit, die meist anstrengende B/NMI-Kontrolle über einen längeren Zeitraum aufrechtzuerhalten. Dies erschwert die Anwendung als unterstützendes Alltagshilfsmittel und schränkt möglicherweise auch die Trainingseffektivität der Neurorehabilitation ein.

Im Gegensatz zu Schlaganfallüberlebenden ist bei Tetraplegikern nach zervikaler Rückenmarksverletzung die motorische Funktion in beiden Händen beeinträchtigt. Da die meisten Aktivitäten des täglichen Lebens (englisch: activities of daily living, ADL) bimanuelle Manipulationen beinhalten, ist eine bilaterale Exoskelettsteuerung erforderlich. Eine solche Steuerung konnte bis heute jedoch noch nicht bei Tetraplegikern gezeigt werden.

Um die verfügbaren B/NMI-Systeme weiter zu verbessern, untersuchten wir zunächst, ob eine sichere B/NMI Exoskelettsteuerung für die gesamte obere

Extremität bei Halbseitenlähmung nach chronischem Schlaganfall umsetzbar ist. Im Gegensatz zum einfachen Greifen war die Steuerung komplexerer Aufgaben, die die gesamte obere Extremität einbeziehen, mit etablierten B/NMI-Systemen nicht zu realisieren. Der Grund dafür liegt in der hohen Dimensionalität solcher Mehrgelenksysteme, die eine zu umfangreiche Menge an Steuerbefehlen erfordern würde. Wir kombinierten daher die B/NMI-Steuerung mit kamerabasierter Robotiksteuerung, um eine semiautonome Ganzarm-Exoskelett-Steuerung zu implementieren. Auf diese Weise konnten ADL-Aufgaben in eine Abfolge von EEG/EOG-getriggerten Teilaufgaben aufgeteilt werden, was die Komplexität für den Benutzer deutlich reduzierte. Während z.B. Trinken in EOG-induziertes Greifen, Heben und Zurückstellen des Bechers unterteilt wurde, basierten Greif- und Öffnungsbewegungen auf intuitiver SMR-Steuerung. Die Machbarkeit einer solchen neuartigen B/NMI-Steuerung wurde angenommen, wenn die Ausführungen innerhalb von 3 s initialisiert (flüssige Steuerung) und mindestens 75 % der Teilaufgaben innerhalb dieser Zeit ausgeführt wurden (zuverlässige Steuerung). Die Machbarkeit wurde sowohl bei gesunden Probanden als auch bei chronischen Schlaganfallüberlebenden gezeigt. Dabei wurden über keine Nebenwirkungen berichtet, was den Rückschluss auf eine sichere Anwendung zuließ.

In ähnlicher Weise wurde die Machbarkeit und Sicherheit der bilateralen B/NMI-Kontrolle nach zervikaler Rückenmarksverletzung untersucht. Um die bilaterale B/NMI-Steuerung zu ermöglichen, wurden die etablierten EEG-basierten Greif- und EOG-basierten Öffnungs- oder Stopp-Befehle durch einen neuartigen EOG-Befehl erweitert, der mittels längeren horizontalen Augenbewegungen (>1 s) nach links oder rechts erlaubt, die Lateralität zu wechseln. Studienergebnisse mit gesunden Probanden und Tetraplegikern zeigten eine Initialisierung von Greifbewegungen unter 3 s sowie eine sichere Anwendung, da ein unbeabsichtigtes Greifen gestoppt werden konnte, bevor eine vollständige Bewegung ausgeführt wurde. Die Überlegenheit der neuartigen bilateralen Steuerung wurde durch eine höhere Genauigkeit von bis zu 22 % bei Tetraplegikern im Vergleich zu einer bilateralen Steuerung ohne neuartigen EOG-Befehl gezeigt.

Da eine zuverlässige B/NMI-Kontrolle kognitiv anspruchsvoll ist, z. B. durch die Vorstellung der gewünschten Bewegungen, untersuchten wir schließlich, ob die Herzfrequenzvariabilität (englisch: heart rate variability, HRV) als Biomarker zur Vorhersage eines nachlassenden Kontrollvermögens verwendet werden kann. Insbesondere wird bei Schlaganfallüberlebenden häufig über eine kontinuierliche Abnahme der Kontrollfähigkeit aufgrund kognitiver Beeinträchtigungen berichtet. Bezugnehmend auf die bekannte Hirn-Herz-Achse zeigten wir bei gesunden Probanden, dass eine Abnahme der HRV sowohl spezifisch als auch prädiktiv für eine Verringerung der B/NMI-Kontrollfähigkeit innerhalb einer einzelnen Trainingssitzung ist. Der prädiktive Zusammenhang wurde durch eine Granger-Kausalitätsanalyse gezeigt.

Zusammenfassend konnten wir wichtige Verbesserungen bei B/NMI-Kontrollparadigmen erzielen, die sowohl eine komplexe Ganzarm-Exoskelett-Kontrolle als auch eine individuelle Leistungsüberwachung innerhalb einer Trainingseinheit auf Basis der HRV beinhalten. Beide Studienergebnisse tragen dazu bei, den Einsatz als Standardtherapie in der Schlaganfall-Neurorehabilitation weiter voranzutreiben. Insbesondere die prädiktive Eigenschaft der HRV ebnet den Weg für adaptive B/NMI-Steuerungsparadigmen, um individuelle Unterschiede bei beeinträchtigten Schlaganfallüberlebenden zu berücksichtigen. Darüber hinaus zeigten wir die Machbarkeit und sichere Anwendung einer neuartigen Implementierung für die bilaterale B/NMI-Kontrolle, die für die zuverlässige Bedienung von zwei Hand-Exoskeletten nach Rückenmarksverletzung notwendig ist.

7. Declaration of contribution others

I hereby declare that the doctoral dissertation submitted with the title: "Enhancing brain/neural-machine interfaces for upper limb motor restoration in chronic stroke and cervical spinal cord injury" was written independently using only the stated sources and aids and that quotes and excerpts, literal or otherwise, are marked correspondingly. I declare on oath that these statements are true and that I have concealed nothing. I am aware that false declarations or affirmations in lieu of an oath can be punished with a jail sentence of up to three years or with a fine.

Marius Nann

1. Publication:

Crea, S.*, Nann, M.*., Trigili, E.*., Cordella, F., Baldoni, A., Badesa, F. J., Catalan, J. M., Zollo, L., Vitiello, N., Aracil, N. G., Soekadar, S. R. (2018). Feasibility and safety of shared EEG/EOG and vision-guided autonomous whole-arm exoskeleton control to perform activities of daily living. *Scientific Reports*, 8(1), 10823.

* authors contributed equally to this work

Marius Nann, Prof. Dr. Loredana Zollo, Prof. Dr. Nicola Vitiello, Prof. Dr. Nicolas Garcia Aracil and Prof. Dr. Surjo R. Soekadar created the research concept and designed the study to equal parts. Dr. Simona Crea, Marius Nann and Dr. Emilio Trigili selected the methods to equal parts with support of Dr. Francesca Cordella. Study subjects were recruited by Dr. Francesca Cordella and Prof. Dr. Loredana Zollo. Data was acquired by Dr. Simona Crea, Marius Nann, Dr. Emilio Trigili, Dr. Francesca Cordella to equal parts with support of Dr. Andrea Baldoni, Dr. Francisco J. Badesa and José M. Catalán. The majority of data analysis, interpretation of results and preparation of manuscript was conducted by Marius Nann with support of Dr. Simona Crea and Dr. Emilio Trigili.

Prof. Dr. Surjo R. Soekadar supervised the study and supported interpretation of results and preparation of manuscript.

2. Publication:

Nann, M.*, Cordella, F.*., Trigili, E., Lauretti, C., Bravi, M., Miccinilli, S., Catalan, J. M., Badesa, F. J., Crea, S., Bressi, F., Garcia-Aracil, N., Vitiello, N., Zollo, L.*., Soekadar, S. R.* (2021). Restoring Activities of Daily Living Using an EEG/EOG-Controlled Semiautonomous and Mobile Whole-Arm Exoskeleton in Chronic Stroke. *IEEE Systems Journal*, 15(2), 2314-2321.

* authors contributed equally to this work

Marius Nann, Prof. Dr. Loredana Zollo, Prof. Dr. Nicola Vitiello, Prof. Dr. Nicolas Garcia Aracil and Prof. Dr. Surjo R. Soekadar created the research concept and designed the study to equal parts with support of Dr. Simona Crea and Prof. Dr. Federica Bressi. Marius Nann and Dr. Francesca Cordella selected the methods to equal parts with support of Dr. Emilio Trigili. Study patients were recruited by Marco Bravi and Dr. Sandra Miccinilli with support of Dr. Francesca Cordella, Prof. Dr. Federica Bressi and Prof. Dr. Loredana Zollo. Data was acquired by Marius Nann, Dr. Emilio Trigili and Dr. Francesca Cordella to equal parts with support of Dr. Clemente Lauretti, Dr. Francisco J. Badesa, José M. Catalán, Marco Bravi and Dr. Sandra Miccinilli. The majority of data analysis, interpretation of results and preparation of manuscript was conducted by Marius Nann with support of Dr. Francesca Cordella. Prof. Dr. Surjo R. Soekadar supervised the study and supported interpretation of results and preparation of manuscript.

3. Publication:

Nann, M., Peekhaus, N., Angerhöfer, C., Soekadar, S. R. (2020). Feasibility and Safety of Bilateral Hybrid EEG/EOG Brain/Neural–Machine Interaction. *Frontiers in Human Neuroscience*, 14(521), 580105.

Marius Nann and Niels Peekhaus created the research concept and study design with support of Prof. Dr. Surjo R. Soekadar. Marius Nann and Niels Peekhaus selected the methods to equal parts. Subjects and patients for experiments were recruited by Niels Peekhaus and Cornelius Angerhöfer. The majority of data was acquired by Niels Peekhaus with support of Marius Nann and Cornelius Angerhöfer. Data analysis was conducted to equal parts by Marius Nann and Niels Peekhaus. The majority of results interpretation were conducted by Marius Nann and Niels Peekhaus with support of Cornelius Angerhöfer. Majority of manuscript preparation was done by Marius Nann with support of Niels Peekhaus and Cornelius Angerhöfer. Prof. Dr. Surjo R. Soekadar supervised the study and supported preparation of manuscript.

4. Publication:

Nann, M., Haslacher, D., Colucci, A., Eskofier, B., von Tscharner, V., Soekadar, S.R. (2021). Heart rate variability predicts decline in sensorimotor rhythm control. *Journal of Neural Engineering*, 18(4), 0460b5.

Marius Nann and Prof. Dr. Surjo R. Soekadar created the majority of the research concept and designed the study with support of Annalisa Colucci. Most of the methods were selected by Marius Nann with support of David Haslacher, Prof. Dr. Bjoern Eskofier and Prof. Dr. Vinzenz von Tscharner. Marius Nann recruited the study subjects and acquired the data. Data analysis was conducted by Marius Nann with support of David Haslacher. Results were interpreted by Marius Nann with support of David Haslacher and Prof. Dr. Surjo R. Soekadar. Manuscript was prepared by Marius Nann. Prof. Dr. Surjo R. Soekadar supervised the study and supported preparation of manuscript.

Acknowledgments

Creating this thesis was an exciting and instructive journey for me. On this journey, I met many interesting and great persons who contributed in all kind of ways to this work. Among them, there are some persons to whom I feel deeply grateful. To the following I'd like to express my appreciation and sincere:

Surjo Soekadar for being my supervisor, for giving me the chance to pursue my Ph.D under his mentorship, and, most importantly, for teaching me more than just neuroscience.

Christoph Braun for being my co-supervisor and for providing me great support and a social network especially in challenging times.

Bjoern Eskofier for being my co-supervisor and for giving me the chance to pursue my Master thesis in Canada, the initial start of the whole adventure.

Vinzenz von Tscharner for his decisive impulse to begin a Ph.D, for his constant advice and support in all kind of topics and for teaching me skills which I still draw on.

Jürgen Mellinger for his invaluable and selfless help and his willingness to support me in all kind of programming questions.

Inka Montero and Pia Schmidt for their precious help and advice in all kind of questions regarding the Ph.D program.

Annette Dreher for her constant availability and her invaluable feedback during numerous test sessions.

The members of the Applied/Clinical Neurotechnology Lab in Tübingen/Berlin for their great support and company playing a major role in the success of this Ph.D thesis.

